Improvement of the electron transfer in *S. oneidensis* and production of glucose-based platform chemicals

Zur Erlangung des akademischen Grades einer

DOKTORIN DER NATURWISSENSCHAFTEN

(Dr. rer. nat.)

von der KIT-Fakultät für Chemie und Biowissenschaften

des Karlsruher Instituts für Technologie (KIT)

genehmigte

DISSERTATION

von

Veronica Palma Delgado

1. Referent: Prof. Dr. Johannes Gescher
2. Referent: Prof. Dr. Reinhard Fischer
Tag der mündlichen Prüfung: 11.12.2019

I.   Erklärung an Eides statt

Hiermit erkläre ich, diese Arbeit selbstständig angefertigt und keine anderen als die angegebenen Quellen und Hilfsmittel verwendet habe. Alle Teile, die wörtlich oder inhaltlich aus anderen Werken entnommen sind, sind von mir durch Angabe der Quelle gekennzeichnet. Weiterhin habe ich beim Anfertigen dieser Arbeit die Regeln zur Sicherung der guten wissenschaftlichen Praxis des KIT beachtet und alle Primärdaten gemäß Abs. A (6) am Institut archiviert. Des Weiteren versichere ich, dass die elektronische mit der schriftlichen Form dieser Arbeit übereinstimmt.

Karlsruhe, 11. Dezember 2019

Veronica Palma Delgado

II.   Acknowledgements

To my grandparents,

who died during my time in Germany.

I want to thank my professor Johannes Gescher for giving me the opportunity to do my PhD in his laboratory and for all the new things I could learn throughout my studies.

I also want to thank my laboratory colleagues for the funny moments, little distractions and new experiences.

And thank you, Thomas, for being there when I needed you.

III.   Publications and conference contributions

Publication 1: Paper

Delgado, Veronica Palma; Paquete, Catarina M.; Sturm, Gunnar; Gescher, Johannes (2019): "Improvement of the electron transfer rate in *Shewanella oneidensis* MR-1 using a tailored periplasmic protein composition". In Bioelectrochemistry 129, pp. 18–25. DOI: 10.1016/j.bioelechem.2019.04.022.

Publication 2: Book chapter

Palma-Delgado, Veronica; Gescher, Johannes; Sturm, Gunnar (2019): "Electrode-Assisted Fermentations: Their Limitations and Future Research Directions". In Sonia M. Tiquia-Arashiro, Deepak Pant (Eds.): Electrochemical Technologies. Milton: CRC Press, pp. 85–96. DOI: 10.1201/9780429487118.

Conference contributions

EU-ISMET 2018 (Newcastle, England)
Talk: "Increasing the microbe-electrode electron transfer using a tailored periplasmic protein composition"

VAAM 2019 (Mainz, Germany)
Poster: "Microbe-electrode interaction as a tool for anaerobic production of platform chemicals"

IV. Zusammenfassung

Das Hauptziel dieser Doktorarbeit war es, die Elektronentransferrate des Mikroorganismus *S. oneidensis* MR-1 auf Anodenoberflächen zu verbessern und mit seiner Hilfe Itakonsäure ausgehend von Glukose als neuem Substrat zu produzieren. Aufgrund der Komplexität dieses Vorhabens wurde die Doktorarbeit in drei Teilprojekte aufgeteilt.

Das erste Teilprojekt basierte auf der Hypothese, dass eine Reduktion der Komplexität des periplasmatischen Elektronentransfernetzwerks und eine anschließende Überexpression des wichtigen periplasmatischen Elektronen-Shuttle-Cytochroms STC zu einer Beschleunigung der Elektronentransferrate und somit des gesamten Metabolismus führen könnte. Genauer gesagt, wurden die periplasmatischen Cytochrome NrfA, CcpA, NapB und das Protein NapA mit STC ersetzt, was zu einer 3,6-fach erhöhten Expression des STC kodierenden Gens *cctA* und einem 2,5-fachen Anstieg der periplasmatischen Flavin-Konzentration führte. Die resultierende 4-fach Mutante zeigte in anoxischen Zellsuspensionsassays mit Eisencitrat als Elektronenakzeptor eine 1,7-fach erhöhte Elektronentransferrate im Vergleich zu *S. oneidensis* MR-1. Des Weiteren war die erreichte Gesamtstromproduktion in bioelektrochemischen Systemen mit einer Graphit-Fleece-Elektrode als Elektronenakzeptor unter anoxischen Bedingungen mit der entwickelten 4-fach Mutante 1,5-fach höher. Außerdem war es möglich zu zeigen, dass eine bisher vermutete Redundanz von STC und FccA im Elektronentransfer nicht komplett gegeben ist, da eine zusätzliche Substitution von FccA mit STC zu Elektronentransferraten auf Wildtyp-Niveau führte.

Im zweiten Teilprojekt wurden verschiedene Strategien getestet, um *Shewanella* zu ermöglichen Glukose als Substrat zu nutzen. Dabei war das Einsetzen eines Plasmids mit den Genen für den Glukosetransporter GalP und die Kinase Glk aus *E. coli* die effizienteste Strategie. Die Kombination aus dieser Strategie und dem im ersten Teilprojekt entwickelten Chassis-Stamm erlaubten es *Shewanella* 50 mM Eisen(III)citrat innerhalb von 24 h komplett zu reduzieren. Im Vergleich von 4-fach Mutante mit Glukose-Modul und Wildtyp mit Glukose-Modul konnte ein 1,7-fach schnellerer Glukoseverbrauch festgestellt

werden. Eine andere getestete Strategie – die Deletion des Repressors NagR – stellte sich unter anoxischen Bedingungen als wirkungslos heraus.

Das dritte Teilprojekt zielte auf die Ermöglichung der Glukose-basierten Itakonsäure-Produktion ab, weshalb das zuvor getestete Glukose-Modul sowie das Enzym CadA von *Aspergillus terreus* in einem Plasmid in *Shewanella* eingefügt wurden. Zusätzlich wurden verschiedene Gene deletiert, um die metabolische Komplexität zu reduzieren und die Produktion von Nebenprodukten zu vermeiden. Genauer gesagt wurden die Gene *sucCD, pykA, aceA, ptA* und *ackA* aus dem Genom entfernt. Zellsuspensionsassays unter oxischen und anoxischen Bedingungen zeigten, dass die Produktion von kleinen Itakonsäure-Mengen nur unter oxischen Bedingungen möglich war. Wegen der geringen Mengen von Itakonsäure, die während dieser Experimente produziert werden konnten, wäre weitere Forschung an der Stammoptimierung notwendig. Nichtsdestotrotz konnte gezeigt werden, dass die Integration von *cadA* die Itakonsäure-Produktion ermöglicht und somit das grundlegende Konzept valide ist.

V. Abstract

The main aim of this thesis was to accelerate the extracellular electron transfer to an anode catalyzed by the microorganism *S. oneidensis* MR-1 and to enable the production of itaconic acid based on glucose as a new substrate. Due to the complexity, the thesis was divided into three sub-projects.

The first sub-project was based on the hypothesis that a reduction of the complexity of the periplasmic electron transfer network and a subsequent overexpression of the crucial periplasmic electron shuttling cytochrome STC could lead to an acceleration of the electron transfer rate and, thereby, of the whole metabolism. In particular, the periplasmic cytochromes NrfA, CcpA, NapB and the protein NapA were substituted with STC, which led to a 3.6-fold increased expression of *cctA* encoding STC and a 2.5-fold increase of the periplasmic flavin concentration. The resulting quadruple mutant showed a 1.7-fold increased electron transfer rate compared to *S. oneidensis* MR-1 in anoxic cell suspension assays with ferric iron citrate as electron acceptor. Also, the achieved total current production in bioelectrochemical systems with a graphite fleece electrode as electron acceptor under anoxic conditions was 1.5-fold higher with the developed quadruple mutant. Besides, it was possible to demonstrate that a so far suspected redundancy of STC and FccA in the electron transfer is not completely given because the additional substitution of FccA with STC led to electron transfer rates similar to the wild type.

In the second sub-project, different strategies of enabling glucose consumption in *Shewanella* were tested. Inserting a plasmid containing the genes for the glucose transporter GalP and the kinase Glk from *E. coli* resulted as the most efficient strategy. The combination of this strategy with the developed chassis strain from the first sub-project enabled *Shewanella* to reduce 50 mM ferric iron citrate completely within 24 h. A 1.7-fold faster glucose consumption could be observed in the quadruple mutant comprising the glucose module compared to the wild type comprising the glucose module. Another tested strategy – the deletion of the repressor NagR – was revealed to be ineffective under anoxic conditions.

The third project aimed at facilitating a glucose-based itaconic acid production by introducing a plasmid comprising the previously tested glucose module and the enzyme CadA from *Aspergillus terreus.* Additionally to the insertion of *cadA*, various genes were knocked out in order to reduce the metabolic complexity and to avoid the production of by-products. More specifically, the genes *sucCD*, *pykA*, *aceA*, *ptA* and *ackA* were deleted. Cell suspension assays under oxic and anoxic conditions revealed that the production of small quantities of itaconic acid was only possible under oxic conditions. Due to the small quantities of itaconic acid obtained during these experiments, further investigation on optimizing the strain would be necessary. Nevertheless, the concept of facilitating itaconic acid production by inserting *cadA* could be proven valid.

VI. Table of contents

VII. List of figures

VIII.   List of tables

IX. List of abbreviations

Abbreviation	Description
A	Surface of the anode
A. terreus	*Aspergillus terreus*
AAFs	Anode-assisted fermentations
AceA	Isocitrate lyase
AckA	Acetate kinase
AMP	Adenosine mononucleotide phosphate
APS	Ammonium persulfate
A_{total}	Total heme absorbance
BESs	Bioelectrochemical systems
BSA	Serum albumin protein
c	Concentration
C_0	Concentration of the redox species
CAFs	Cathode-assisted fermentations
CcpA	Diheme cytochrome c5 peroxidase
CTAB	Cetyl trimetylammonium bromide
CymA	Tetraheme *c*-type cytochrome
d	Layer thickness
D_0	Diffusion coefficient of he redox species
DMSO	Dimethyl sulfoxide
ε	Molar extinction coefficient
ED	Entner-Doudoroff
EMP	Embden-Meyerhof-Pamas
ET	Electron transfer
FAD	Flavin adenine dinucleotide
FccA	Flavocytochrome A
Ferrozine	3-(2-pyri-dyl)-5,6-diphenyl-1,2,4-triazine-p,p'-disulfonic acid
FMN	Flavin mononucleotide
GalP	Galactose-proton symporter

GlcNAc	N-acetylglucosamine permease
GlF	Glucose facilitator
GlK	Glucokinase
HEPES	4-(2-Hydroxyethyl)piperazine-1-ethanesulfonic acid
HPLC	High performance liquid chromatography
IA	Itaconic acid
IfcA	Periplasmic tetraheme flavocytochrome
i_p	Peak intensity
MAA	Methacrylic acid
MECs	Microbial electrolysis cells
MESs	Microbial electrosynthesis cells
MFCs	Microbial fuel cells
MMA	Methyl methacrylate
MtrA	Decaheme cytochrome *c*
MtrB	β-barrel protein
MtrC	Decaheme cytochrome *c*
NagK	N-acetylglucosamine kinase
NagP	N-acetylglucosamine permease
NagR	Transcriptional repressor
NapA	Periplasmic nitrate reductase
NapB	Periplasmic nitrate reductase
NrfA	Ammonia-forming nitrite reductase
PGE	Pyrolytic graphite edge
PP	Pentose phosphate
PtA	Phosphate acetyltransferase
PTS	Phosphotransferase system
PykA	Pyruvate kinase
RF	Riboflavin
SDS-PAGE	Polyacrylamide gel electrophoresis
STC	Small tetraheme *c*-type cytochrome

SucCD	Succinyl-CoA synthetase
TCA	Trichloroacetic acid
TCA cycle	Tricarboxylic acid cycle
TEA	Terminal electron acceptor
TEMED	Tetramethylethylendiamin
TMB	3,3′,5,5′-Tetramethylbenzidine dihydrochloride hydrate
TPM	Transcripts per million
υ	Scan rate

1. Introduction

Today's industry is in large parts based on fossil feedstock. Because of rising concerns about the future cost, availability and environmental impact of fossil feedstock, research on new technologies based on renewable feedstock has increased in the last decades (Hirsch et al. 2006). One research branch is focused on the utilization of microorganisms since many natural metabolites can be used for chemical synthesis of polymers.

Genetic and chemical engineering offer many possibilities to develop new bioprocesses that overcome classic issues like low product yields and high production costs. Following this line of research, this thesis will contribute to the fundamental research on improving *Shewanella oneidensis* for microbe-electrode interaction and finding new fields of application.

1.1 *Shewanella oneidensis*

1.1.1 General information

S. oneidensis MR-1 is a facultative anaerobe, Gram-negative γ-proteo-bacterium, which was discovered in 1988 by Charles Myers and Ken Nealson in Lake Oneida in Upstate New York, USA (Myers and Nealson 1988).

S. oneidensis is known for the broad spectrum of electron acceptors it can use under anoxic conditions. The bandwidth of usable electron acceptors stretches from soluble substances like dimethyl sulfoxide (DMSO), nitrate, nitrite or fumarate to insoluble iron and manganese oxides as well as anodes in bioelectrochemical systems (BESs) (Myers and Nealson 1988; Hau and Gralnick 2007; Romine et al. 2008; Förster et al. 2017). Under anoxic conditions, *Shewanella* is known to metabolize lactate, pyruvate and N-acetyl-glucosamine (Lovley et al. 1989; Pinchuk et al. 2008; Hunt et al. 2010; Brutinel and Gralnick 2012a), while it can use additionally acetate and some amino acids under oxic conditions (Myers and Nealson 1988; Myers et al. 2000; Heidelberg et al. 2002; Tiedje 2002; Viamajala et al. 2002; Middleton et al. 2003; Tang et al. 2006).

Due to this versatility combined with an easy genetic tractability (Hau and Gralnick 2007) *S. oneidensis* has become a model organism for studying dissimilatory iron reduction processes and has been applied for bioremediation processes regarding various types of heavy metals (Myers and Nealson 1988; Myers et al. 2000; Heidelberg et al. 2002; Tiedje 2002; Viamajala et al. 2002; Middleton et al. 2003; Tang et al. 2006). Furthermore, an increasing number of applied studies focuses on the electricity generation using *S. oneidensis* under anoxic conditions (Kim et al. 2002; Park and Zeikus 2002; Kim et al. 2003; Logan et al. 2005; Lovley 2006).

As a Gram-negative organism, *S. oneidensis* has a cytoplasmic and an outer membrane that surround the periplasmic space. In order to reduce iron oxides or other insoluble electron acceptors, respiratory electrons which are set free during metabolism in the cytoplasm have to cross both membranes and the periplasmic space (Beliaev and Saffarini 1998; Beliaev et al. 2001; Lies et al. 2005).

1.1.2 Aerobic and anaerobic respiration

S. oneidensis generates energy by coupling the oxidation of organic compounds to the reduction of a wide range of electron acceptors, including oxygen, fumarate and Fe(III) (Myers and Nealson 1988; Meshulam-Simon et al. 2007). Depending on the availability of electron donors and acceptors, *S. oneidensis* adopts two different metabolic modes: aerobic respiration and anaerobic respiration.

Aerobic respiration uses oxygen as terminal electron acceptor (TEA) and is the most productive mode regarding cell energy due to the complete oxidation of a growth substrate. Meanwhile, during anaerobic respiration the carbon and electron source is only partially oxidized. Due to the energetic benefits of oxygen as electron acceptor, the switch between aerobic and anaerobic metabolism has a significant impact on the gene expression (Maier and Myers 2001; Beliaev et al. 2002).

Shewanella's anaerobic metabolism is supported by a large number of redox active multi-heme cytochromes, which is assumed to be one reason for its respiratory diversity (Fredrickson et al. 2008). So far, 41 cytochromes have been discovered in *Shewanella*, which can be classified into three groups according to their physical localization in the bacterium: there are 9 cytoplasmic membrane, 5 outer membrane and 27 periplasmic cytochromes (Romine et al. 2008; Gao et al. 2010).

1.1.3 Electron transfer process in *Shewanella oneidensis*

Based on the anaerobic iron reduction process, the electron transfer mechanism from the cytoplasm to the external electron acceptor is illustrated in Figure 1.

During the anaerobic respiration of organic electron sources in the cytoplasm, electrons are set free and are then transported to the menaquinone pool in the cytoplasmic membrane, which is re-oxidized by the tetraheme *c*-type cytochrome and quinol oxidase CymA (Hartshorne et al. 2007; Firer-Sherwood et al. 2008). CymA has an important role in transporting the electrons into the periplasm since mutants lacking the *cymA* gene are unable to reduce electron acceptors such as ferric iron, fumarate, nitrate, nitrite, DMSO or an anode (Myers and Myers 1997; Schwalb et al. 2003; Lies et al. 2005; Gao et al. 2010). A network of periplasmic redox proteins, which is dominated by *c*-type cytochromes, receives the electrons from CymA (Gralnick and Newman 2007).

The periplasmic tetraheme *c*-type flavocytochrome and fumarate reductase FccA and the small tetratheme *c*-type cytochrome STC are highly abundant in the periplasm (Ross et al. 2011) and seem to act as electron transfer hub between CymA and different electron transfer paths or redox active proteins at the outer membrane (Gralnick and Newman 2007; Schuetz et al. 2009; Coursolle and Gralnick 2010; Fonseca et al. 2013; Alves et al. 2015; Sturm et al. 2015).
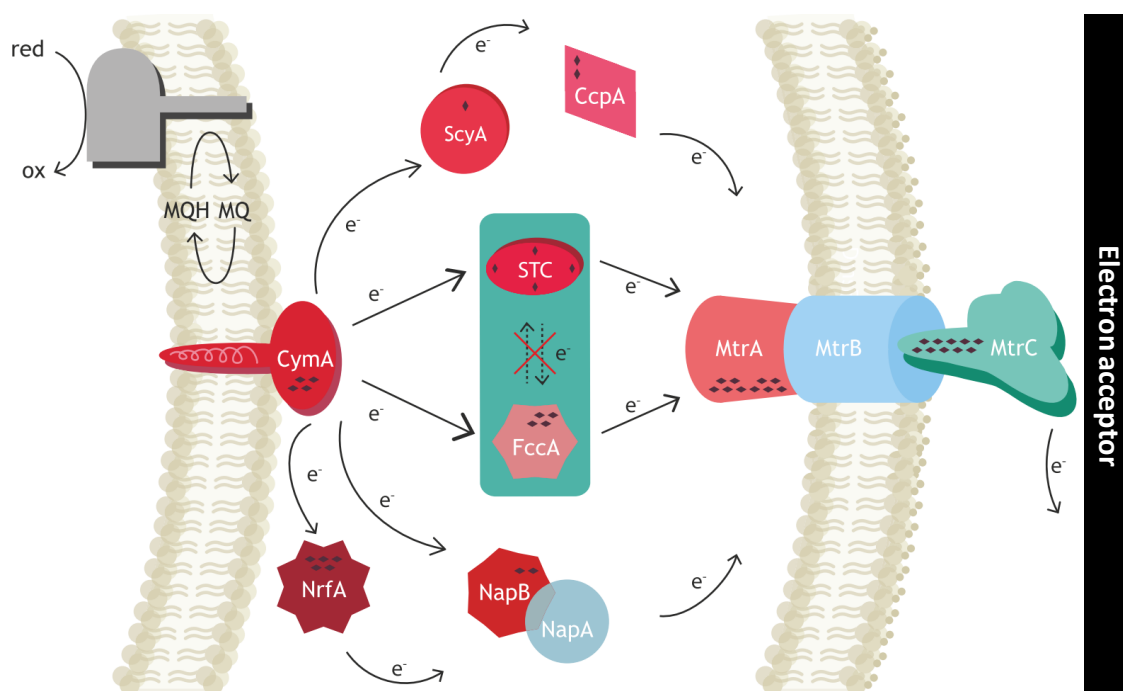
Figure 1: Scheme of electron transfer in *S. oneidensis*. Electrons set free during the metabolism in the cytoplasm pass the cytoplasmic membrane via CymA to the periplasm. Here, a network of periplasmic redox active cytochromes transports the electrons to the outer membrane protein complex MtrABC which allows them to cross the outer membrane. Once on the cell surface, the electrons reduce an external electron acceptor.

Sturm and colleagues showed that a simultaneous deletion of the genes corresponding to STC and FccA resulted in a strong inhibition of growth on ferric iron and nitrate compared to the wild type as well as a complete inability to grow on DMSO (Sturm et al. 2015). Both cytochromes seem to have redundant functions regarding the distribution of electrons (Fonseca et al. 2013; Sturm et al. 2015) but cannot exchange electrons with each other (Fonseca et al. 2013).

Since FccA and STC are able to interact with CymA and MtrA, one could assume that they could build a "bridge" between the cytoplasmic and outer membrane. However, studies showed that such a static connection is impossible because both proteins use the same heme to contact CymA and MtrA and, therefore, have to move and even change orientation between both membrane cytochromes in order to transfer electrons (Alves et al. 2015).

To reduce external ferric iron or an anode, electrons have to be transported through the outer membrane to the cell surface, which is facilitated by a heterotrimeric protein complex composed of MtrA, MtrB and MtrC. MtrA is a metal reducing cytochrome located at the periplasmic side of the outer membrane and works as periplasmic electron acceptor, MtrC is the terminal reductase on the cell surface and MtrB is a membrane associated β-barrel protein, which seems to connect MtrA and MtrC enabling the exchange of electrons between both (Shi et al. 2012). Several studies demonstrated that mutants lacking any of these proteins have a diminished ability to reduce extracellular ferric iron or lose this ability completely (Beliaev et al. 2001; Bretschger et al. 2007; Gao et al. 2010; Schicklberger et al. 2011).

Firer-Sherwood and colleagues investigated the redox potential of *c*-type cytochromes that are important for the dissimilatory metal reduction. They discovered that the individual redox potentials have overlapping windows, which in all likelihood facilitates the electron transfer and directs it along the redox potential gradient between CymA and the terminal electron acceptor (Firer-Sherwood et al. 2008).

In recent years, two mechanisms have been proposed to explain the electron transport over longer distances to insoluble electron acceptors: direct and indirect transport. Figure 2 illustrates both mechanisms schematically.

Shewanella's cellular appendices, so-called nanowires, were shown to resemble extensions of the periplasm and the outer membrane. Containing typical periplasmic protein content and having functional expressions of MtrC and OmcA on the surface, these appendices are conductive and facilitate direct electron transport (Gorby et al. 2006; Bouhenni et al. 2010; El-Naggar et al. 2010; Pirbadian et al. 2014; Subramanian et al. 2018).

For the indirect electron transport from the outer membrane to a terminal electron acceptor, flavins were identified to have a crucial role (Covington et al. 2010; Brutinel and Gralnick 2012b; Kotloski and Gralnick 2013). While earlier studies reported only about the electron shuttle functionality of flavins, more recent investigations argue based on conducted differential pulse voltammetry experiments that flavins might also have a role as cofactors of outer membrane

cytochromes (Okamoto et al. 2013; Okamoto et al. 2014a; Okamoto et al. 2014b; Xu et al. 2016). Currently, there is an ongoing scientific discussion about which of these two functions has major impact on the external electron transport.
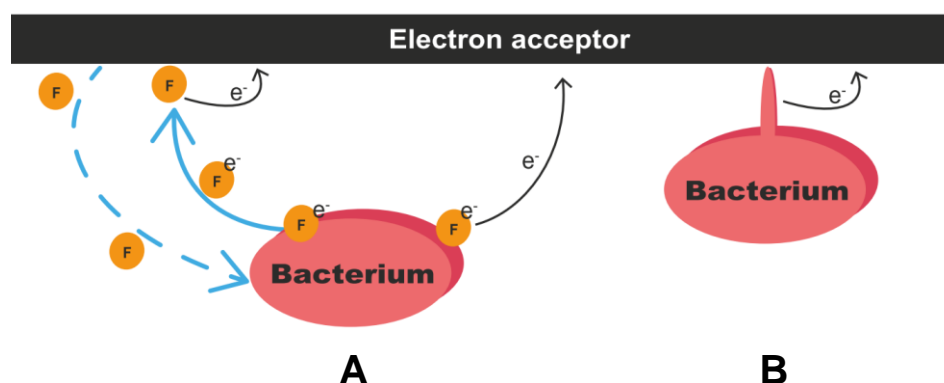
Figure 2: A: Scheme of indirect electron transfer via flavins as shuttles (left) and cofactors (right). **B:** Scheme of direct electron transfer via cellular appendices.

Especially in the case of insoluble terminal electron acceptors such as electrodes, a study by Marsili and colleagues showed that endogenously expressed and secreted flavins allow for long-distance electron transport and that they are responsible for roughly 70% of the electron transfer rate (Marsili et al. 2008). While essential for the respiration of insoluble electron acceptors, the importance of flavins for the reduction of soluble electron acceptors like ferric citrate decreases due to the dispersion of the electron acceptor and the resulting easier cell contact. Nevertheless, secreted flavins lead to an acceleration of the electron transfer rate (von Canstein et al. 2008).

Besides the long-range electron transport to electron acceptors, flavins are also assumed to be beneficial for the intercellular electron transport in biofilms (Okamoto et al. 2013; Okamoto et al. 2014a; Okamoto et al. 2014b).

Depending on the growth conditions, flavins are reported to accumulate in varying concentrations from 25 nM to 500 nM in supernatants of *S. oneidensis* cultures (Marsili et al. 2008; von Canstein et al. 2008; Velasquez-Orta et al. 2010; Zhai et al. 2016; Delgado et al. 2019).

During flavin synthesis, the proteins encoded by *ribBA, ribD, ribH* and *ribE* have been shown to be responsible for the generation of riboflavin (RF) (Brutinel et al. 2013). The riboflavin kinase RibF can transform RF to flavin mononucleotide (FMN) and flavin adenine dinucleotide (FAD) (Brutinel and Gralnick 2012b). Another important gene is the bacterial FAD exporter *bfe*, which is responsible for exporting FAD into the periplasm (Kotloski and Gralnick 2013). In the periplasm, FAD can be hydrolyzed by the periplasmic 5' nulceotidase UshA to FMN and AMP or bind as a cofactor to proteins like FccA or MtrC (Covington et al. 2010).

The electron transport mechanisms described above allow investigating strategies for the improvement of the electron transport to extracellular electron acceptors and make *Shewanella* an excellent organism for such studies.

1.1.4 Glucose metabolism

S. oneidensis is known for preferably using small organic molecules like lactate and pyruvate as a carbon and energy source. Five- and six-carbon carbohydrates like glucose cannot be metabolized without previous adaptation or genetic modifications.

For most sustainable biotechnological applications such as the use of agricultural organic residues (e.g. cellulose), *S. oneidensis* must be able to use these carbohydrates. Besides, larger carbohydrates can be cheaper than the naturally preferred smaller substrates (glucose: 0.35 US$ / kg (Song and Lee 2006) vs. lactic acid: 1.38 US$ / kg for 50% purity (Wee et al. 2006)). Furthermore, the natural availability of lactate is limited (Biffinger et al. 2009). Therefore, it is necessary to adapt *Shewanella's* metabolism in order to design biotechnological processes that are potentially profitable on an industrial scale.

It is already common to use glucose as carbon source for other microorganisms in various biotechnological processes like for example the production of itaconic acid using *Aspergillus terreus* (Willke and Vorlop 2001; da Cruz et al. 2018) or the production of glutamic acid using *Corynebacterium glutamicum* (Ramesh et al. 2014).

Even though *S. oneidensis* comprises the major part of the Entner-Doudoroff (ED) and the pentose phosphate (PP) pathways (Nakagawa et al. 2015), it is unable to gain energy using glucose as carbon source. Previous studies demonstrated that a natural adaption over time enables the use of glucose, when either exposed first to lactate, than to a mixture of lactate and glucose, and finally only to glucose as electron donor (Howard et al. 2012) or when exposed directly to glucose as electron donor under oxic conditions (Serres and Riley 2006; Biffinger et al. 2008; Biffinger et al. 2009). Nevertheless, some investigations concentrated on facilitating the metabolic utilization of glucose through genetic modifications under oxic and anoxic conditions employing different electron acceptors. So far, two basic approaches were tested: on one hand, the insertion of a glucose transporter and a kinase to allow glucose transport into the cell and the conversion of glucose to glucose-6-phosphate, respectively (Choi et al. 2014a; Nakagawa et al. 2015), and, on the other hand, the deletion of the transcriptional repressor *nagR,* which enables the subsequent expression of genes for an N-acetylglucosamine permease (*nagP*) and kinase (*nagK*) (Chubiz and Marx 2017).

For the first research direction, glucose transporters and kinases from different microorganisms were introduced into *Shewanella.* Choi and colleagues inserted the glucose facilitator GlF and the glucokinase GlK of *Zymomonas mobilis* into *Shewanella's* genome and showed that this mutant was capable of using glucose as sole carbon source under oxic conditions and under anoxic conditions with ferric citrate as electron acceptor (Choi et al. 2014a). They also demonstrated that this mutant was able to produce current in BESs using glucose as substrate.

Earlier experiments showed that for *E. coli* the glucose/galactose-proton symporter GalP and the hexokinase GlK are crucial for the metabolic usage of glucose, when the phosphotransferase system (PTS) is disabled. Mutants lacking PTS and one or both of these genes lost their ability to grow with glucose as carbon source or at least suffered severe growth inhibition (Flores et al. 1996; Flores et al. 2002; Hernández-Montalvo et al. 2003). Based on these findings, the research group around Nakagawa chose to insert the glucose transporter GalP and the kinase GlK from *E. coli* into *Shewanella's* genome,

which led to a mutant able to consume glucose under oxic conditions and under anoxic conditions with fumarate as electron acceptor. Meanwhile, experiments under anoxic conditions without electron acceptor (fermentation) showed no significant cell growth in the studied timeframe (Nakagawa et al. 2015). Moreover, they reported on the influence of different electrode potentials in MFCs on the metabolite production and on the level of gene expression (Nakagawa et al. 2015).

Chubiz and Marx studied via transcriptomic analysis the genomic basis of *S. oneidensis* MR-1 strains that naturally adapted to glucose consumption in order to identify the enabling genetic mutations. They observed that the transcriptional repressor *nagR* was naturally deleted in all strains, resulting in the consecutive expression of the N-acetylglucosamine permease (GlcNAc) NagP and the kinase NagK. These genetic alterations allow the transport of glucose into the cell and its phosphorylation to glucose-6-phosphate. On account of these findings, Chubiz and Marx designed a mutant lacking *nagR* and confirmed that this deletion enables growth on glucose. Another finding of this study was that – once adapted to glucose consumption – *Shewanella* almost exclusively uses the Entner-Doudoroff pathway for metabolizing glucose, even though the entire pentose phosphate and the almost complete Embden-Meyerhof-Parnas (EMP) pathway are available as well (Chubiz and Marx 2017).

No matter how the glucose consumption was achieved – natural adaptation, gene insertion or gene deletion – the facilitation of a glucose metabolism also resulted in a deterioration of the capability to grow on lactate (Chubiz and Marx 2017).

The studies of Choi and Nakagawa showed that biomass formation and electrical current generation are less efficient when using glucose as carbon source compared to lactate (Choi et al. 2014a; Nakagawa et al. 2015). Nevertheless, enabling glucose consumption is still appealing from an industrial point of view because of the high cost differences between both substrates. Furthermore, the glucose metabolism plays a crucial role for the use of more complex molecules such as cellobiose and cellulose as carbon source, which can be converted into glucose (Climent et al. 2011).

1.2 Fermentation

1.2.1 Conventional fermentation

If neither oxygen for aerobic respiration nor other external electron acceptors for anaerobic respiration are available, some microorganisms are able to gain energy through fermentation. Electrons that are released during substrate oxidation reduce an internal electron acceptor, which initiates a cascade of oxidation and reduction reactions. In order to keep the fermentation going, the redox balance between substrate and product must be maintained, which limits the range of possible products obtained from a substrate and results often in the production of various by-products (Moat et al. 2002).

Over millennia up to this day, mankind has used fermentations for producing, refining and conserving food and beverages like cheese, bread, sauerkraut, vinegar, wine and beer. Also, biogas production is based on the fermentation of organic residues. Nowadays, metabolic pathway engineering paved the way for industrial production of certain chemicals such as citric acid, glutamic acid or vitamins by using microorganisms in bioreactors (Survase et al. 2006; Max et al. 2010; Ramesh et al. 2014).

1.2.2 Electrode-assisted fermentations

To overcome the metabolic limitations of redox balanced fermentations, bioelectrochemical systems are used to perform electrode-assisted fermentations. A BES is a bioreactor composed of a counter, working and reference electrode, in which desired products and electricity can be generated by means of concomitant electrochemical and biological processes. Most commonly, calomel or silver chloride reference electrodes are used, while platinum electrodes are normally used as counter electrodes. The working electrode is frequently composed of carbon and graphene materials due to their high conductivity, chemical stability and rather low cost (Walcarius et al. 2013). In comparison with other electron acceptors like ferric iron, fumarate or DMSO, an electrode offers the advantage of not being consumed over time.

Electrodes as electron acceptor offer the biotechnological possibility of developing pathways that do not need to be stoichiometrically balanced with respect to the oxidation states of substrates and products. This allows the production of substances more oxidized than the substrates (Flynn et al. 2010). Figure 3 depicts the basic working principle of electrode-assisted fermentations.

By modifying the electrode potential, it is possible to influence the intracellular redox balance and, thereby, change the production yield or even produce other chemicals (Flynn et al. 2010; Zhou et al. 2013; Choi et al. 2014b; Nakagawa et al. 2015). Also, microbial cell growth and density can be optimized (Aelterman et al. 2008; Torres et al. 2009).
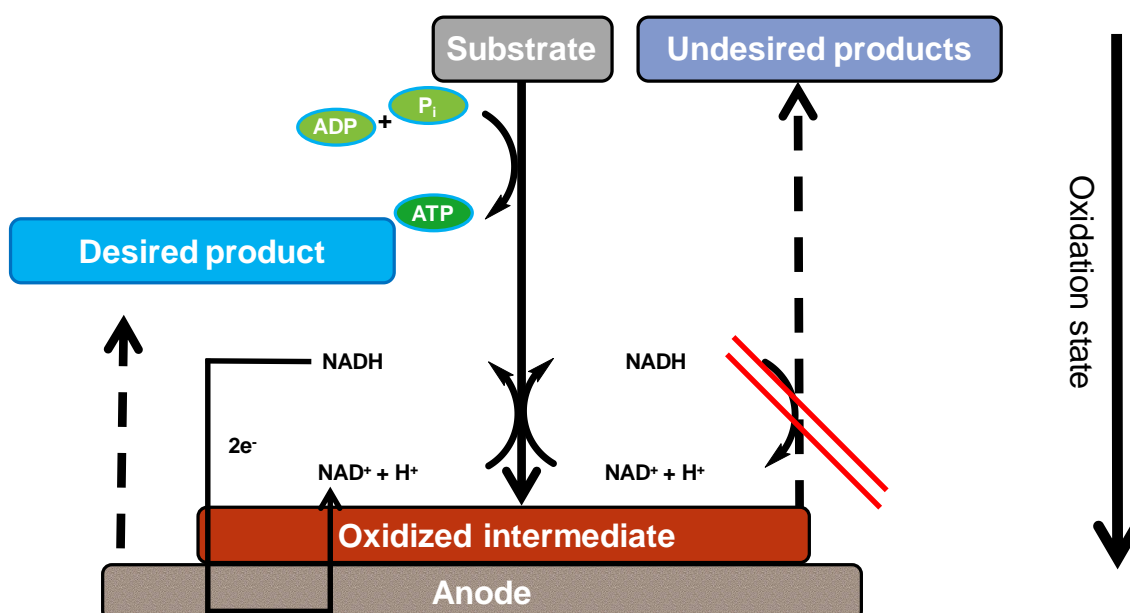
Figure 3: Scheme of unbalanced fermentation. By using an anode as non-depletable electron acceptor, it is possible to produce chemical compounds with a higher oxidation state than the substrate.

There are two different types of electrode-assisted fermentations: anode-assisted fermentations (AAFs) and cathode-assisted fermentations (CAFs). In the first case, the working electrode serves as external electron acceptor allowing the production of metabolites with a higher oxidation state than the substrate's (e.g. glycerol to ethanol) and avoiding the formation of by-products

by means of conducting the surplus electrons to the anode generating electrical current. As a result, NADH recycling leads to proton gradients for ATP generation (Kracke and Krömer 2014). In the case of CAFs on the other hand, the working electrode is used as an electron source facilitating the production of an end product with a lower oxidation state than the substrate (e.g. glucose to butanol). Here, the electrons provided through the cathode lead to a higher NADH production, which increases the reduction of chemical molecules producing additional ATP (Kracke and Krömer 2014).

Depending on the intended application, there are three general operating modes of BESs that allow performing electrode-assisted fermentations: microbial fuel cells (MFCs), microbial electrolysis cells (MECs) and microbial electrosynthesis cells (MESs). In MFCs and MECs the bacteria are placed in the anode compartment (AAFs) while in MESs the microorganisms are inserted in the cathode compartment (CAFs). Figure 4 shows these BES modes schematically.

The main goal of MFCs, besides the production of valuable substances, is the generation of electrical current by extracting the chemical energy from complex organic substrates. After powering external devices, remaining electrons are transported directly to the cathode compartment where they reduce O_2 to H_2O. Some examples of this process are the production of acetoin using lactate (Bursac et al. 2017) or glucose (Förster et al. 2017) as substrate and the production of ethanol using glycerol as carbon source (Flynn et al. 2010).

In MECs on the other hand, the production of valuable compounds is combined with the formation of hydrogen at the cathode. Since the low redox potential of the H^+ / H_2 couple ($E_0^{'} = -414$ mV) requires an overpotential that cannot be completely provided by the current produced at the anode, the cathode potential is lowered by an additional external power source. In contrast to the MFCs, the cathode compartment is sealed to exclude oxygen.

In MESs, microorganisms are placed in the cathode compartment using carbon dioxide (CO_2) and electrical current as sources for the production of platform chemicals.
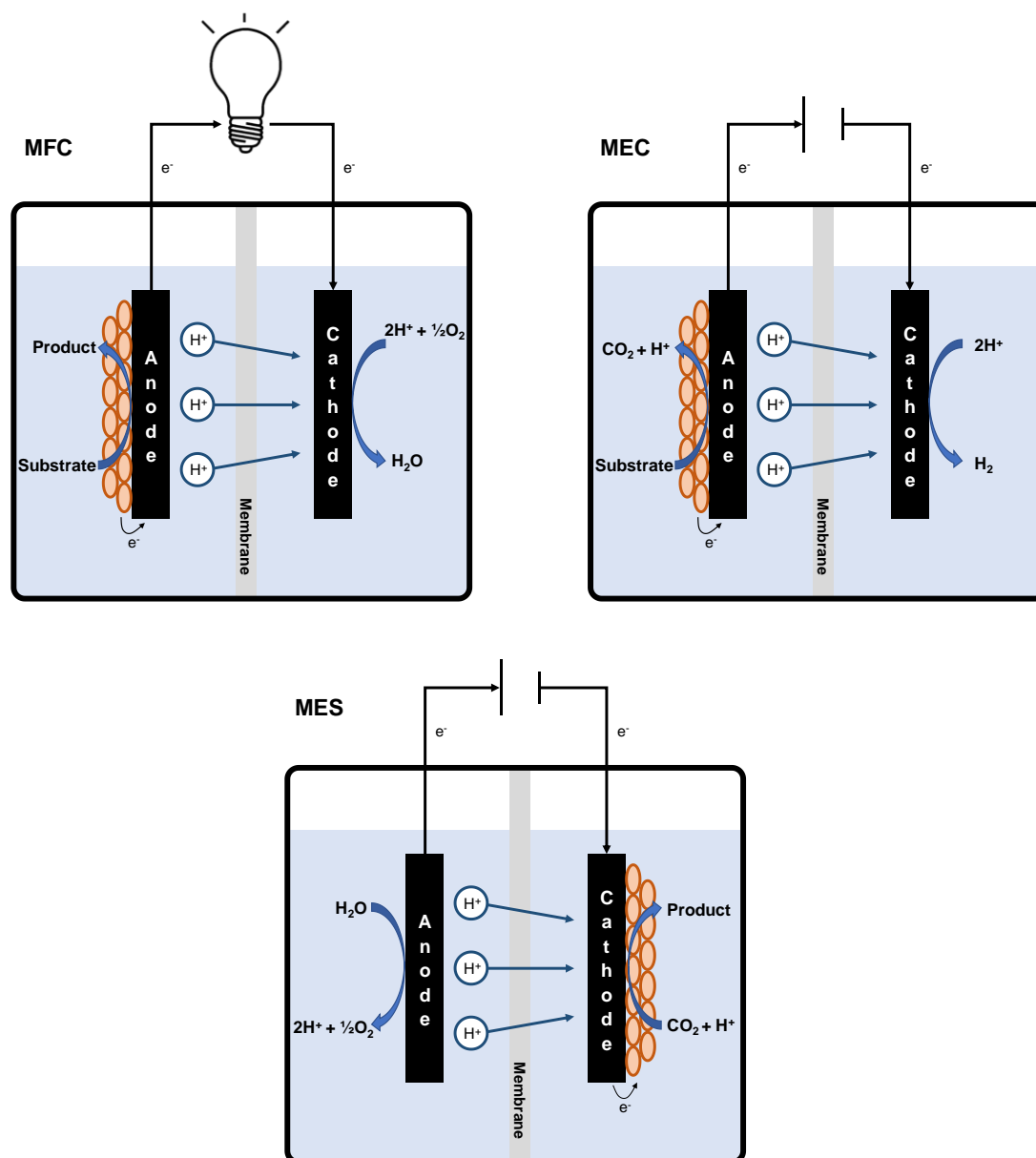
Figure 4: Schemes of AAFs (MFC and MEC) and CAFs (MES).

Unfortunately, not all microorganisms are suitable for a deployment in MFCs since an efficient connection of cellular metabolism to an anode as electron acceptor is vital. Required mechanisms for the transport of respiratory electrons to the cell surface and further on to an anode have been intensively studied in exoelectrogenic bacteria like *Shewanella* or *Geobacter* (Flynn et al. 2010; Bursac et al. 2017; Förster et al. 2017).

Since this work is focusing on the production of platform chemicals and the generation of electricity using pure *S. oneidensis* cultures, only MFCs are relevant in the following.

1.3   Platform chemicals – Itaconic acid

As already mentioned at the beginning of this chapter, the development of processes for the environmentally friendly and sustainable production of chemical compounds has gained momentum in recent years. This is because of an increasing awareness that it is about time to replace petro-chemical processes that, more often than not, require high pressures and high temperatures combined with pollutant components such as toxic solvents. Furthermore, the demand for biodegradable end products is strongly increasing in times of (micro-)plastic debates. Besides the mere scientific and technological challenges of developing new processes, they also have to be economically and quantitatively competitive with already established processes and the obtained products must have at least the same quality as the current ones. Therefore, several studies aimed at identifying the most promising chemicals that could be produced via biotechnological processes. One of the most quoted publications in this regard is a study of the U.S. Department of Energy, which identified the top value added chemicals from biomass. Itaconic acid (IA) was among the top 12 value-added compounds based on sugar or synthesis gas (Werpy et al. 2004). This unsaturated C5 dicarboxylic acid is also called methylene succinic acid or 2-methylidenebutanedioic acid.

Itaconic acid is currently used as platform chemical in various application fields such as chemical and pharmaceutical industry. Today, round about 50% of the worldwide IA production is used as polymer stabilizer in the production of latex. In emulsion paints, the addition of IA is beneficial for the paint's adhesion (da Cruz et al. 2018).

Additionally, itaconic acid has potential for replacing maleic anhydride and sodium tripolyphosphate, which are used for the production of unsaturated polyester resin and detergent builder, respectively (Weastra s.r.o. 2012).

Water treatment technologies make use of IA to bind heavy metals and other pollutants (El-Halah et al. 2019). The pharmaceutical industry takes advantage of different properties of itaconic acid. While its hardening characteristic is used for contact lenses or dental glass ionomer cement, it serves as absorbent in diapers and sanitary napkins (Okabe et al. 2009). Also, the antiseptic property allows the utilization for purposes of wound healing and the prevention of bacterial contamination (Tomić et al. 2010).

Besides the development of new applications, the future potential for an broadened commercial use of itaconic acid lies in a substitution of other – petroleum-based – chemicals in established or new processes (Willke and Vorlop 2001; Robert and Friebel 2016). Some processes like the IA-based production of methyl methacrylate (MMA) or methacrylic acid (MAA) were already tried and tested but necessitate lower IA prices in order to be profitable (Weastra s.r.o. 2012). MAA, for example, can be derived from IA via decarboxylation (Carlsson et al. 1994). Both, MAA and MMA, are important monomers for the plastics industry (Bauer, Jr. 2000).

Wilke and Vorlop gave an overview of the different processes that were used throughout the history of itaconic acid production and stated that none of the so far proposed chemical synthesis processes is able to compete with the biotechnological production via fermentation by fungi (Willke and Vorlop 2001). Kinoshita discovered in 1932 for the first time that itaconic acid can be produced biologically by a fungus which then was called *Aspergillus itaconicus* (Kinoshita 1932). Several years later, Calam et al. reported that *Aspergillus terreus* is able to produce IA with an even higher productivity than *A. itaconicus* (Calam et al. 1939). Today's IA production is almost completely realized via fermentation with *A. terreus* based on glucose as substrate (Okabe et al. 2009).

Figure 5 depicts the glucose-based biosynthesis pathway of itaconic acid in *A. terreus*. After entering the cytosol, the glucose is converted via glycolysis to pyruvate. Part of the formed pyruvate is transported into the mitochondrion and part of it is metabolized together with CO_2 to oxaloacetate in the cytosol. Subsequently, the oxaloacetate is transformed to malate, which also can enter into the mitochondrion and forms part of the TCA cycle. Inside the

mitochondrion, pyruvate is converted to acetyl-CoA releasing a CO_2 molecule. Acetyl-CoA is then metabolized to citrate and, thereby, enters the TCA cycle. The next step of the TCA cycle is the formation of *cis*-aconitate, which can be transported back into the cytosol, where it is transformed into itaconate via CadA. Finally, the itaconate is transported to the cell surface as itaconic acid (Bentley and Thiessen 1957a).

Figure 5: Biosynthesis of itaconic acid in *Aspergillus terreus* based on glucose via glycolysis and TCA cycle.

The yearly worldwide production is around 40,000 tons and there are different predictions of the future development. While a "business as usual" development is predicted to lead to an annual production of 52,000 tons in 2025, major breakthroughs in production processes and application fields might as well result in a demand of 170,000 tons per year (Carvalho et al. 2018).

Even though there has been a noticeable price reduction in the recent years from 4,000 US$ / ton in 2001 (Willke and Vorlop 2001), over 2,000 US$ / ton in 2009 (Okabe et al. 2009) to a current trading price of 1,650 US$ / ton (Carvalho et al. 2018), a further significant price reduction is necessary to make itaconic acid more competitive with similar compounds. Werpy et al. estimated a competitive price of 500 US$ / ton (Werpy et al. 2004), whereas other authors state that IA already is cost-competitive with acrylic acid and only moderate price reductions are required to compete with other chemicals such as maleic anhydrate or fumaric acid (Carvalho et al. 2018).

Using new, cheaper substrates or reducing other process costs is one way to decrease production costs of itaconic acid. In the last decades, a great number of researchers worked in another direction and investigated the improvement of *A. terreus'* productivity or the utilization of other microorganisms for the itaconic acid production in the hope that these might allow higher yields or cheaper processes.

The first attempt to increase *A. terreus'* productivity was made by studying various wild type strains in order to identify the strain with the highest itaconic acid productivity (Batti and Schweiger 1963). In the 1990's Yahiro et al. developed a mutant strain of *A. terreus* via mutagenesis, which showed a higher IA productivity (Yahiro et al. 1995). No further strain improvements that led to a more efficient, industrial applicable *A. terreus* strain were reported in the reviewed literature. The reviews of Kuenz and Krull and da Cruz et al. give an overview of different strains for the production of itaconic acid and their yield, IA concentration and productivity or process time (da Cruz et al. 2017; Kuenz and Krull 2018).

In order to use genetic engineering for improving *A. terreus* or enabling other organisms to produce itaconic acid, it is necessary to understand which genes are pivotal for the formation of IA. Studies of Bentley and Thiessen (Bentley and Thiessen 1957a, 1957b, 1957c) as well as Bonnarme et al. (Bonnarme et al. 1995) suggested that the key protein for the IA production is *cis*-aconitate decarboxylase (CAD). This assumption was confirmed by Dwiarti et al. (Dwiarti et al. 2002) and, in 2008, the gene *cad1* encoding CAD was cloned successfully

for the first time in the yeast *Saccharomyces cerevisiae* (Kanamasa et al. 2008). Later, *cad1* was called *cadA* to be conform with the nomenclature guidelines of *Aspergillus* (Steiger et al. 2013). CadA is localized in the cytosol (Jaklitsch et al. 1991) and catalyzes the conversion of *cis*-aconitate to itaconate (Bentley and Thiessen 1955).

Afterwards, several researchers inserted the gene *cadA* in other organisms like *Aspergillus niger*, *Ustilago maydis*, *Candida sp., Corynebacterium glutamicum* and *E. coli* in order to produce itaconic acid (van der Straat et al. 2014; Geiser et al. 2016; Vuoristo et al. 2015a; Okamoto et al. 2015; Otten et al. 2015).

Due to itaconic acid's potential to substitute petro-based chemicals such as acrylic acid, maleic anhydrate and fumaric acid (Carvalho et al. 2018) and the necessity to develop new processes to reduce the production costs of IA, this research is focused on the development of a new metabolic pathway in the microorganism *S. oneidensis* that could potentially be used on industrial scale in the future.

1.4 Goal of this work

The overall goal of this work is the application of *S. oneidensis* in MFCs in order to produce IA based on glucose in an efficient manner. Therefore, in this thesis fundamental research will be performed in three sub-projects: First of all, the electron transfer in *S. oneidensis* is supposed to be improved in order to accelerate the metabolism and to produce more electrical current in MFCs. This work is based on the hypothesis that a tailored composition of periplasmic cytochromes can lead to faster electron transfer chains. Hence, the genes for several periplasmic cytochromes will be replaced by copies of the *cctA* gene encoding STC.

Secondly, *S. oneidensis* will be enabled to metabolize glucose by completing the ED pathway. For this purpose, three strategies will be tested: the insertion of the glucose transporter GalP and the kinase GlK from *E. coli*, the knockout of the transcriptional repressor *nagR*, and the natural adaptation on glucose.

Finally, a new metabolic pathway for the production of itaconic acid will be designed and combined with the glucose consumption facilitator deemed best in the second sub-project. This approach is based on the hypothesis that the introduction of the *A. terreus* gene *cadA* can enable the production of IA in *S. oneidensis* and that the deletion of the genes *sucCD*, *pykA*, *aceA*, *ptA* and *ackA* can contribute to enhancing the production of IA by avoiding the formation of some by-products. The developed strains will be tested under oxic and anoxic conditions.

2. Material and methods

2.1 Primers, bacterial strains and plasmids

Table 1 summarizes the primers designed and used in this work, Table 2 the strains and Table 3 the plasmids.

Table 1: Primers used in this work.

No.	Primer	Sequence 5´→3´
1	500 up(*ccpA*)_for_ *S. oneidensis* MR-1	CGGCCAGTGCCAAGCTTGCATGCCTGCAGGCC TAAATAGGGATAGCGCC
2	500 up(*ccpA*)_rev_ *S. oneidensis* MR-1	GAAAAGCACACTTAATAGTTTTTTGCTCATCTGG TTTTCTCCCTTATTAACC
3	500 down(*ccpA*)_for_ *S. oneidensis* MR-1	CGTACTTCTGCGTCTGTTCTGAAGAAGTAAAGG TTAAACCTAAGAAGCATTTAGCATA
4	500 down(*ccpA*) _rev_ *S. oneidensis* MR-1	ATGATTACGAATTCGAGCTCGGTACCCGGGTTG ATGAACGCCGTGG
5	500 up(*nrfA*)_for_ *S. oneidensis* MR-1	CGGCCAGTGCCAAGCTTGCATGCCTGCAGGAC TCTTGGAGGGGTGTAGTG
6	500 up(*nrfA*)_rev_ *S. oneidensis* MR-1	CTCATCTCCGCGTTGC
7	500 down(*nrfA*)_for_ *S. oneidensis* MR-1	CGTACTTCTGCGTCTGTTCTGAAGAAGTAATCAT CCTTGAAGATGAGCTAACC
8	500 down(*nrfA*)_rev_ *S. oneidensis* MR-1	ATGATTACGAATTCGAGCTCGGTACCCGGGTTT CTGCCGCGTTATCG
9	500 up(*napA*)_for_ *S. oneidensis* MR-1	CGGCCAGTGCCAAGCTTGCATGCCTGCAGGCC CCATTCCTCCCTCTC
10	500 up(*napA*)_rev_ *S. oneidensis* MR-1	GAAAAGCACACTTAATAGTTTTTTGCTCATAGTG TTTCCTCACTCATTTTTTC
11	500 down(*napA*)_for_ *S. oneidensis* MR-1	CGTACTTCTGCGTCTGTTCTGAAGAAGTAAGCC TTCATTTGATAGCGATG
12	500 down(*napA*)_rev_ *S. oneidensis* MR-1	ATGATTACGAATTCGAGCTCGGTACCCGGGCCT TTAAAGTTCAGGCAATTTTTC
13	500 up(*napB*)_for_ *S. oneidensis* MR-1	CGGCCAGTGCCAAGCTTGCATGCCTGCAGGCC CCTGCTCACGGG
14	500 up(*napB*)_rev_ *S. oneidensis* MR-1	TGGTCATTCTCCGCCTTG
15	500 down(*napB*)_for_ *S. oneidensis* MR-1	CGTACTTCTGCGTCTGTTCTGAAGAAGTAAACC ACACTTCCCTGCAC

16	500 down(*napB*)_rev_ *S. oneidensis* MR-1	ATGATTACGAATTCGAGCTCGGTACCCGGGTTT TTGGGCGGCAC
17	500 up(*fccA*)_for_ *S. oneidensis* MR-1	CGGCCAGTGCCAAGCTTGCATGCCTGCAGGAG ACTTAACCCCTCAACACCAC
18	500 up(*fccA*)_rev_ *S. oneidensis* MR-1	AGTTGTTCCTCCGCCGTACAT
19	500 down(*fccA*)_for_ *S. oneidensis* MR-1	CGTACTTCTGCGTCTGTTCTGAAGAAGTAATATC AATAGGTTCTAGGTTAA
20	500 down (*fccA*)_rev_ *S. oneidensis* MR-1	CATGATTACGAATTCGAGCTCGGTACCCGGGCG ACTAAGTCGACA
21	*cctA*_for_ *S. oneidensis* MR-1	ATGAGCAAAAAACTATTAAGTG
22	*cctA*_rev_ *S. oneidensis* MR-1	TTACTTCTTCAGAACAGACG
23	*cctA*_for (overlap_*fccA*)_ *S. oneidensis MR-1*	GTAGATGAAATGTACGGCGGAGGAACAACTATG AGCAAAAAACTATTAAG
24	*cctA*_for (overlap_*nrfA*)_ *S. oneidensis* MR-1	TTTACAACAAAAATGCAACGCGGAGATGAGATG AGCAAAAAACTATTAAG
25	*cctA*_for (overlap_*napB*)_ *S. oneidensis* MR-1	ACACATTGCCCCCAAGGCGGAGAATGACCAATG AGCAAAAAACTATTAAG
26	*pMQ150*_for	CGGCCAGTGCCAAG
27	*pMQ150*_rev	CATGATTACGAATTCGAGCTC
28	Δ*ccpA*_for_ *S. oneidensis* MR-1	CGGCAGAAAAACAGTCC
29	Δ*ccpA*_rev_ *S. oneidensis* MR-1	GTAAATACCAAGGCGCAA
30	Δ*nrfA*_for_ *S. oneidensis* MR-1	GTAGTACTTCATCACCAGCCA
31	Δ*nrfA*_rev_ *S. oneidensis* MR-1	GCCAGACGAACCCTTCT
32	Δ*napA*_for_ *S. oneidensis* MR-1	GGTATGACCATTTCTGCG
33	Δ*napA*_rev_ *S. oneidensis* MR-1	GTGATGATCGCTATGCTG
34	Δ*napB*_for_ *S. oneidensis* MR-1	AGAATGACCAATGAGCAAAAAC
35	Δ*napB*_rev_ *S. oneidensis* MR-1	CGCTTATCTTTCATTTCGTC

36	Δ*fccA*_for_ *S. oneidensis* MR-1	GAAATCTGCTGCCCAGACA
37	Δ*fccA*_rev_ *S. oneidensis* MR-1	GCATGCCTAAACGTTTAGC
38	500 up(*sucCD*)_for_ *S. oneidensis* MR-1	CGGCCAGTGCCAAGCTTGCATGCCTGCAGGAA TGATCTTTGGTGCTTTCACAG
39	500 up(*sucCD*)_rev_ *S. oneidensis* MR-1	ACTGCGGCTGACAAATTTGGATTTGATTAGAAGT ATATGGATAGATCATC
40	500 down(*sucCD*)_for_ *S. oneidensis* MR-1	TTCTAGTGCCGCAAATTTGTCAGCCGCAGTGAT GATCTATCCATATACTTCTAATCAAATCC
41	500 down(*sucCD*)_rev_ *S. oneidensis* MR-1	CATGATTACGAATTCGAGCTCGGTACCCGGGTG GTAACGCCAGTGCTACG
42	500 up(*pykA*)_for_ *S. oneidensis* MR-1	CGGCCAGTGCCAAGCTTGCATGCCTGCAGGCT AGAGCAGGGCACAATTAGTAAC
43	500 up(*pykA*)_rev_ *S. oneidensis* MR-1	TCTTGACTGTTCGGTTTTAG
44	500 down(*pykA*)_for_ *S. oneidensis* MR-1	TAGATTAACGCTAAAACCGAACAGTCAAGAAAG ATACTCCGTTAAAGTTAAAAAAATC
45	500 down(*pykA*)_rev_ *S. oneidensis* MR-1	CATGATTACGAATTCGAGCTCGGTACCCGGGTG GTATTAATTTCCCACACTG
46	500 up(*aceA*)_for_ *S. oneidensis* MR-1	CGGCCAGTGCCAAGCTTGCATGCCTGCAGGAC AAACATCAAAGGTATAATACCAATC
47	500 up(*aceA*)_rev_ *S. oneidensis* MR-1	GCCAACCATGTTGTTGTTTTAC
48	500 down(*aceA*)_for_ *S. oneidensis* MR-1	ATCTCACGGGTAAAACAACAACATGGTTGGCAG TGTCACTCCTTTCTGTGTGG
49	500 down(*aceA*)_rev_ *S. oneidensis* MR-1	CATGATTACGAATTCGAGCTCGGTACCCGGGAC CGAGCAAGGCATGCG
50	*glK*_for (overlap pBAD202)_ *E. coli*	GTTTAACTTTAAGAAGGAGATATACATACCATGA CAAAGTATGCATTAGTCG
51	*glK*_rev_*E. coli*	TTACAGAATGTGACCTAAGGTCTG
52	*galP*_for (overlap glK)_*E. coli*	TTACGCCAGACCTTAGGTCACATTCTGTAAGGA GGGCATCATGCC
53	*galP*_rev (overlap pBAD202)_ *E. coli*	CCGCCAAAACAGCCAAGCTGGAGACCGTTTTTA ATCGTGAGCGCCTATTTC
54	*galP*_rev_*E. coli*	TTAATCGTGAGCGCCTATTTC
55	*cadA*_for_*A. terreus*	AAACTGCGCGAAATAGGCGCTCACGATTAAGAA TTCAGGAGGACAGCTATGACCAAACAGAGCGCA G

56	*cadA*_rev (overlap *pBAD202*) _*A. terreus*	CCGCCAAAACAGCCAAGCTGGAGACCGTTTTTA AACCAGCGGGCTTTTC
57	*cadA*_rev_short_*A. terreus*	TTAAACCAGCGGGCTTTTC
58	Δ*sucCD*_for_ *S. oneidensis* MR-1	CACAATGTCAGCTCGGTCTAG
59	Δ*sucCD*_rev_ *S. oneidensis* MR-1	ACGATATCGTTTACCACAACTAC
60	Δ*pykA*_for_ *S. oneidensis* MR-1	GTATGCCTGTAAAGAGATTTAC
61	Δ*pykA*_rev_ *S. oneidensis* MR-1	TGTATCAACAGCAATGAAGG
62	Δ*aceA*_for_ *S. oneidensis* MR-1	CACAGCATTATTTAGGCCAAGAC
63	Δ*aceA*_rev_ *S. oneidensis* MR-1	CTCCGATTTTAGCCGCTGA
64	Δ*ptA*_for_*S. oneidensis* MR-1	GCTTGGCTTTTTCGACATCGC
65	Δ*ackA*_rev_ *S. oneidensis* MR-1	CTATTTTTAAGATGAGCGCCATATC
66	*pBAD202*_for	GATTAGCGGATCCTACCTGAC
67	*pBAD202*_rev	CTCTCATCCGCCAAAACAG

Regions of 500 bp up- and downstream of the genes *ccpA* (primers 1 to 4), *nrfA* (primers 5 to 8), *napA* (primers 9-12), *napB* (primers 13 to 16), *fccA* (primers 17 to 20), *sucCD* (primers 38 to 41), *pykA* (primers 42 to 45) and *aceA* (primers 46 to 49) were amplified via PCR. *CctA* was amplified using primers 21 to 25.

The resulting up- and downstream regions of the genes *nrfA*, *ccpA*, *napA*, *napB* and *fccA* and the amplified *cctA* gene were inserted into the BamHI and SalI cleaved suicide vector *pMQ150* by isothermal *in vitro* assembly (Gibson et al. 2009) and transformed into *E. coli* WM3064 (Saltikov and Newman 2003).

Afterwards, the integration of copies of the *cctA* gene into the *S. oneidensis* MR-1 genome and the corresponding deletions of the genes *ccpA, nrfA, napA, napB* and *fccA* were achieved as described previously (Saltikov and Newman 2003). The same procedure was carried out for the deletion of the genes *sucCD*, *pykA* and *aceA*, *pta* and *ackA*.

The genes *glK* and *galP* from *E. coli* and *cadA* from *A. terreus* were amplified using the primers 50 to 54 and 57. The fusion of *glK* and *galP* was achieved using the primers 50, 53 and 56. The additional fusion of *cadA* to the fragment *glk_galP* was performed using the primers 50 and 56. The resulting fragments were inserted into the NcoI and PmeI cleaved vector *pBAD202* by isothermal *in vitro* assembly (Gibson et al. 2009), regulated under the arabinose promoter and transformed into *E. coli* WM3064 (Saltikov and Newman 2003).

The primers 26-37 and 58-67 were used to check if the insertions or deletions were successful and to detect unintended mutations.

Table 2: Bacterial strains used in this study.

No.	Strain	Reference
1	*S. oneidensis* MR-1	Venkateswaran et al. 1999
2	*S. oneidensis ΔnrfA::cctA*	This study
3	*S. oneidensis ΔnrfA::cctA_ΔccpA::cctA*	This study
4	*S. oneidensis ΔnrfA::cctA_ΔccpA::cctA_ΔnapA::cctA*	This study
5	*S. oneidensis ΔnrfA::cctA_ΔccpA::cctA_ΔnapA::cctA_ΔnapB::cctA*	This study
6	*S. oneidensis ΔnrfA::cctA_ΔccpA::cctA_ΔnapA::cctA_ΔnapB::cctA _ΔfccA::cctA*	This study
7	*S. oneidensis glk_galP_pBAD202*	This study
8	*S. oneidensis ΔnrfA::cctA_ΔccpA::cctA_ΔnapA::cctA_ΔnapB::cctA _glk_galP_pBAD202*	This study
9	*S. oneidensis ΔnagR*	This study
10	*S. oneidensis glK_galP_cadA_pBAD202*	This study
11	*S. oneidensis ΔsucCD*	This study
12	*S. oneidensis ΔsucCD_ΔpykA*	This study
13	*S. oneidensis ΔsucCD_ΔpykA_ΔaceA*	This study
14	*S. oneidensis ΔsucCD_ΔpykA_ΔaceA_ΔptA_ΔackA*	This study
15	*S. oneidensis ΔsucCD_ΔpykA_ΔaceA_glk_galP_cadA_pBAD202*	This study
16	*S. oneidensis ΔsucCD_ΔpykA_ΔaceA_ΔptA_ΔackA_glk_galP_ cadA_pBAD202*	This study
17	*E. coli pMQ150*	Shanks et al. 2006

18	*E. coli* WM3064	Saltikov and Newman 2003
19	*E. coli* WM3064_up(ccpA)_cctA_down(ccpA)_pMQ150	This study
20	*E. coli* WM3064_up(nrfA)_cctA_down(nrfA)_pMQ150	This study
21	*E. coli* WM3064_up(napA)_cctA_down(napA)_pMQ150	This study
22	*E. coli* WM3064_up(napB)_cctA_down(napB)_pMQ150	This study
23	*E. coli* WM3064_up(fccA)_cctA_down(fccA)_pMQ150	This study
24	*E. coli_pBAD202*	Invitrogen
25	*E. coli_glk_galP_pBAD202*	This study
26	*E. coli_up(nagR)_down(nagR)_pMQ150*	This study
27	*E. coli* WM3064_up(sucCD)_down(sucCD)_pMQ150	This study
28	*E. coli* WM3064_up(pykA)_down(pykA)_pMQ150	This study
29	*E. coli* WM3064_up(aceA)_down(aceA)_pMQ150	This study
30	*E. coli* WM3064_down(ackA)_up(ptA)_pMQ150	Bursac et al. 2017
31	*E. coli* WM3064_glK_galP_pBAD202	This study
32	*E. coli* S116_cad1_pASK43	JG Laboratory
33	*E. coli* WM3064_glK_galP_cadA_pBAD202	This study

Table 3: Plasmids used in this study.

No.	Name	Relevant genotype	Reference
1	*pMQ150*	Km^R, r6k, *ura*3, *sacB*	Shanks et al. 2006
2	*pBAD202*	Km^R, P_{ara}	Invitrogen
3	*up(nrfA)_cctA_down(nrfA)_pMQ150*	Km^R, r6k, *ura*3, *sacB*	This study
4	*up(ccpA)_cctA_down(ccpA)_pMQ150*	Km^R, r6k, *ura*3, *sacB*	This study
5	*up(napA)_cctA_down(napA)_pMQ150*	Km^R, r6k, *ura*3, *sacB*	This study
6	*up(napB)_cctA_down(napB)_pMQ150*	Km^R, r6k, *ura*3, *sacB*	This study
7	*up(fccA)_cctA_down(fccA)_pMQ150*	Km^R, r6k, *ura*3, *sacB*	This study
8	*up(sucCD)_down(sucCD)_pMQ150*	Km^R, r6k, *ura*3, *sacB*	This study
9	*up(pykA)_down(pykA)_pMQ150*	Km^R, r6k, *ura*3, *sacB*	This study
10	*up(aceA)_down(aceA)_pMQ150*	Km^R, r6k, *ura*3, *sacB*	This study

11	*down(ackA)_up(ptA)_pMQ150*	Km^R, r6k, *ura*3, *sacB*	Bursac et al. 2017
12	*glK_galP_pBAD202*	Km^R, P$_{ara}$	This study
13	*up(nagR)_down(nagR)_pMQ150*	Km^R, r6k, *ura*3, *sacB*	This study
14	*cad1_pASK43*	Amp	JG Laboratory
15	*glK_galP_cadA_pBAD202*	Km^R, P$_{ara}$	This study

2.2 Chemicals, enzymes and kits

Chemicals and biochemicals were obtained from the companies Sigma Aldrich (Munich, Germany), Carl Roth (Karlsruhe, Germany) and Promega (Mannheim, Germany). Enzymes were purchased from New England Biolabs (Frankfurt am Main, Germany), AppliChem (Darmstadt, Germany), Merk (Darmstadt, Germany) and Thermo Fisher Scientific (Waltham, USA). The nitrogen gas bottles were obtained from basi Schöberl GmbH & Co.KG (Rastatt, Germany).

2.3 Bacterial strain preservation and growth conditions

For strain preservation, overnight cultures (OD> 1.5) were supplemented with 10% (v/v) glycerol, frozen in cryotubes using liquid nitrogen and stored at -80°C.

Frozen strains were cultivated on LB agar plates before inoculation in liquid medium.

Depending on the experiment, bacterial cultures were grown under oxic conditions in LB broth overnight at 37°C for *E. coli* strains and at 30°C for *S. oneidensis* strains. For other experiments, minimal medium (Table 10) was used under oxic and anoxic conditions. All aerobic cultures were shaken in the incubator at 180 rpm.

If required, the autoclaved solid or liquid medium was supplemented with antibiotics (100 µg ml^{-1} ampicillin or 50 µg ml^{-1} kanamycin), 0.3 mM 2,3-diaminopimelinic acid (DAP), 10% sucrose, 50 mM glucose, 1 mM arabinose or a combination of these components.

2.4   Media

All media were prepared with de-ionized water, stirred during pH adjustment and autoclaved afterwards. Heat-labile components were supplemented sterilely via filtration (Ø= 0.2 µm) (Sarstedt, Nümbrecht, Germany).

Table 4: Composition of LB medium.

Component	Amount/liter [g/l]
Tryptone extract	10
Yeast extract	5
NaCl	5
pH value= 7.4	

Table 5: Composition of SOB medium.

Component	Amount/liter [g/l]
Trypton extract	20.00
Yeast extract	5.00
NaCl	0.58
KCl	0.19
pH value= 7.4	

Table 6: Composition of SOC medium; no additional H_2O was added.

Component	Amount
$MgCl_2$ solution (1 M)	1.9 g
Glucose solution (2 M)	3.6 g
SOB medium (Table 5)	Up to 1.0 l total volume
pH value= 7.4	

Table 7: Composition of 2% LB agar medium for plates.

Component	Amount/liter [g/l]
Tryptone extract	10
Yeast extract	5
NaCl	5
Agar	20
pH value= 7.4	

Table 8: Composition of the 100-fold trace element solution.

Component	Amount/liter [mg/l]	End concentration [µM]
$CoCl_2$	64.9	5.0
$CuSO_4 \cdot 5H_2O$	5.0	0.2
$Fe(II)Cl_2 \cdot 4H_2O$	107.4	5.4
H_3BO_3	350.0	56.6
$MnSO_4 \cdot H_2O$	22.0	1.3
Na_2EDTA	2,501.5	67.2
$Na_2MoO_4 \cdot 2H_2O$	94.4	3.9
$Na_2SeO_4 \cdot 6H_2O$	39.5	1.5
NaCl	58.4	10.0
$NiCl_2 \cdot 6H_2O$	118.9	5.0
$ZnSO_4 \cdot 7H_2O$	28.8	1.0
pH value= 7.0		

Table 9: Composition of 10-fold minimal medium salts (M4 [10x]).

Component	Amount/liter [g/l]	End concentration [mM]
K_2HPO_4	2.21	12.69
KH_2PO_4	0.99	7.27
HEPES	14.07	50.00
$NaHCO_3$	1.68	20.00
$(NH_4)_2SO_4$	11.89	89.98
NaCl	87.70	1,500.68
pH value= 7.4		

Table 10: Composition of minimal medium for anoxic experiments (M4 medium).

Component	Amount/liter	End concentration [mM]
M4 [10x]	100.00 ml	See Table 9
Trace element solution [100x]	10.00 ml	See Table 8
$MgSO_4 \cdot 7H_2O$ solution [1 M]	1.00 ml	1.00
$CaCl_2 \cdot 2H_2O$ solution [0.1 M]	1.00 ml	0.10
Na-D,L-lactate 50% (w/w) or glucose	11.20 g 9.91 g	50.00 50.00
Casamino acids	1.00 g	0.10% (w/v)

In order to prepare minimal medium using Fe(III)-citrate as electron donor, Fe(III)-citrate was added to 300 ml de-ionized water and boiled in the microwave until it dissolved completely. After cooling to room temperature, the pH was slowly adjusted to pH 6 with 1 M NaOH and the other components (Table 11) were added. Afterwards, dH_2O was added until 900 ml total solution volume, then the pH was adjusted to 7.4 and, finally, dH_2O was added until reaching 1 l total solution volume.

The final Fe(III)-citrate concentration in the medium was 50 mM for growth experiments and 100 mM for adaptation experiments. Oxygen was removed

from the medium (Table 11) by cycles of nitrogen purging and subsequent vacuum application (20 cycles, overall duration 45 min).

Table 11: Composition of minimal medium using Fe(III)-citrate as electron acceptor.

Component	Amount/liter	End concentration [mM]
Fe(III)-citrate	12.25 g or 24.50 g	50.00 or 100.00
M4 [10x]	100.00 ml	See Table 9
Trace element solution [100x]	10.00 ml	See Table 8
$MgSO_4$ $7H_2O$ solution [1 M]	1.00 ml	1.00
$CaCl_2$ $2H_2O$ solution [0.1 M]	1.00 ml	0.10
Na-D,L-lactate 50% (w/w) or glucose	11.20 g 9.91 g	50.00 50.00
Casamino acids	1.00 g	0.10% (w/v)
pH= 7.4 adjusted with 1 M NaOH		

For the minimal medium used for bioelectrochemical experiments (Table 12), at first the oxygen was removed from the medium and then it was autoclaved. During the entire experiment the reactors were stirred with a magnetic stirrer and kept anoxic by purging with nitrogen gas.

Table 12: Minimal medium composition for bioelectrochemical experiments.

Component	Amount/liter	End concentration [mM]
M4 medium [10x]	100.00 ml	Table 9
Trace element solution [100x]	10.00 ml	Table 8
$MgSO_4$ solution [1 M]	1.00 ml	1.00
$CaCl_2$ solution [0.1 M]	1.00 ml	0.10
Na-D,L-lactate 50% (w/w) or glucose	11.21 g 9.91 g	50.00 50.00
Casamino acids	1.00 g	0.10% (w/v)
pH= 7.4		

For experiments using fumarate as electron acceptor, the oxygen was removed from the minimal medium (Table 13) as described above.

Table 13: Composition of minimal medium using fumarate as electron acceptor.

Component	Amount/liter	End concentration [mM]
M4 medium [10x]	100.00 ml	Table 9
Trace element solution [100x]	10.00 ml	Table 8
$MgSO_4$ solution [1 M]	1.00 ml	1.00
$CaCl_2$ solution [0.1 M]	1.00 ml	0.10
Na-D,L-lactate 50% (w/w)	11.21 g	50.00
Fumaric acid	5.80 g	50.00
Casamino acids	1.00 g	0.10% (w/v)
pH= 7.4		

Table 14: Composition of minimal medium wash buffer.

Component	Amount/liter	End concentration [mM]
M4 [10X]	100.0 ml	Table 9
Trace elements [100x]	10.0 ml	Table 8
$MgSO_4$ solution [1 M]	1.0 ml	1.0
$CaCl_2$ solution [0.1 M]	1.0 ml	0.1
pH= 7.4		

2.5   Molecular biological methods

2.5.1   DNA extraction

2.5.1.1 Plasmid isolation

5-10 ml of the overnight culture were harvested, centrifuged at 16,000 rpm (Eppendorf, Hamburg, Germany) and isolated using the kit "Wizard® Plus SV Minipreps DNA purification system" according to the manufactures suggestions (Promega, Mannheim, Germany). Afterwards, the DNA was stored at -20ºC.

2.5.1.2 Genomic DNA extraction

The genomic DNA of *S. oneidensis* was extracted following the Marmur method (Marmur 1961) and, afterwards, used to amplify the studied genes as well as the up- and downstream regions of genes that were deleted. Table 15 summarizes the components used for the DNA extraction.

Table 15: Components for the extraction of *S. oneidensis* MR-1 DNA.

Solution	Composition
Tris-EDTA (TE) resuspension buffer	10 mM Tris/HCl pH= 8 1 mM NaEDTA
Lysis solution	10% SDS
Proteinase K solution	20 mg·ml^{-1} Proteinase K in TE buffer (pH= 8)
NaCl solution	5 M NaCl
CTAB / NaCl solution	10% (w/v) CTAB (cetyl trimetylammonium bromide) 0.7 M NaCl
Chloroform / isoamylalcohol	100 ml 24:1 (v/v) $CHCl_3$:$C_5H_{12}O$
Isopropanol	400 µl
EtOH solution	70% (v/v) CH_3CH_2OH/H_2O
Tris-EDTA (TE) buffer	1 mM Tris/HCl pH= 8 1 mM NaEDTA

10 mg cells were resuspended in 570 µl TE buffer. 30 µl lysis solution and 3 µl proteinase K solution (20 mg ml^{-1}) were added. This mixture was shaken and incubated at 52°C for 1 h.

Afterwards, 100 µl of 5 M NaCl solution were added to increase the salt concentration at room temperature. Then, 80 µl CTAB were added and the mixture was shaken and incubated at 65°C for 10 min. The addition of NaCl facilitates the precipitation of the CTAB-nucleic acid, which is a cationic surfactant that solubilizes the cell wall.

In the next step, the addition of 780 µl chloroform / isoamylalcohol led to the emulsification of the CTAB complex into the organic phase. After that, the mixture was centrifuged at 16,000 rpm for 5 min for an optimal separation of aqueous and organic phase, which resulted in the precipitation of the CTAB complex between both phases. This step was repeated with the aqueous phase.

Subsequently, 400 µl isopropanol were added to precipitate the DNA. After tapping the mixture gently, the DNA precipitated immediately. Then, the mixture was centrifuged at 16,000 rpm for 5 min. The liquid was extracted carefully and the pellet was washed twice with 200 µl EtOH to dissolve the salts allowing for their elimination and improving the DNA purification. Afterwards, it was centrifuged at 16,000 rpm for 5 min and EtOH was carefully extracted. The EtOH rest was evaporated at room temperature. Finally, the DNA was resuspended in 100 µl TE buffer and stored at 4°C.

2.5.2 Polymerase chain reaction

The polymerase chain reaction (PCR) method was utilized for the *in vitro* amplification of DNA fragments from genomic DNA or plasmids. A thermal cycler (C1000^{TM}, S1000, Bio-Rad, Munich, Germany) was used to carry out the reactions. Each PCR assay requires the presence of template DNA, primers, nucleotides and DNA polymerase, whereby the primers need to be specific for each target sequence. Table 1 comprises all primers used in this study.

IProof™ high fidelity DNA polymerase (BIO-RAD laboratories, Munich, Germany) or the PCRBIO HiFi polymerase (PCR Biosystems London, England) were used to perform PCRs and the Gibson reaction. The preparations of the reactions are described in Table 16 and Table 18. While iProof™ is a pure polymerase, HiFi polymerase is a solution that already contains dNTPs and DMSO.

For the analytic detection of PCR products and estimation of product size, the MangoMix™ (bioline, Luckenwalde, Germany) reaction mix was used. This 2-fold reaction mix is composed of MangoTaq™ DNA polymerase, $MgCl_2$ and dNTPs. For the preparation of the PCR solution, the primers and the MangoMix™ solution were diluted in a ratio of 2:1. See Table 20 for the concentration of the primers.

Table 16: Components of the preparative PCR phusion using the iProof™ polymerase.

Component	Volume [µl]
5x iProof™ buffer	10.0
iProof™ DNA polymerase [2 U µl^{-1}]	0.5
dNTPs [10 mM]	1.0
DMSO	1.5
Primer forward [2 µM]	12.5
Primer reverse [2 µM]	12.5
DNA template: <500 ng gDNA or <100 ng cDNA	Pick colony or µl template
ddH$_2$O	Up to 50 µl final volume

Table 17: PCR program of the preparative PCR using the iProof™ polymerase.

Phase	Temperature [°C]	Duration [min]
Initial denaturation	98	2:30
Denaturation	98	0:10
Annealing of primer	T_m*	0:30
Elongation	72	0:30 / kb**
Final elongation	72	10:00
End	12	∞

T_m* = Annealing temperature of primer, specific for each primer

**The iProof™ polymerase achieves 1 kb per 30 s.

Table 18: Components of the preparative PCR using the HiFi polymerase.

Component	Volume [µl]
5x HiFi buffer	10.0
PCRBIO HiFi polymerase [2 U µl^{-1}]	0.5
Primer forward [10 µM]	2.0
Primer reverse [10 µM]	2.0
Template DNA: <500 ng gDNA or <100 ng cDNA	Pick colony or µl template
ddH$_2$O	Up to 50 µl final volume

Table 19: PCR program of the preparative PCR using the HiFi polymerase.

Phase	Temperature [°C]	Duration [min]
Initial denaturation	95	2:30
Denaturation	95	0:10 - 0:30
Annealing of primer	T_m*	0:30
Elongation	72	0:30 / kb**
Final elongation	72	10:00
End	12	∞

T_m* = annealing temperature of primer, specific for each primer

**The HiFi polymerase achieves 1 kb per 30 s.

Table 20: Components of the standard MangoMix™ PCR reaction.

Component	Volume [µl]
MangoMix™ solution	7.50
Primer forward [2 µM]	3.75
Primer reverse [2 µM]	3.75
Template DNA: <500 ng gDNA or <100 ng cDNA	Pick colony or µl template

Table 21: Standard MangoMix™ PCR cycler program.

Phase	Temperature [°C]	Duration [min]
Initial denaturation	95	2:20
Denaturation	95	0:10
Annealing of primer	T_m^*	0:30
Elongation	72	0:30 / kb**
Final elongation	72	10:00
End	12	∞

T_m^* = annealing temperature of primer, specific for each primer

**The MangoTaq™ polymerase achieves 1 kb per 30 s.

2.5.3 DNA purification

For the purification of DNA from PCR, restriction or ligation reactions, the kit "Wizard® SV Gel and PCR Clean-Up System" from Promega (Mannheim, Germany) was used according to the manufacturer's guidelines.

The DNA concentration was measured using the NanoDrop™ 2000 spectrophotometer (Thermo Scientific™, Waltham, USA). For the measurements, 1 µl DNase free water or medium was used for the blank depending on how the DNA was resuspended. After the blank, 1 µl of the sample was measured.

2.5.4 DNA sequencing

All plasmids and PCR products were sequenced by the company MWG Eurofins Genomics (Ebersberg, Germany).

2.5.5 Cloning methods

2.5.5.1 Restriction enzymes

The plasmid *pMQ150* was digested using the restriction enzymes SalI and BamHI and for the plasmid *pBAD202* PmeI and NcoI were used (NEB, Frankfurt am Main, Germany). 10-20 ml of an overnight culture were centrifuged at 16,000 rpm (Eppendorf 5418, Hamburg, Germany) and isolated. Afterwards, 20 µg of the plasmid were mixed softly with 1 µl of each corresponding enzyme, 5 µl of 10x CutSmart® buffer (NEB, Frankfurt am Main, Germany) and up to 50 µl final volume with ddH$_2$O. The reaction was incubated at 37ºC for 1 h 30 min and the linear vector was analyzed via gel electrophoresis. As a control, 10 µl of the plasmid without digestion were used. The fragments were excised and purified using the "Wizard® SV Gel and PCR Clean-Up System" from Promega (Mannheim, Germany).

2.5.5.2 Fusion of DNA fragments via PCR

The fusion of linear DNA fragments (with the respective overlap of each other) was conducted via PCR using the corresponding flanking primers.

Table 22: Standard reaction for fusion PCR using HiFi polymerase.

Component	Volume [µl]
5x HiFi buffer	10.0
Primer forward [2 µM]	12.5
Primer reverse [2 µM]	12.5
Fragment 1	Depending on the concentration
Fragment 2	(together max. 100 ng)
PCRBIO HiFi polymerase [2 U µl^{-1}]	1.0
ddH$_2$O	Up to 50 µl final volume

Table 23: Standard reaction for fusion PCR using iProof™ polymerase.

Component	Volume [µl]
5x iProof™ buffer	10.0
Primer forward [2 µM]	12.5
Primer reverse [2 µM]	12.5
Fragment 1	Depending on the concentration
Fragment 2	(together max. 100 ng)
iProof™ polymerase [2 U µl^{-1}]	1.0
dNTPs [10 mM]	1.0
DMSO	1.5
ddH$_2$O	Up to 50 µl final volume

2.5.5.3 Isothermal *in vitro* ligation using Gibson reaction

Gibson isothermal assembly is a method for assembling multiple DNA sequences in a single reaction volume. The reaction is composed of a T5 5´-3´-exonuclease, a DNA polymerase and a DNA ligase. First, the 5´-3´ exonuclease activity removes the 5´ end sequences and exposes the complementary sequence (3´-5´) for annealing at 50ºC, at which temperature the exonuclease is unstable and allows annealing. Then, the polymerase activity fills in the gaps at the annealed regions (3´-5´) and leaves the strand. Finally, the DNA ligase assembles the DNA fragments (in this work the vector with the DNA fragments) (Gibson et al. 2009).

Previous to this process, the DNA fragments were amplified using the respective primers for the necessary overlaps of 30-50 bp to a vector and other DNA fragments via PCR (Table 16 and Table 17 or Table 18 and Table 19). The fragments were then mixed with the vector in equimolar concentration. 5 µl were added to 15 µl reaction (Table 25), whereby the total DNA concentration must not exceed 100 ng, and incubated in a thermal cycler (C1000™ Biorad, Munich, Germany) for 1 h 30 min at 50ºC. Afterwards, the solution was dialyzed using a 0.025 µm nitrocellulose membrane (Merck Millipore, Darmstadt,

Germany) for 30 min to remove the salts and it was used for the transformation of competent cells.

Table 24: Composition of the 5x buffer for the *in vitro* ligation reaction.

Component	Concentration [mM]
TRIS-HCl [1 M] (pH= 7.5)	500
MgCl$_2$ 6H$_2$O [1 M]	50
dNTPs [10 mM]	1
DTT [1 M]	50
NAD$^+$ [100 mM]	5
PEG-8000 Da	25% (w/v)
ddH$_2$O	250 µl

Table 25: Master Mix for the *in vitro* ligation.

Component	Amount [µl]
Buffer (5x) see Table 24	80
Phusion polymerase [2.0 U µl^{-1}] or iProof™ polymerase [2.0 U µl^{-1}]	5
Tag DNA ligase [40.0 U µl^{-1}]	40
T5 exonuclease [0.1 U µl^{-1}]	16
ddH$_2$O	239

2.5.6 Transformation technique: Electroporation

The integration of the plasmids into the *E. coli* and *S. oneidensis* cells was performed via electroporation. To conduct the electroporation, 5 ml cells were grown in LB overnight (Table 4) and 1% preculture were introduced in 25 ml SOB medium (Table 5) and incubated for 2 to 4 h. The cells were centrifuged at 6,000 rpm (Eppendorf, Hamburg, Germany) for 10 min at room temperature, washed twice with ddH$_2$O to remove the salts and resuspended in 500 µl ddH$_2$O. 100 µl cells were added into the electroporation cuvette (Bio-Rad,

Munich, Germany) with 10 µl of the desired dialyzed plasmid and softly mixed. Then, the cells received an electric pulse (1.8 kV, 5 ms) with the MicroPulser (Bio-Rad, Munich, Germany) and 500 µl SOC (Table 6) were added immediately. The electric potential allows for the introduction of the plasmid into the cell through the pores and the SOC medium helps to restore the cell membrane. After this, the cells were incubated at 30ºC for *S. oneidensis* and 37ºC for *E. coli* for at least 1 h. As last step, the cells were plated on an LB agar medium plate containing an antibiotic and incubated overnight at 30 or 37ºC depending on the strain. If required, DAP was added to the SOC medium and the plates.

2.5.7 Conjugation

To delete or replace genes in the *S. oneidensis* genome, the conjugation method was applied. The suicide plasmid *pMQ150* was selected to transport the desired fragments 500 bp up- and 500 bp downstream and, in case of substitutions, the gene *cctA*. Via electroporation the plasmid was integrated in the strain *E. coli* WM3064, which is able to replicate the R6K-ORI and cannot grow without DAP.

Afterwards, *E. coli* WM3064 with the corresponding plasmid and *S. oneidensis* were grown separately in LB medium overnight. 1 ml of each culture was centrifuged at 8,000 ×g for 1 min at room temperature (J-26 XP Avanti centrifuge, Beckman Coulter, Indianapolis, USA) and washed two times with fresh LB medium. After this, the *E. coli* cells were resuspended into 500 µl of LB medium and, afterwards, the *Shewanella* cells were resuspended in the same medium.

Then, 250 µl were plated on a LB agar plate and incubated at 30ºC for 8 h. 1 ml of LB was poured on the plate to scrape off cells. 1:5, 1:25 and 1:125 dilutions of the resuspended culture were prepared and 100 µl of each dilution were plated on an LB agar plate supplemented with 25 µg ml^{-1} kanamycin and grown for 24 to 48 h. In this step, only *Shewanella* clones grow which have integrated the plasmid into the genome.

The clones were picked and patched on another 25 µg ml^{-1} kanamycin LB agar plate. Two selected clones were grown overnight and 1 ml of each one was washed twice, diluted in a ratio of 1:10 and incubated for 4 hours. After this, 1:100, 1:500 and 1:1000 dilutions were prepared and 100 µl of each dilution were plated on a 10% sucrose LB agar plate and incubated for a period of 24 to 48 h. The clones were picked and patched on a sucrose LB agar plate and on an LB agar plate supplemented with 25 µg ml^{-1} kanamycin. Clones not able to grow on kanamycin plates but on sucrose plates contain with a 50% probability the desired mutations. Potential candidates were tested for the deletions and insertions via PCR with the corresponding primers. The primers *pMQ150_*for and *pMQ150_*rev bind to the plasmid and were used as negative control.

2.5.8 Electrophoretic methods

Agarose gel electrophoresis

Electrophoresis was used to separate the DNA fragments (for example PCR reaction or restriction-digested plasmid) in an electric field from the anode to the cathode according to the size. For this, a 1% (w/v) agarose gel in TAE buffer (Table 26) was prepared by melting the agarose (Table 27) in the microwave and supplementing 0.1 µl ml^{-1} of Midori Green (Nippon genetics, Düren, Germany) to stain the DNA. To estimate the size of the bands, 10 µl of the 0.5 or 1 kb DNA ladder marker (0.5 µg µl^{-1}) (Thermo Fisher Scientific, Schwerte, Germany) was used and a 6x loading dye buffer (Table 28) (Thermo Fisher Scientific, Schwerte, Germany) was added to the samples not containing MangoMix™. The electrophoresis was performed putting the polymerized agarose gel into the PerfectBlue™ Mini S gel box (PEQLAB Biotechnologie GmbH, Erlangen, Germany), covering it with TAE buffer (Table 26), loading the samples into the wells, closing the gel box and connecting to the Bio-Rad's PowerPac™ HC (Munich, Germany) at a voltage of 120 V.

The analytic detection of PCR products and the estimation of their size were conducted under UV light in the GelDoc™ employing the software Image Lab 5.1 (Biorad, Munich, Germany).

PCR products that were going to be used in further cloning processes were visualized under LED light (FastGene B/G LED Transilluminator, FG-08, NIPPON Genetics EUROPE GmbH, Düren, Germany) to avoid DNA mutations. Afterwards, these products were cut and cleaned using the "Wizard® SV Gel and PCR Clean-Up System" (section 2.5.3).

Table 26: Composition of the TAE buffer.

Component	Amount/liter [g/l]	Concentration [mM]
Tris	4.85	40.00
EDTA	0.37	1.00
Na-acetate [20 mM] to adjust the pH to 8		

Table 27: Composition of 1% agarose gel.

Component	Amount
Agarose	0.6 g
TAE buffer (Table 26)	60.0 ml

Table 28: Composition of the 6x loading dye buffer.

Component	Amount in 28.5 ml
Xylene cyanol	0.05 g
Orange G	0.05 g
Glycerin	12.00 ml
TAE buffer [50x]	1.50 ml
ddH$_2$O	15.00 ml

2.6 Protein biochemical methods

2.6.1 Polyacrylamide gel electrophoresis (SDS-PAGE)

For the separation of the periplasmic proteins containing heme groups according to their size, a polyacrylamide gel electrophoresis (SDS-PAGE) was performed following the protocol of Laemmli (Laemmli 1970). The gel is composed of a stacking gel and a separating gel (see Table 31).

All samples were prepared with the same total concentration, mixed with the SDS electrophoresis protein loading buffer [1x] (Table 29) and heated in the Thermomixer® Compact (Eppendorf, Hamburg, Germany) at 95ºC for 1 min. Afterwards, the protein samples were loaded into the wells of the stacking gel, which was previously introduced in a buffer tank. At the beginning, the gel was run at 120 V for 10 min and, then, at 150 V for 30 to 45 min. To identify the size of the bands, the BlueStar prestained protein marker (Nippon, Düren, Germany) was utilized.

Table 29: Composition of the 6x SDS electrophoresis protein loading buffer.

Component	Amount [ml]
Glycerin [50%]	6.5
2 M TRIS / HCl (pH= 6.8)	1.5
20% (w/v) SDS stock	6.0
β-mercaptoethanol [15%]	3.0
0.5% (w/v) bromophenol blue	3.0

Table 30: Tris-glycine SDS running buffer.

Component	Amount/liter [g/l]
TRIS / HCl (pH= 8.8)	3.0
SDS	1.0
Glycine	14.4

Table 31: Composition of the SDS-PAGE gel.

Component	Amount
4% stacking gel	
30% (w/v) acrylamide / 0.8% (w/v) methylenbisacrylamide	825.00 µl
2 M TRIS-HCl, pH= 6.8 (buffer)	375.00 µl
20% (w/v) SDS stock	30.00 µl
TEMED (tetramethylethylendiamine)	7.50 µl
APS (ammonium persulfat) [100 mg ml^{-1}]	30.00 µl
ddH$_2$O	4.38 ml
10% separating gel (9 ml / gel, 375 mM TRIS, 0.1% SDS)	
30% (w/v) acrylamide / 0.8% (w/v) methylenbisacrylamide)	3.00 ml
2 M TRIS-HCl, pH= 8.8 (buffer)	2.25 ml
20% (w/v) SDS stock	45.00 µl
TEMED (tetramethylethylendiamin)	9.00 µl
APS (ammonium persulfat) [100 mg ml^{-1}]	45.00 µl
ddH$_2$O	3.70 ml

2.6.2 Heme staining

For the detection of the *c*-type cytochromes, a heme staining was performed and visualized by a heme-coupled peroxidase staining as described previously (Thomas et al. 1976).

After the bands were separated via vertical electrophoresis using the Mini-Protean Tetra System (Biorad, Munich, Germany), the gel was washed with dH$_2$O to remove the salts (electrophoresis buffer). Then, it was soaked with a solution of 12.5% (w/v) TCA (trichloroacetic acid) for 30 min to fix the proteins and limit the diffusion. Afterwards, the gel was washed with dH$_2$O to remove the SDS (SDS interferes with staining). 10 mg of TMB (3,3′,5,5′-Tetramethylbenzidine dihydrochloride hydrate) were diluted in 9 ml H$_2$O and

poured on the gel (TMB acts as electron donor giving the electrons to H_2O_2).
Right after this, 1 ml of a 0.5 M citric acid solution and 40 µl of H_2O_2 were
added. These three last components are necessary to detect the heme
proteins. During all additions, the gel was gently agitated using an orbital shaker
DRS-12 at 25 to 30 rpm (NeoLab, Heidelberg, Germany). The SDS-PAGE gel
was visualized with the Molecular Imager® ChemiDoc XRS GelDoc™ (Biorad,
Munich, Germany) using the software Image Lab 5.1 (Biorad, Munich,
Germany) in mode "protein" with option "Auflicht" or "coomassie blue".

2.6.3 BSA protein assay

The total protein concentration of the periplasmic samples was determined
according to the Bradford method (Bradford 1976). The aim of this assay is that
the reagent coomassie brilliant blue binds with the basic side chains of the
amino acids non-specifically producing a color change from brown to blue.

For the determination of the concentration, a standard calibration curve was
performed using the bovine serum albumin protein (BSA) with the following
concentrations: 0, 20, 40, 60, 80 and 100 µg ml^{-1}.

The samples were prepared without dilution and with a dilution in a ratio of 1:5,
1:25 and 1:125. Afterwards, they were diluted in a ratio of 1:10 using the
Bradford reagent (Table 32), loaded in a 96-well plate and measured at a
wavelength of 595 nm in the microplate reader IMark (Biorad, Munich,
Germany).

Table 32: Composition of the Bradford reagent.

Component	Amount
Coomassie Brilliant Blue G-250	100 mg
≥ 85% phosphoric acid	100 ml
96% ethanol	50 ml
dH$_2$O	until 1000 ml total volume

2.6.4 Determination of heme groups

For the quantification of the periplasmic heme concentration, the method of Berry and Trumpower (Berry and Trumpower 1987) was carried out. Periplasmic fractions were mixed with a solution containing 200 mM NaOH, 40% pyridine and 3 µl of a 0.1 M solution $K_3Fe(CN)_6$, which led to the complete oxidation of the heme groups contained in the sample. After the first measurements, 2 to 5 mg of sodium dithionite were added as electron donor to reduce Fe(III) to Fe(II) until the stabilization of the peak at 552 nm.

All samples were scanned from 400 to 600 nm using the spectrophotometer Cary50 UV/VIS (Varian, Darmstadt, Germany). After each measurement, sodium dithionite was added until peak stabilization at 552 nm. The total heme absorbance (A_{total}) was calculated using Equation 1 and the heme concentration (*c*) was determined according to the Beer-Lambert equation (Equation 2), where the molar extinction coefficient (ε) is 24 mM^{-1}.

$$A_{total} = [A_{550}(red) - A_{550}(ox)] - [A_{535}(red) - A_{535}(ox)] \quad \text{(Equation 1)}$$

Beer-Lambert law:

$$A_{total} = \varepsilon * c * d \quad \text{(Equation 2)}$$

With A_{total}= absorbance, ε= molar extinction coefficient, *c*= concentration, *d*= layer thickness

2.7 Isolation of the periplasmic fraction

At first, *Shewanella* strains were grown anoxically with 50 mM ferric iron citrate as electron acceptor and 50 mM lactate as electron donor (see Table 11) and washed two times with minimal medium buffer (Table 14). In order to isolate the periplasmic fractions, the method of Cerny and Pitts was followed (Cerny and Teuber 1971; Pitts et al. 2003). The cells were washed with 20 mM HEPES (pH 7.4) and resuspended (1 ml buffer / 1.5 g cells). Afterwards, polymyxin B sulfate was added with a final concentration of 1 mg/ml and the suspension was incubated for 1 h at 37ºC. Polymyxin B sulfate binds to the lipopolysaccharides

of the membrane resulting in their destabilization. After centrifuging the suspension at 15,000 ×g and 4°C for 45 min, the resulting supernatant contained the periplasmic fraction.

2.8   Determination of Fe(II)

All samples taken during experiments using Fe(III)-citrate as electron acceptor were stopped with 1 M HCl to avoid the oxidation of Fe(II) with atmospheric oxygen and the samples were diluted 1:10 or 1:100 depending on the Fe(II) concentration.

To quantify the Fe(II), a ferrozine reagent (3-(2-pyri-dyl)-5,6-diphenyl-1,2,4-triazine-p,p'-disulfonic acid) was used following the protocol of Stookey et al. (Stookey 1970). This reagent was dissolved in a 50% (w/v) ammoniumacetate solution to neutralize the pH value (Stookey 1970; Ruebush et al. 2006), 180 µl of this solution were added to 20 µl samples and incubated 5 min at room temperature. Afterwards, the samples were read at 595 nm in the microplate absorbance reader iMark^{TM} (Bio-Rad, Munich, Germany). For the standardization of the measurements, a calibration curve was established using $(NH_4)_2Fe(SO_4)_2$ $6H_2O$ dissolved in HCl.

2.9   Analytical methods

2.9.1 Chromatographic methods

High Performance Liquid Chromatography (HPLC)

To identify and quantify the produced and consumed organic acids, their concentration was measured via HPLC (Thermo Fisher, Waltham, USA), which separates and purifies the compounds according to their polarity. The components were injected continuously into the mobile phase (which was composed of 5 mM of H_2SO_4) using a high pressure pump to set a specific flow rate (0.6 ml min^{-1}). The mobile phase was introduced into the cation exchanger column (300 x 7.8mm Aminex HPX-87H, Bio-Rad, Munich, Germany), which

contained a specific chromatographic packing material (the stationary phase) to allow for the separation of the components. This process was performed at 60ºC. After the separation, the "Hitachi Diode array UV detector L2455" detected the components in form of bands at 210 nm and the resulting chromatogram was analyzed with the software EZChrom Elite (Agilent, Waldbronn, Germany).

Before inserting samples into the HPLC, they were centrifuged at 6,000 rpm (Eppendorf 5418, Hamburg, Germany) and filtered using a membrane syringe filter with a pore size of 0.2 µm (VWR™ international, Ohio, USA). Then, 150 µl were mixed with 15 µl of H_2SO_4 in a microtiter plate and covered with a special plastic that attaches to the microtiter. A calibration curve was prepared for each relevant chemical compound that could be present in a sample.

2.9.2 Flavin quantification

Liquid samples of the BESs were collected at different points of time. The samples were centrifuged at 6,000 rpm for 5 min (Eppendorf 5418, Hamburg, Germany) and filtered through a membrane syringe filter with a pore size of 0.2 µm (VWR™ international, Ohio, USA). 200 µl of each sample were transferred to a microtiter plate and read in a Tecan Infinite M200 PRO plate reader (Tecan, Austria) at 440 nm excitation and 525 nm emission. Different concentrations ranging from 25 nM to 2.5 µM of a mixture of FMN and RF (80:20) were used for establishing a standard calibration curve.

2.10 Electrochemical methods

2.10.1 Bioelectrochemical systems (BESs)

The bioelectrochemical systems described previously by Förster et al. were used in this study to analyze and compare the current production of the strains. Figure 6 displays the design of the used BESs. Precultures were grown overnight in LB medium (Table 4), washed twice using washing buffer (minimal medium without electron acceptor or donor, Table 14) and resuspended in

minimal medium with 50 mM lactate (Table 12) at an OD_{600} of 0.5. The bioelectrochemical experiments were carried out at 30°C under potentiostatic control (PG8850RM, uniscan instruments, Göttingen, Germany), using a platinum counter (1.25 cm^2), a graphite felt working (36 cm^2, SIGRATHERM, SGLGGroup, Wiesbaden, Germany) and an Ag/AgCl reference electrode (Meinsberg, Waldheim, Germany) (sat. KCl, 0.199 V vs. SHE). The data were analyzed with the software UiEchem (Bio-Logic, Glosopp, UK). Throughout the experiments, the BESs were stirred with a magnetic stirrer and kept anoxic by purging with nitrogen gas.

Reference electrode
Counter electrode
Graphite working electrode
Stir bar
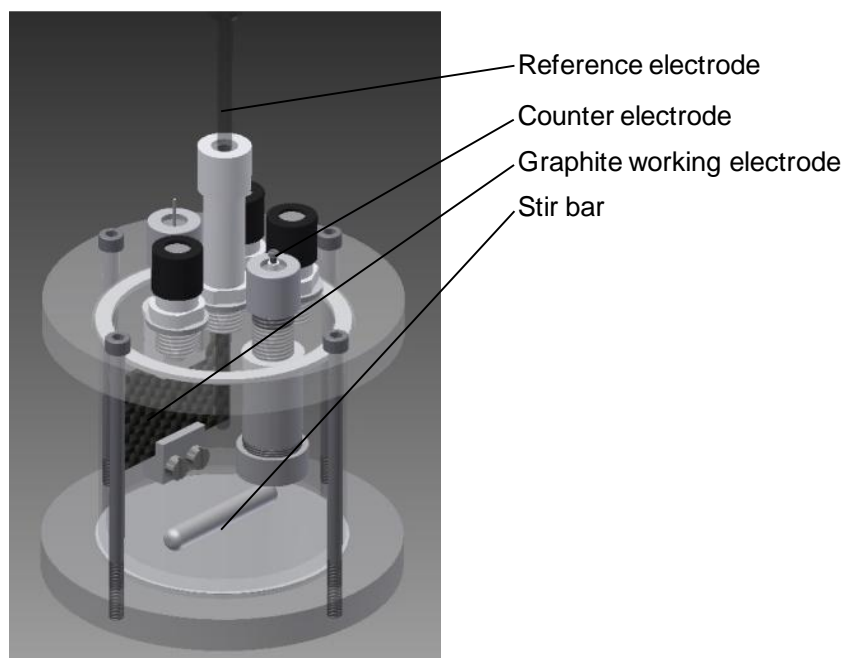
Figure 6: Schema of the reactor used in this study with a capacity of 270 ml and composed of a graphite felt working electrode (36 cm^2), a platinum counter electrode (1.25 cm^2) and an Ag/AgCl reference electrode (sat. KCl, 0.199 V vs. SHE) (Förster et al. 2017).

2.10.2 Cyclic voltammetry

The electrochemical setup was a three-electrode system composed of a pyrolytic graphite edge (PGE) electrode as working electrode, an Ag/AgCl (3 M KCl, 0.210 V vs. SHE (Bard and Faulkner 2002)) reference electrode and a silver wire as counter electrode. Prior to use, the PGE electrode was polished with alumina slurry (1 µm, Buehler, Lake Bluff, IL, USA). All electrochemical

experiments were performed at room temperature (approx. 25⁰C) in an anaerobic chamber filled with N_2 (residual oxygen < 5 ppm). Experiments were performed at different scan rates with the periplasmic fractions of the individual strains diluted in 500 mM phosphate buffer at pH 7.0, normalized to contain the same amount of cells.

Cyclic voltammetry was performed with an Autolab electrochemical analyzer (PGSTAT-128N, Metrohm, Herisau, Switzerland) controlled by GPES software. The electrochemical data were analyzed using the QSOAS program available at www.qsoas.org (Fourmond 2016). According to the Randles-Sevcik equation, the anodic and cathodic peak intensities (i_p) were plotted versus the square root of the scan rate:

$$i_p = (2.69 \times 10^5)\, n^{3/2}\, A\, D_0^{1/2}\, C_0\, v^{1/2} \quad \text{(Equation 3)}$$

With n= number of electrons, A= surface of the electrode, D_0= diffusion coefficient of the redox species, C_0= concentration of the redox species and v= scan rate

By assuming that the analytes are identical in all strains, and taking into consideration that all the experiments were performed with the same setup and electrode, the ratio between the concentration of the periplasmic fraction of the mutant and wild type strains (C_{mut}/C_{wt}) were determined.

2.11 Bioinformatical methods

2.11.1 CLC software

For the design of primers and different synthetic pathways, as well as for the verification of deletions and insertions of genes, the software CLC Main Workbench (Qiagen, Hilden, Germany) was used. This program was also used to analyze the transcriptome data.

2.11.2 Chromas

The software Chromas (Technelysium, South Brisbane, Australia) was used to identify and clarify possible mutations in certain DNA sequences.

2.11.3 Transcriptomic analysis

For the RNA extraction, cells were previously harvested during 4 h with an initial OD of 0.1 using minimal medium, Fe(III) citrate as electron acceptor and lactate as electron donor (Table 11). Afterwards, 10 ml samples were centrifuged at 15,500 ×g for 2 min, the supernatants were discarded and the pellets were immediately frozen by emerging the redcaps containing the pellets into liquid nitrogen. Right after that, the frozen samples were stored in a Styrofoam box containing dry ice at -80ºC until sending them in for analysis.
The illumina sequence was performed by IMGM (Martinsried, Germany).

Gene expression analysis by quantitative RNA sequencing

The library preparation was performed using the TruSeq mRNA Sample Prep Kit from Illumina based on the Ribo-Zero Bacteria procedure (rRNA-depletion) and the gene expression levels were represented in transcripts per million (TPM). The samples were sequenced with single 75 nt reads (SR75) with an expected coverage of at least 10 million reads per sample, which can be used for subsequent bioinformatic analysis. Afterwards, the data were analyzed using the genome data of *S. oneidensis* MR-1 (NCBI NC-004347.2) and the software CLC based on (Mortazavi et al. 2008).

3. Results

In this chapter, the results of the three sub-projects will be presented. Chapter 3.1 elucidates the improvement of the electron transfer rate in *S. oneidensis* MR-1, chapter 3.2 outlines the facilitation of using glucose as substrate and chapter 3.3 describes experiments aiming at the production of itaconic acid.

3.1 Improvement of the ET rate in *S. oneidensis* MR-1

The first sub-project's aim was the improvement of the electron transfer rate of *S. oneidensis* under anoxic conditions in BESs. Therefore, it was under investigation if tailoring the periplasmic protein content could lead to an increase of the extracellular respiration. Due to the similar biochemistry necessary for ferric iron citrate and graphite fleece electrode reduction and the easier detectability of changes in the ET with this soluble electron acceptor, experiments were first conducted with ferric iron citrate. After identifying a promising strategy, it was applied in BESs.

In order to enhance the periplasmic ET rate, periplasmic proteins that are not relevant for dissimilatory iron reduction were replaced with the electron shuttling *c*-type cytochrome STC. More precisely, the genes *nrfA, ccpA, napA* and *napB* were deleted from the genome and a copy of *cctA* encoding STC was introduced at the respective loci to be under control of the respective native promoters (see schema in Figure 7). In contrast to a plasmid-based overexpression, this kind of control can avoid a high metabolic burden.
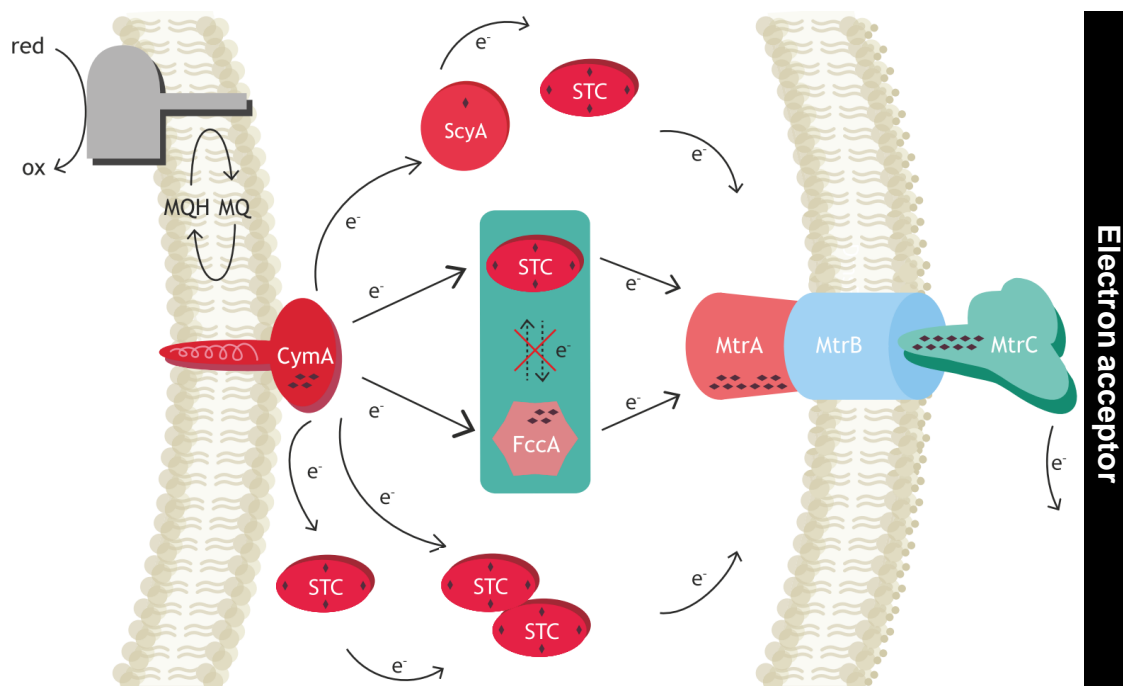
Figure 7: Schematic of tailored periplasmic protein content in *S. oneidensis*.

Hence, four different strains containing 2 to 5 copies of *cctA* were developed for this study via conjugation (section 2.5.7). For the sake of easier readability, a mutant name is assigned to each strain and will be used in the following. Table 33 lists the developed strains and their respective mutant names.

Table 33: Mutant names of the developed strains.

Strain	Mutant name
S. oneidensis ΔnrfA::cctA	Single
S. oneidensis ΔnrfA::cctA_ΔccpA::cctA	Double
S. oneidensis ΔnrfA::cctA_ΔccpA::cctA_ΔnapA::cctA	Triple
S. oneidensis ΔnrfA::cctA_ΔccpA::cctA_ΔnapA::cctA_ΔnapB::cctA	Quadruple

3.1.1 Impact of STC overexpression on the periplasmic heme concentration

To investigate the impact of STC overexpression resulting from the substitution of the above mentioned *c*-type cytochromes with *cctA,* a heme staining of the four mutants and the wild type as reference was performed. All strains were grown anoxically with 50 mM ferric citrate as electron acceptor and 50 mM lactate as electron donor. The periplasmic fraction of each strain was isolated as described in section 2.7 and the protein concentration was quantified following the Bradford method (Bradford 1976). 30 µg of each periplasmic fraction were loaded into the wells of the SDS-PAGE gel (section 2.6.1).

The resulting SDS-PAGE gel is shown in Figure 8 and a gradual increase of STC concentration in the periplasm up to the quadruple mutant through insertion of *cctA* copies can be noticed.
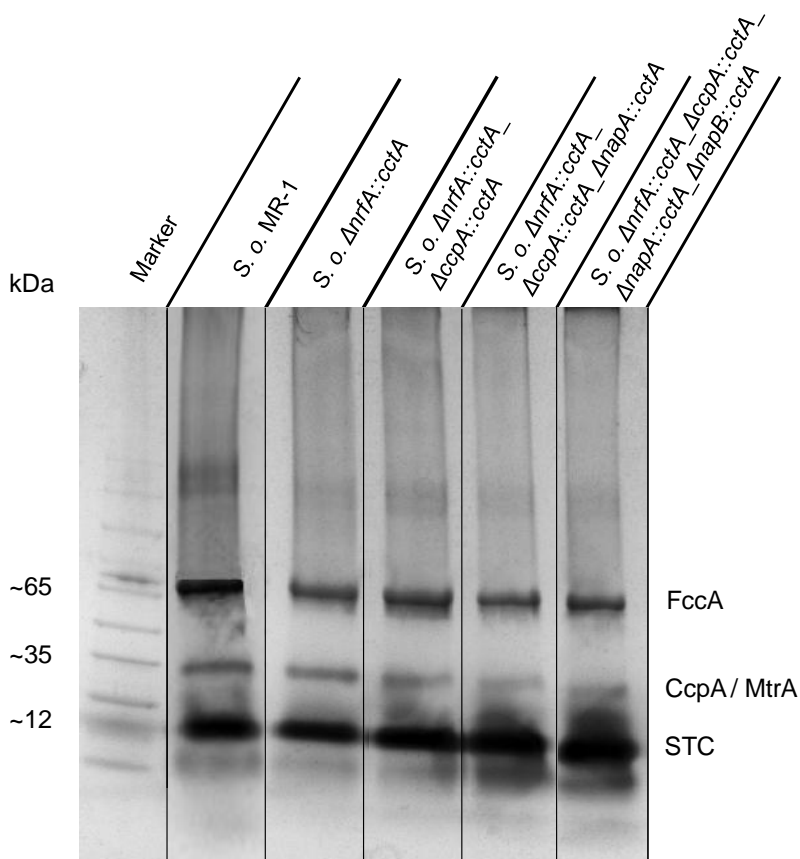
Figure 8: Heme staining of periplasmic fractions (30 µg of protein) from Fe(III)-citrate grown wild type cells and cells of the four developed mutant strains. The respective genotype is indicated in the figure.

Table 34 outlines the number of heme groups of the replaced proteins and STC. STC contains more heme groups than the average of the proteins that have been knocked out. Therefore, the quadruple mutant should exhibit a higher periplasmic heme concentration as well as an increased STC production.

Table 34: Number of heme groups and molecular weight of the studied proteins.

Protein	Number of heme groups per protein	Molecular weight [kDa]
NrfA	5	52.86
NapA	0	92.47
NapB	2	14.56
CcpA	2	35.26
STC	4	12.26
FccA	4	62.42

In order to validate this hypothesis, the periplasmic heme concentration was quantified according to the method of Berry and Trumpower (Berry and Trumpower 1987) described in section 2.6.4. Table 35 shows the measured heme concentrations and the heme per mg of periplasmic protein. The results corroborate the first part of the mentioned hypothesis. With 11.52 ± 0.73 µM heme / mg periplasmic protein, the quadruple mutant contained 32.34% more heme compared to the wild type, which contained 8.69 ± 0.88 µM heme / mg periplasmic protein.

Table 35: Heme concentration and heme per periplasmic protein content of *S. oneidensis* MR-1 and quadruple mutant.

	S. o. MR-1	Quadruple mutant	Increase in quadruple mutant
Heme concentration [µM]	82.94	88.67	6.91%
Heme per protein [µM mg^{-1}]	8.69 ± 0.88	11.52 ± 0.73	32.34%

3.1.2 Impact of up-regulating *cctA* on the ET rate to ferric iron citrate

To study the impact of the four deletions and the concurrent potential up-regulation of STC, cell suspension assays were performed under anoxic conditions with 50 mM Fe(III)-citrate as electron acceptor and 50 mM lactate as electron donor at an OD of 2. The results of these experiments show that each additional substitution with *cctA* led to an increase of the ferric iron reduction rate in comparison to *S. oneidensis* MR-1 and the respective preceding mutants, as displayed in Figure 9. A 1.7-fold increase in ferric iron reduction rate was detected when comparing the quadruple mutant to the wild type. Statistical analyses of these measurements performed in order to verify the differences between the strains confirmed significance and p-values below 0.01. Hence, the up-regulation of STC leads to a significant acceleration of the ET to ferric iron.
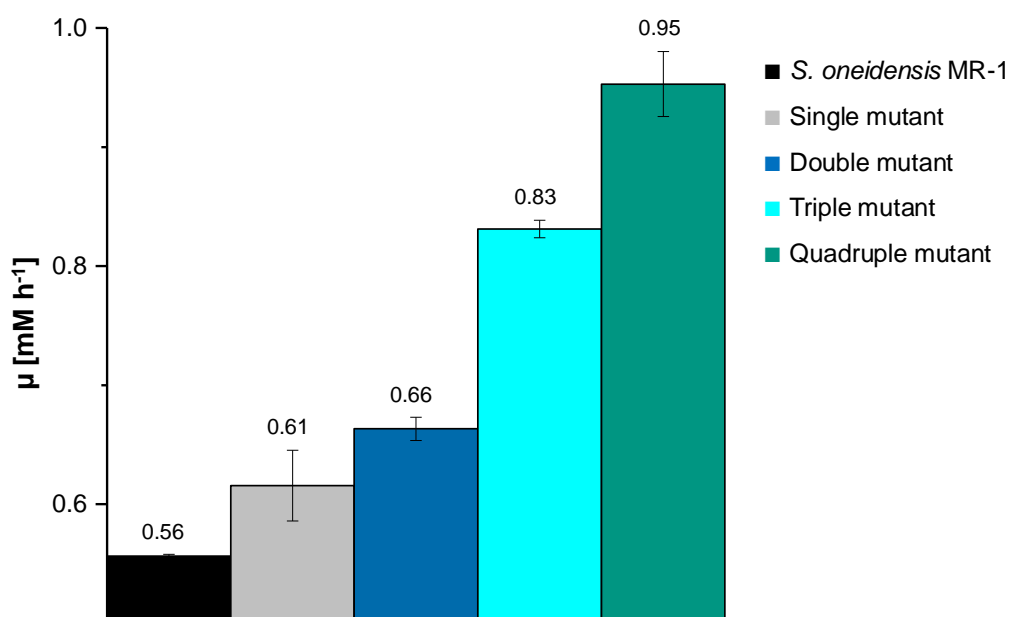
Figure 9: Increase of the ferric iron reduction rates μ [mM h^{-1}]. All experiments were started with OD 2 and carried out under anoxic conditions with 50 mM lactate as electron donor and 50 mM Fe(III)-citrate as terminal electron acceptor.

3.1.3 Cell suspension assays with fumarate as electron acceptor and lactate as electron donor

Cell suspension assays with fumarate as electron acceptor and lactate as electron donor were carried out to answer the question whether the effect of STC overexpression is specific for extracellular ferric iron reduction or a result of a general fitness increase of the strains. As shown in Figure 10, the biomass formation rates of wild type and quadruple mutant do not vary significantly when using fumarate as electron acceptor. Hence, it can be assumed that the beneficial impact of overexpressing *cctA* is not due to a general fitness gain but is specific for an extracellular reduction process.
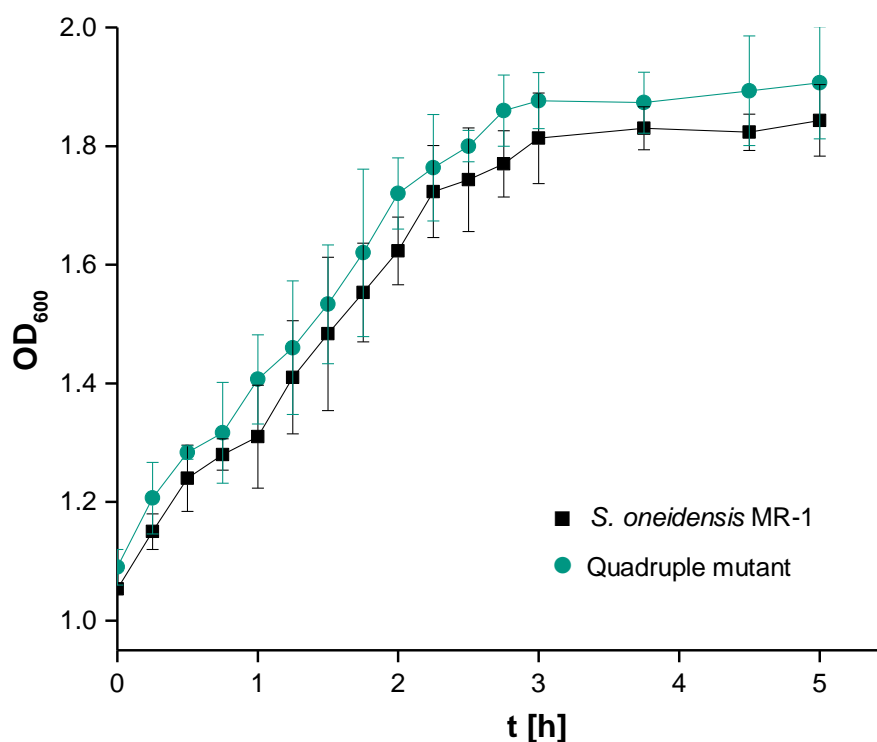
Figure 10: Cell suspensions assays with 50 mM fumarate as terminal electron acceptor and 50 mM lactate as electron donor started with OD_{600} 1 and carried out under anoxic conditions. Comparison of the wild type and quadruple mutant.

3.1.4 Investigation of FccA's functional redundancy compared to STC

Studies of Sturm et al. and Fonseca et al. suggested that STC and FccA have a functional redundancy regarding the ET between the cytoplasmic membrane protein CymA and the outer membrane protein complex MtrABC (Fonseca et al. 2013; Sturm et al. 2015). Therefore, a quintuple mutant lacking FccA and containing an additional *cctA* copy was designed (*S. oneidensis ΔnrfA::cctA_ ΔccpA::cctA_ΔnapA::cctA_ΔnapB::cctA_ΔfccA::cctA*) in order to analyze whether there might be a full functional overlap between the two proteins.

A performed heme staining clearly indicates the successful deletion of *fccA* (Figure 11). Although FccA is a very prominent periplasmic *c*-type cytochrome, the measured heme concentration of the quintuple mutant (9.38 ± 1.05 µM heme mg^{-1} periplasmic protein) was not significantly higher compared to the wild type and lower compared to the quadruple mutant (Table 35), which provides evidence that the additional insertion of *cctA* did not lead to a replacement of the FccA related heme concentration by STC.
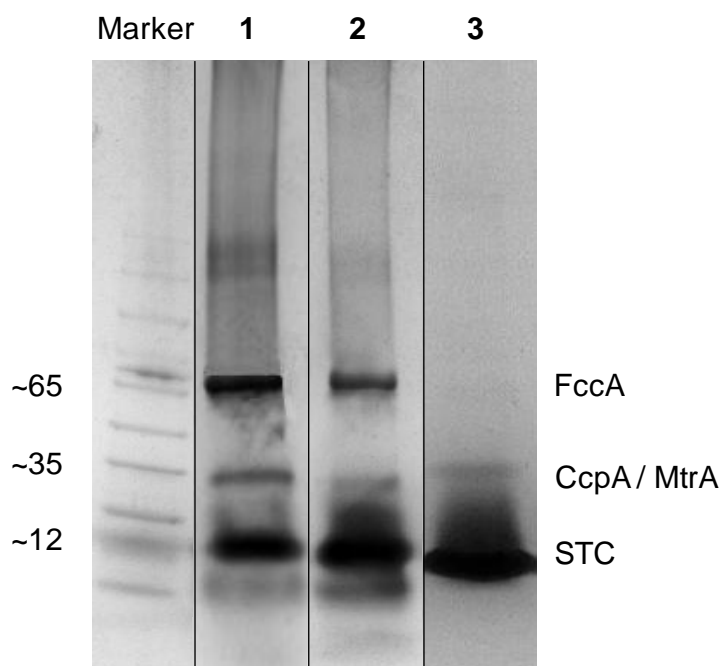
Figure 11: Heme staining of periplasmic fractions from Fe(III)-citrate grown wild type (1), quadruple (2) and quintuple mutant (3) cells. 30 µg of protein of each strain were loaded on the gel.

The quintuple mutant was also tested in cell suspension assays analogously to sections 3.1.2 and 3.1.3. When using ferric iron citrate as electron acceptor, the reduction rate was similar to the wild type's reduction rate but almost two-fold lower in comparison to the quadruple mutant (Figure 12).
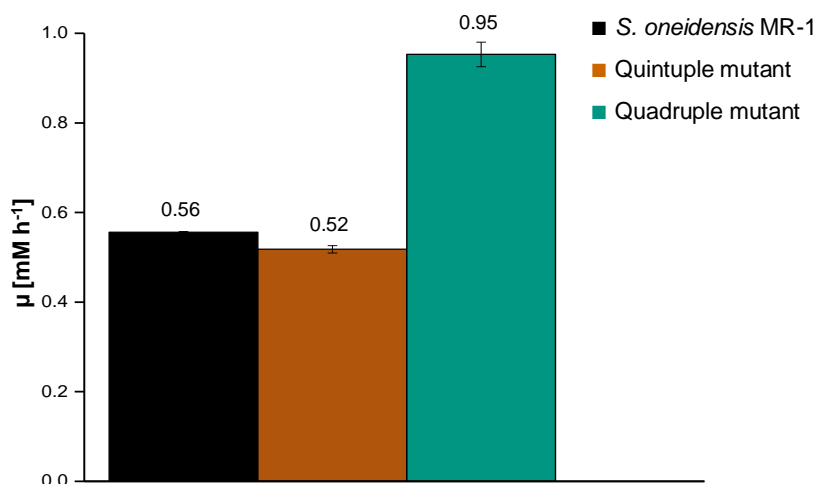
Figure 12: Fe(III)-citrate reduction rates μ [mM h^{-1}] of the quintuple mutant compared to *S. oneidensis* MR-1 and the quadruple mutant.

In the case of fumarate as electron acceptor, the strain was not able to grow as could be expected due to the deletion of the gene encoding for the fumarate reductase FccA (Figure 13).
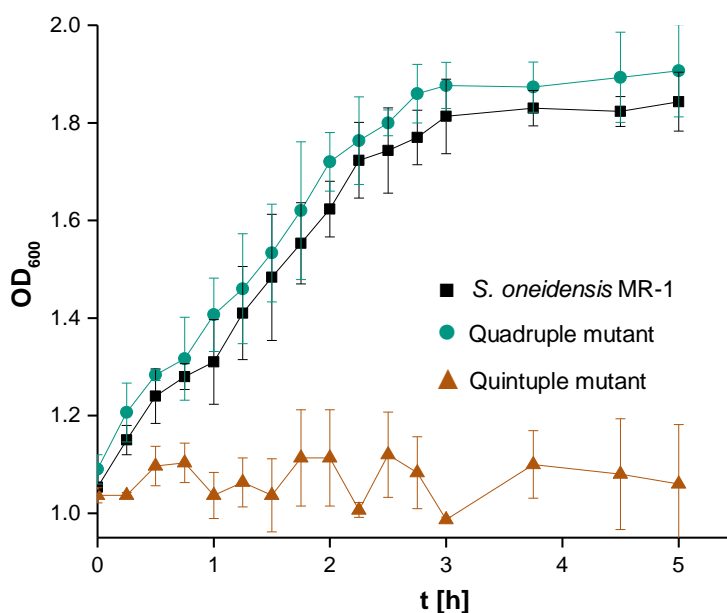
Figure 13: Cell suspensions assays with 50 mM fumarate as terminal electron acceptor and 50 mM lactate as electron donor started with OD$_{600}$ 1 and carried out under anoxic conditions. Comparison of the wild type, quadruple and quintuple mutant.

3.1.5 Cyclic voltammetry of periplasmic fractions

After observing the aforementioned changes in the ET rate of the quadruple and quintuple mutant compared to the wild type, the question arose whether the rearrangement of the periplasmic protein content resulted in detectable differences in the characteristics of observable redox species. Therefore, after isolating the periplasmic fraction of wild type, quadruple and quintuple mutant as described in section 2.7, cyclic voltammetry experiments were performed in cooperation with Catarina Paquete from the ITQB of the university of Lisbon, Portugal. Electrochemical experiments of the periplasmic fractions (section 2.10.2) showed a titration of the redox species present in all samples at approximately -200 mV (Figure 14). The anodic and cathodic peak intensities (i_p) were calculated according to the Randles-Sevcik equation (Equation 3) and the observed linearity between i_p and the scan rate $\upsilon^{1/2}$ (Figure 15) indicates that the redox species were diffusing in the bulk to the electrode.
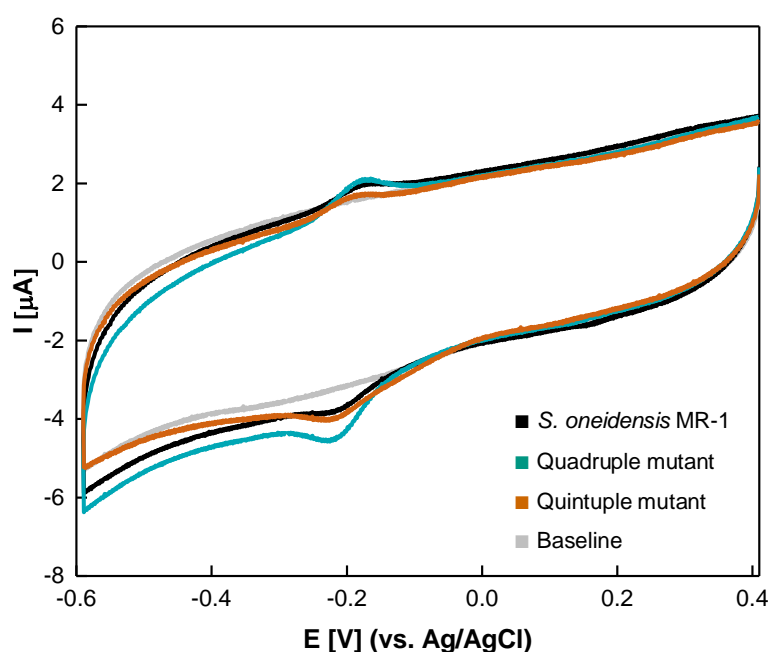
Figure 14: Cyclic voltammetry of the periplasmic fractions of wild type, quadruple mutant and quintuple mutant obtained at a scan rate of 200 mV s^{-1}. The baseline is the raw voltammogram obtained with buffer.
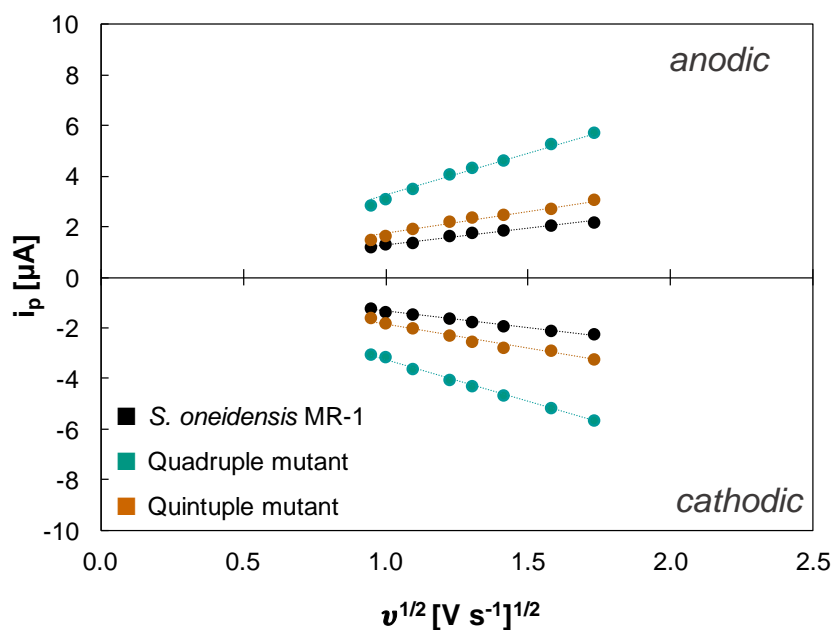
Figure 15: Slope of i_p against $\upsilon^{1/2}$ obtained for the periplasmic fractions of the wild type, quadruple and quintuple mutant. The trend lines are shown as dashed lines.

Since soluble flavins and various periplasmic cytochromes including STC titrate around -200 mV (see Figure 16), the periplasmic fractions were precipitated with trichloroacetic acid (TCA) to denaturate the proteins in order to ascertain if the redox species were flavins.
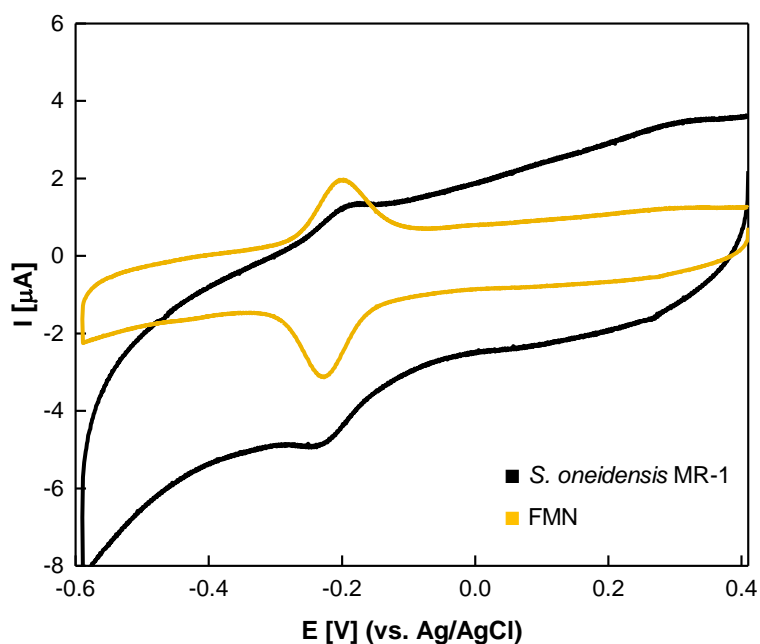
Figure 16: Raw voltammograms of the periplasmic fraction of the wild type and FMN.

UV-visible spectroscopy revealed that the supernatants of the three strains and flavins absorb at the same wavelength of approximately 450 nm (Figure 17A). Further electrochemical experiments with the samples after TCA treatment showed a redox signal similarity to soluble flavins (Figure 17B). These findings suggest that the observed redox species are soluble flavins, which are present in the periplasmic fractions of the analyzed *S. oneidensis* strains.

In order to analyze if there are differences in the periplasmic flavin concentration of the different samples, the ratios between the redox species concentration of each mutant and the wild type were calculated using the Randles-Sevcik equation (Equation 3). A roughly 2.5-fold increase of flavin concentration could be observed in the quadruple mutant compared to the wild type. In contrast, the quintuple mutant only showed an approximately 1.4-fold higher flavin content in comparison to the wild type. Table 36 summarizes the results of these calculations and Figure 15 illustrates the slopes of i_p against $\upsilon^{1/2}$ for the three strains.
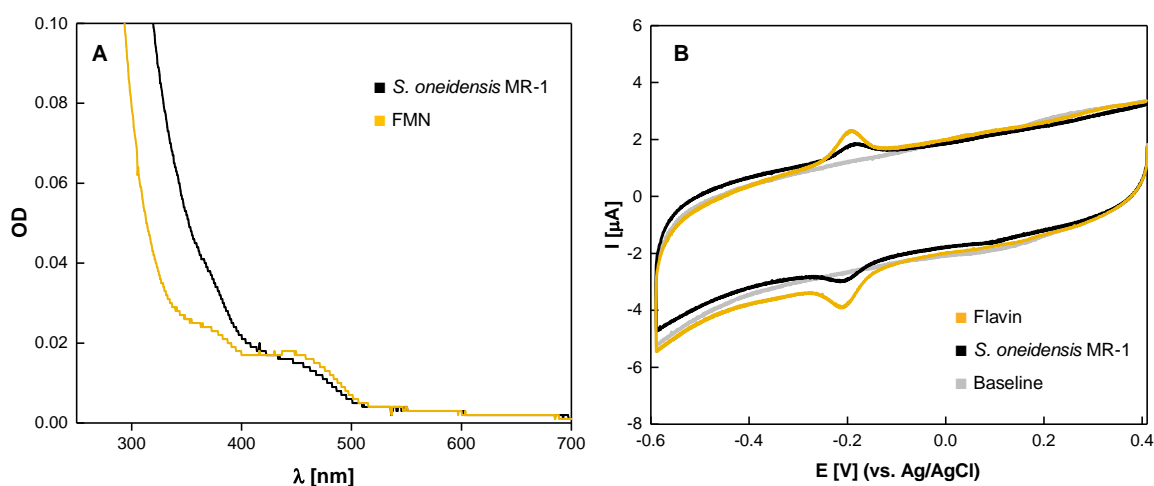
Figure 17: A: UV-visible spectroscopy of the periplasmic fraction of the wild type after TCA treatment compared to FMN. **B:** Cyclic voltammetry of the periplasmic fraction of the wild type after TCA treatment and of FMN obtained at a scan rate of 200 mV s^{-1}. The baseline is the raw voltammogram obtained with buffer prior to the experiment.

Table 36: Slope of i_p against $\upsilon^{1/2}$ (Figure 15) of the anodic and cathodic signal and ratio of the concentration of the redox species in the different mutant strains in relation to the wild type determined for both, anodic and cathodic peak.

Strain	Anodic slope [$\mu A/(V\ s^{-1})^{1/2}$]	Cathodic slope [$\mu A/(V\ s^{-1})^{1/2}$]	C_{mut}/C_{wt} (anodic)	C_{mut}/C_{wt} (cathodic)
Wild type	1.29	-1.33	-	-
Quadruple mutant	3.27	-3.27	2.53	2.46
Quintuple mutant	1.74	-1.87	1.35	1.41

3.1.6 Transcriptomic analysis of wild type, quadruple and quintuple mutant

With the intention to analyze the overexpression of STC quantitatively and to identify potential mechanisms that might cause the increased periplasmic flavin concentration, a transcriptomic analysis was performed (cf. section 2.11.3).

Inserting four additional copies of *cctA* led to a 3.6-fold increase of *cctA* expression in the quadruple mutant compared to the wild type (Table 37B). Interestingly, the replacement of *fccA* with *cctA* did not result in a further increase of the expression rate in the quintuple mutant (Table 37B). Altogether, *cctA* turned into the third highest expressed protein in both mutant strains, while it was ranked 51st in the wild type (Table 37A). Possibly, the already very high expression rate of *cctA* in the quadruple mutant might be the reason why the further insertion of *cctA* did not lead to an additional increase of transcripts in the quintuple mutant.

Table 37: Results of transcriptomic analysis of *S. oneidensis* MR-1 (WT), quadruple mutant (4x) and quintuple mutant (5x). **A:** Top 10 ranking of overall transcribed genes (average TPM) in *S. oneidensis* MR-1, quadruple and quintuple mutant. **B:** Fold changes of selected transcribed genes ranked by highest absolute fold change (≥ 3 as well as ≤ -3) in the quadruple and quintuple mutant compared to the wild type for all statistically significant changes (FDR p-value ≤ 0.05). Grey font: deleted genes in the respective mutants.

A

Gene	WT	Gene	4x	Gene	5x
omp35	15,759.8	omp35	23,524.4	omp35	18,197.7
lpp	14,948.7	lpp	16,023.0	lpp	14,007.8
cspA	10,775.5	cctA	13,860.8	cctA	12,118.3
pflB	10,769.6	pflB	13,493.7	cspA	10,914.5
rpmI	10,450.8	rpmI	10,459.4	rpmI	10,658.3
tufA	8,190.7	cspA	9,563.6	pflB	10,196.4
rplA	7,830.2	rplA	8,656.7	rplJ	8,384.0
rplJ	7,809.1	tufA	8,077.0	tufA	8,184.8
rpsK	7,451.5	rplJ	8,013.3	rpoA	8,051.4
rpoA	7,445.5	tufB	7,414.6	rpsK	7,998.3

B

	4x vs. WT		5x vs. WT
Gene	Fold change	Gene	Fold change
napD	169.1	napD	146.4
napG	55.5	napG	48.3
napH	19.9	napH	17.1
speF	7.7	cctA	3.3
potE	6.9	tnpA_30	3.3
SO_0312	5.5	gpT	3.2
tnpA_20	5.5	SO_2687	3.2
tnpA_134	5.0	SO_2673	3.1
SO_4761	4.3	tnpA_114	-51.0
ifcA	3.8	nrfA	-7,456.7
cctA	3.6	napB	-9,132.7
tnpA_30	3.2	napA	-11,087.7
cysJ	-3.1	fccA	-26,869.0
glgX	-3.2	ccpA	-295,305.4
SO_0547	-3.2		
malQ	-3.5		
glgB	-4.0		
glnK_1	-4.1		
SO_0760	-4.7		
tnpA_114	-27.0		
nrfA	-7,786.9		
napB	-9,537.1		
napA	-11,578.7		
ccpA	-308,383.7		

In a next step, the proteins that were so far shown to be involved in flavin synthesis (see also section 1.1.3) were analyzed aiming to uncover possible mechanisms for the increased flavin secretion. However, neither the quadruple nor the quintuple mutant showed a statistically significant increase of the *ribA-F*, *ushA* or *bfe* expression in comparison to the wild type (Table 38). This finding leads to the assumption that the increased flavin content is not due to an improvement of flavin production.

When comparing the whole transcriptome of the wild type and the quadruple mutant, only a limited number of genes were shown to be more positively affected in expression than *cctA* (Table 37, Table 39). *NapDGH*, which are part of the *napDAGHB* operon in the wild type, presented an increase of their expression that could be explained with the insertion of *cctA* at the position of *napA* and *napB*. While the periplasmic protein NapD is involved in NapA maturation, NapG and NapH build the cytoplasmic membrane bound ubiquinol oxidase of the periplasmic nitrate reductase.

Table 38: Transcriptional changes of genes related to riboflavin synthesis of quadruple (4x) and quintuple mutant (5x) compared to the wild type (WT); FDR p-values ≤ 0.05.

Name	4x vs. 5x	4x vs. WT	5x vs. WT
ribB	-1.77	-1.52	1.17
ribC	1.17	1.18	1.00
ribA	-1.07	1.10	1.18
ribE	-1.05	-1.05	-1.00
ribBA	-1.00	-1.02	-1.02
ribD	1.04	-1.01	-1.05
ribF	-1.03	-1.04	-1.01
btuB / bfe	-1.11	-1.14	-1.03
ushA	-1.31	-1.24	1.06

Table 39: Transcriptomic expression of all genes showing fold changes in transcription level with an absolute value higher than 2 (≥ 2 as well as ≤ -2) and FDR p-values ≤ 0.05. *S. oneidensis* MR-1: WT, quadruple mutant: 4x and quintuple mutant: 5x.

4x vs. WT				5x vs. WT				4x vs. 5x			
Name	Log fold change	Fold change	FDR p-value	Name	Log fold change	Fold change	FDR p-value	Name	Log fold change	Fold change	FDR p-value
napD	7.402	169.115	0.000	napD	7.194	146.411	0.000	fccA	14.053	16,991.796	0.000
napG	5.795	55.538	0.000	napG	5.595	48.338	0.000	tnpA_20	2.572	5.946	0.004
napH	4.312	19.866	0.000	napH	4.095	17.087	0.000	speF	2.567	5.925	0.000
speF	2.950	7.726	0.000	cctA	1.742	3.345	0.000	potE	2.386	5.226	0.000
potE	2.779	6.863	0.000	tnpA_30	1.713	3.278	0.000	SO_4761	2.195	4.577	0.000
SO_0312	2.461	5.507	0.000	gpT	1.699	3.248	0.000	tnpA_134	2.044	4.124	0.007
tnpA_20	2.460	5.504	0.007	SO_2687	1.675	3.192	0.000	SO_0312	2.031	4.088	0.000
tnpA_134	2.314	4.974	0.004	SO_2673	1.626	3.087	0.002	ifcA	1.916	3.774	0.000
SO_4761	2.090	4.256	0.000	gp48	1.573	2.975	0.000	SO_1259	1.355	2.559	0.000
ifcA	1.912	3.765	0.000	gpM	1.416	2.669	0.000	SO_3040	1.320	2.497	0.033
cctA	1.830	3.554	0.000	SO_2688	1.404	2.647	0.000	SO_1420	1.197	2.293	0.000
tnpA_30	1.679	3.203	0.000	nnrS	1.399	2.637	0.000	SO_0910	1.031	2.043	0.000
tnpA_112	1.324	2.504	0.000	gpI	1.387	2.616	0.000	gpM	-1.002	-2.002	0.000
SO_1420	1.205	2.306	0.000	SO_2691	1.366	2.578	0.000	SO_2010	-1.005	-2.006	0.012
nnrS	1.042	2.059	0.000	SO_2686	1.327	2.509	0.000	lys	-1.027	-2.038	0.047
ald	-1.041	-2.058	0.000	ahpF	1.309	2.478	0.000	cysG	-1.037	-2.052	0.000
cysH	-1.042	-2.059	0.000	gpJ	1.300	2.462	0.000	glgA	-1.037	-2.052	0.000
SO_4520	-1.045	-2.063	0.000	tnpA_112	1.282	2.432	0.000	SO_0753	-1.040	-2.056	0.000
glgA	-1.078	-2.112	0.000	SO_2675	1.264	2.402	0.014	pstS_2	-1.044	-2.061	0.033
adhB	-1.143	-2.209	0.000	I	1.243	2.367	0.000	SO_3909	-1.049	-2.069	0.002
cysG	-1.154	-2.226	0.000	SO_2974	1.223	2.334	0.010	SO_1977	-1.054	-2.076	0.000
ompW	-1.180	-2.266	0.000	V	1.192	2.285	0.000	SO_2689	-1.067	-2.095	0.000

Table 39: (Continuation)

4x vs. WT				5x vs. WT				4x vs. 5x			
Name	Log fold change	Fold change	FDR p-value	Name	Log fold change	Fold change	FDR p-value	Name	Log fold change	Fold change	FDR p-value
glnL	-1.199	-2.295	0.000	SO_2957	1.188	2.279	0.000	SO_2918	-1.067	-2.096	0.036
cysK	-1.287	-2.441	0.000	B	1.181	2.267	0.000	relV	-1.071	-2.101	0.001
glgC	-1.324	-2.503	0.000	gp41	1.179	2.265	0.000	SO_4843	-1.087	-2.125	0.017
glnK_2	-1.330	-2.513	0.000	G	1.171	2.252	0.000	sbp	-1.118	-2.171	0.000
cysI	-1.332	-2.518	0.000	katB	1.146	2.212	0.000	SO_0554	-1.125	-2.180	0.000
SO_3972	-1.391	-2.623	0.000	gpG_2	1.145	2.212	0.000	SO_3364	-1.133	-2.193	0.000
glgP	-1.403	-2.644	0.000	gp42	1.145	2.212	0.000	pspB	-1.135	-2.196	0.000
glnA	-1.510	-2.849	0.000	SO_2689	1.137	2.200	0.000	gpG_2	-1.140	-2.204	0.000
cysP	-1.540	-2.909	0.000	SO_2969	1.137	2.199	0.000	SO_3910	-1.142	-2.206	0.002
glnG	-1.564	-2.957	0.000	nrdD	1.132	2.192	0.001	pspC	-1.152	-2.222	0.001
cysJ	-1.616	-3.066	0.000	R	1.106	2.152	0.000	cysW_2	-1.158	-2.231	0.000
glgX	-1.666	-3.174	0.000	emrD	1.087	2.125	0.017	SO_4645	-1.164	-2.241	0.000
SO_0547	-1.681	-3.208	0.000	SO_2972	1.072	2.102	0.000	cysA_2	-1.166	-2.243	0.000
malQ	-1.815	-3.519	0.000	S	1.060	2.085	0.000	SO_1976	-1.167	-2.246	0.000
glgB	-2.005	-4.014	0.000	SO_2970	1.046	2.065	0.000	pdsO	-1.179	-2.264	0.002
glnK_1	-2.020	-4.056	0.000	gpL	1.039	2.055	0.000	SO_2675	-1.183	-2.271	0.010
SO_0760	-2.244	-4.737	0.000	SO_2962	1.012	2.017	0.000	cysH	-1.184	-2.272	0.000
tnpA_114	-4.754	-26.980	0.000	SO_2963	1.007	2.010	0.000	SO_3410	-1.199	-2.297	0.000
nrfA	-12.927	-7,786.948	0.000	yceJ	1.005	2.007	0.002	glnL	-1.203	-2.301	0.000
napB	-13.219	-9,537.143	0.000	mtrC	-1.073	-2.104	0.000	SO_3743	-1.211	-2.315	0.000
napA	-13.499	-11,578.748	0.000	modA_1	-1.088	-2.126	0.000	SO_2688	-1.212	-2.317	0.000
ccpA	-18.234	-308,383.729	0.000	SO_4520	-1.139	-2.202	0.000	gpI	-1.215	-2.322	0.000

Other up-regulated genes in the quadruple mutant encode the ornithinedecarboxylase speF, the putrescine transporter potE, two transposases, an uncharacterized protein, an outer membrane porin as well as the periplasmic tetraheme flavocytochrome IfcA. Of the four genes that were observed to be down-regulated with a fold change ≤ -4 (*glgB*, *glnK_1*, *SO_0760* and *tnpA_114*), none has been reported to have an influence on ET processes, so far.

Since the extracellular ET rate to ferric citrate dropped in the quintuple mutant compared to the quadruple mutant, the question arose whether a different behavior could be observed for some of the aforementioned 10 genes when comparing the quadruple and quintuple mutant with each other. Put differently, it was of interest if other factors apart from the deletion of *fccA* could have caused the observed decline of the ferric iron reduction rate. Out of these 10 genes, *napD*, *napG* and *napH* were equivalently overexpressed in both mutant strains. The seven other genes were down-regulated in the quintuple mutant compared to the quadruple mutant, but only *ifcA* has been proved to be involved in periplasmic electron transfer processes and the encoded protein contains a bound flavin cofactor (Dobbin et al. 1999).

Even though one could draw the conclusion that IfcA might have a pivotal part in improving the ET and increasing the flavin content in the periplasm, the comparison of the TPM values of *ifcA* and *fccA* divulges that *ifcA* expression amounts only to 11% of the *fccA* expression in the wild type and 7% in the quadruple mutant. With regard to *cctA*, *ifcA* expression accounts for 15% and 2% in the wild type and the quadruple mutant, respectively. Thus, it is doubtful that IfcA is responsible for the perceived 2.5-fold increase of periplasmic redox species.

3.1.7 Analysis of extracellular ET to electrode surfaces

So far, the experiments presented in this thesis used Fe(III)-citrate as electron acceptor, which represents a colloidal form of ferric iron that seems to be unable to cross the outer membrane (Shi et al. 2012). After the promising results obtained with the quadruple mutant using Fe(III)-citrate, this strain was tested in BESs (described in section 2.10.1) to study whether a similar improvement of the extracellular ET kinetics is detectable if a graphite fleece electrode is the only TEA.

The bioelectrochemical experiments were started at an OD of 0.5 using M4 medium and 50 mM lactate as the only carbon and electron source. Like the cell suspension assays using ferric iron citrate, these experiments revealed an acceleration of the ET in the quadruple mutant compared to the wild type, as visualized in Figure 18. Right from the start of the experiment, the quadruple mutant showed higher current densities and after 26.9 h it reached maximum current densities which were 23% higher than the wild type's. During the experiment duration of 48 h, the mutant generated in total 47.2% more current than the wild type.

In addition to tracking the current densities, the extracellular flavin content and the lactate consumption were measured after 24 and 48 h. After 24 h, shortly before reaching maximum current densities, no significantly higher flavin content could be detected in the mutant's supernatant in comparison to the wild type. However, after 48 h, the extracellular flavin concentration was 23.8% higher in the mutant BES compared to the wild type. The 17.2% higher lactate consumption of the quadruple mutant could be an indicator for an increased cell density after 48 h of growth, which, on the other hand, could be an explanation for the higher flavin concentration.
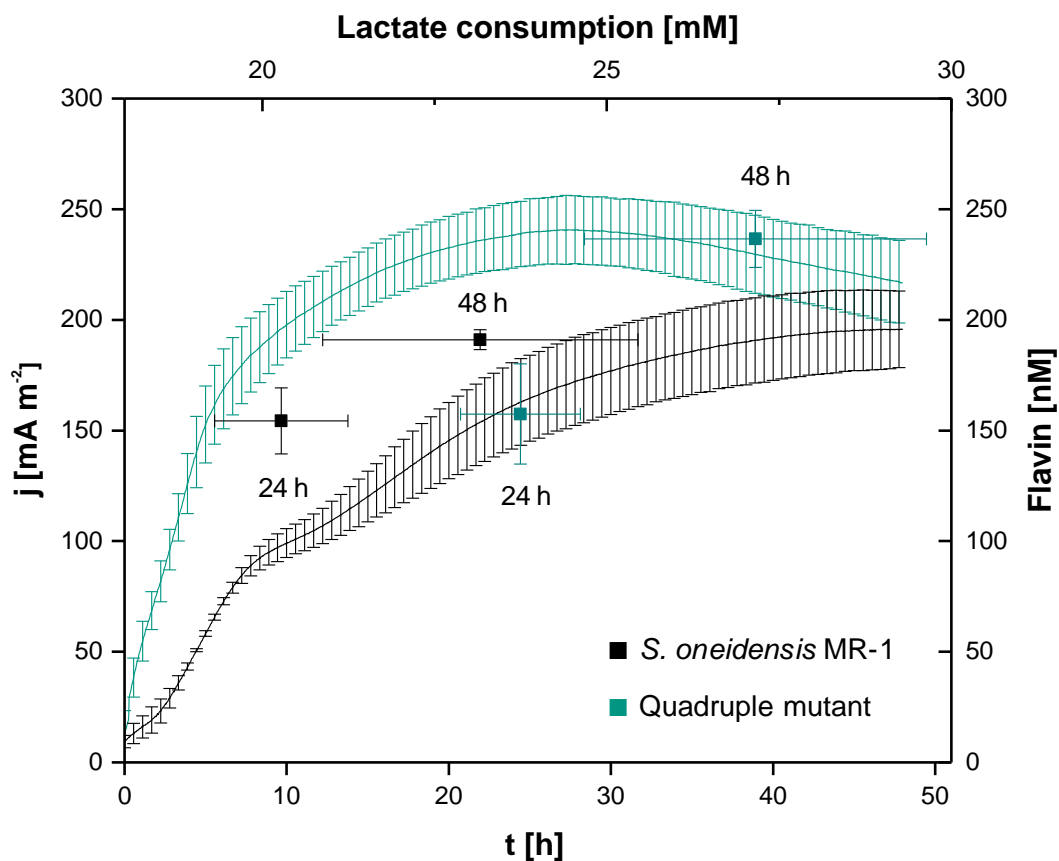
Figure 18: Current production, lactate consumption and extracellular flavin production of the quadruple mutant compared to the wild type using minimal medium containing 50 mM lactate as electron donor. A graphite fleece electrode was the only available electron acceptor. The black and green lines display the achieved current densities of wild type and quadruple mutant, respectively. The analogously colored squares represent the flavin concentration and the consumed lactate after 24 and 48 h.

The quintuple mutant was also tested in BESs (see Figure 19). As expected after the results in section 3.1.4, the total current production was lower than the current produced with the quadruple mutant and even the wild type produced more current when using a graphite electrode as electron acceptor. In particular, the quintuple mutant produced 58.3% less current compared to the quadruple mutant and 38.6% less in comparison to the wild type. These experiments also confirmed the crucial role of FccA in the electron transfer.
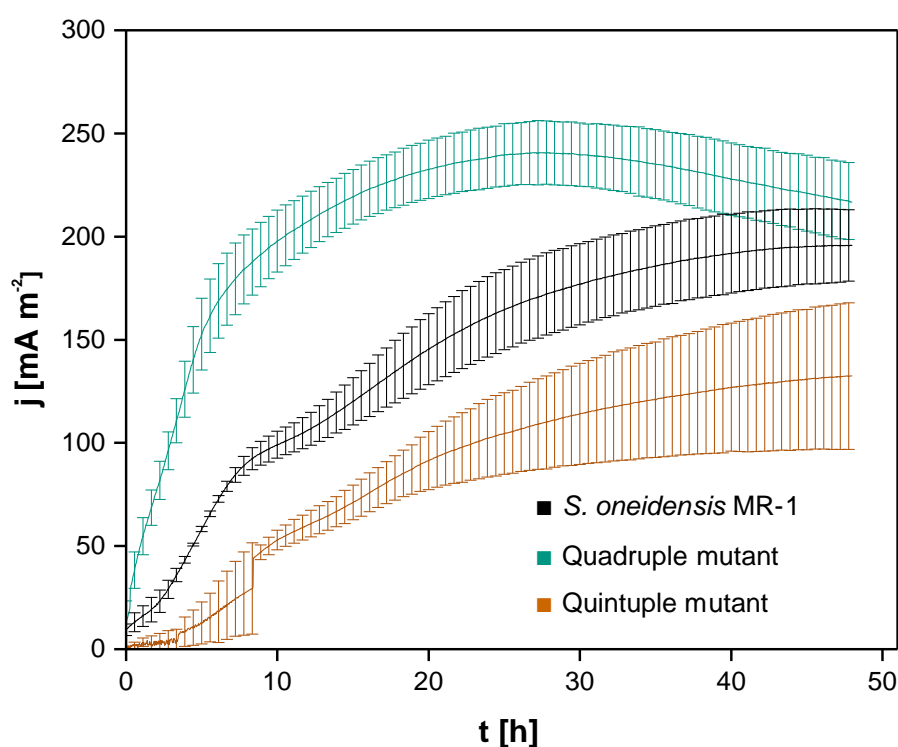
Figure 19: Current production of the quintuple mutant compared to the wild type and the quadruple mutant using minimal medium containing 50 mM lactate as electron donor. A graphite fleece electrode was the only available electron acceptor. The brown, black and green lines display the achieved current densities of the quintuple mutant, wild type and quadruple mutant, respectively.

3.2 Facilitation of a new carbon and electron source: Glucose

As already mentioned in the introduction, *S. oneidensis* is known for preferably using small carbohydrates such as lactate and pyruvate as carbon and electron source. Since these substrates are rather expensive, the utilization of other cheaper substrates is a promising field of investigation for the development of new sustainable biotechnological applications. Based on previous works, three different strategies for facilitating the use of glucose as substrate were tested and compared in order to identify the most efficient approach under anoxic conditions.

The first strategy was the natural adaptation of *S. oneidensis* to glucose, the second was the knock out of the transcriptional repressor *nagR* and the last one was the insertion of the genes *glk* and *galP* from *E. coli* in order to initiate the ED pathway as depicted in Figure 20.
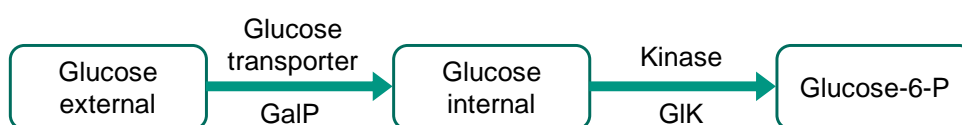
Figure 20: Schema of the glucose module introduced in *S. oneidensis.*

Derived from these strategies, the following strains were tested:

- *S. oneidensis* MR-1
- *S. oneidensis ΔnagR*
- *S. oneidensis glk_galP_pBAD202*

Before starting the experiments, all strains were cultivated identically: First, the strains were grown on LB agar plates, afterwards on LB agar plates supplemented with 20 mM glucose, then in LB solution supplemented with 20 mM glucose and, as last cultivation step, in M4 with Fe(III)-citrate as TEA and glucose as electron donor.

After these adaptations, growth experiments were started at an OD of 0.05 using M4, Fe(III)-citrate as TEA and glucose as electron donor. Figure 21 illustrates the results of the growth experiments, which clearly show that the strain containing the glucose module out-performs the other tested strains by far and that neither wild type nor *nagR* phenotype were able to reduce the ferric iron citrate completely when using glucose as substrate.
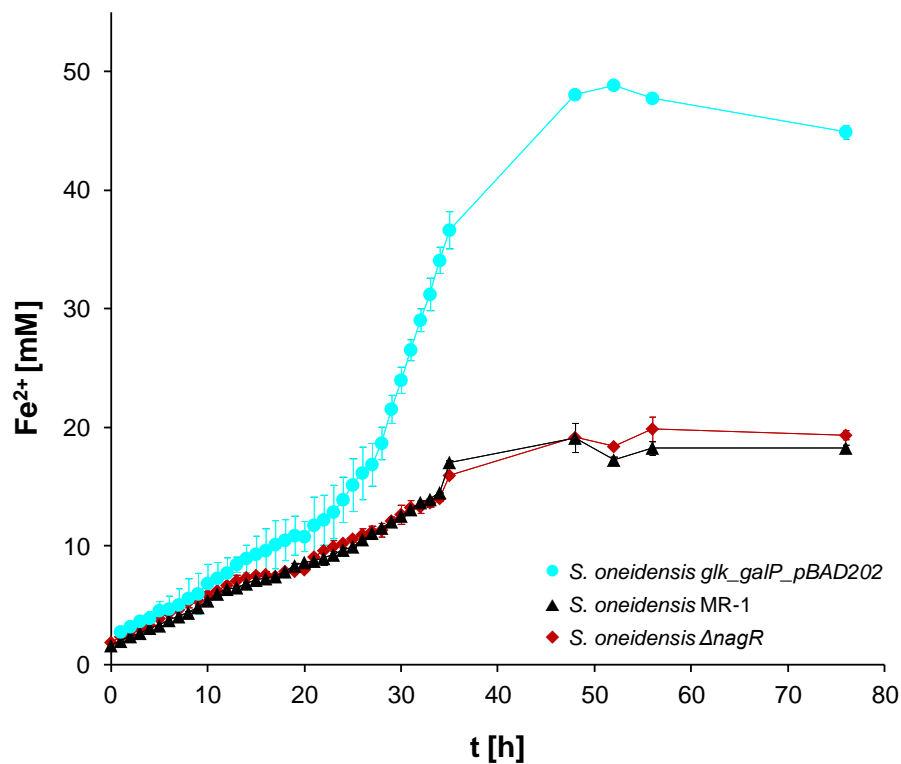
Figure 21: Growth experiments with *S. oneidensis* MR-1, *S. oneidensis ΔnagR* as well as the wild type containing the glucose module. All strains were previously adapted to glucose. The experiments were started at an OD of 0.05 using 50 mM glucose as carbon and energy source and 50 mM Fe(III)-citrate as TEA.

After these promising results, the glucose module was introduced into the quadruple mutant described in section 3.1 in order to test whether the previously shown improvement of the ET rate can also be observed when metabolizing glucose. As can be seen in Figure 22, the insertion of the glucose module into the quadruple mutant led to a faster ferric iron reduction compared to the strains tested before. More specifically, the quadruple mutant *glk_galP_pBAD202* revealed a 1.7-fold increased ferric iron reduction rate compared to *S. oneidensis glk_galP_pBAD202* and reached the maximal ferric iron reduction 23 h faster.
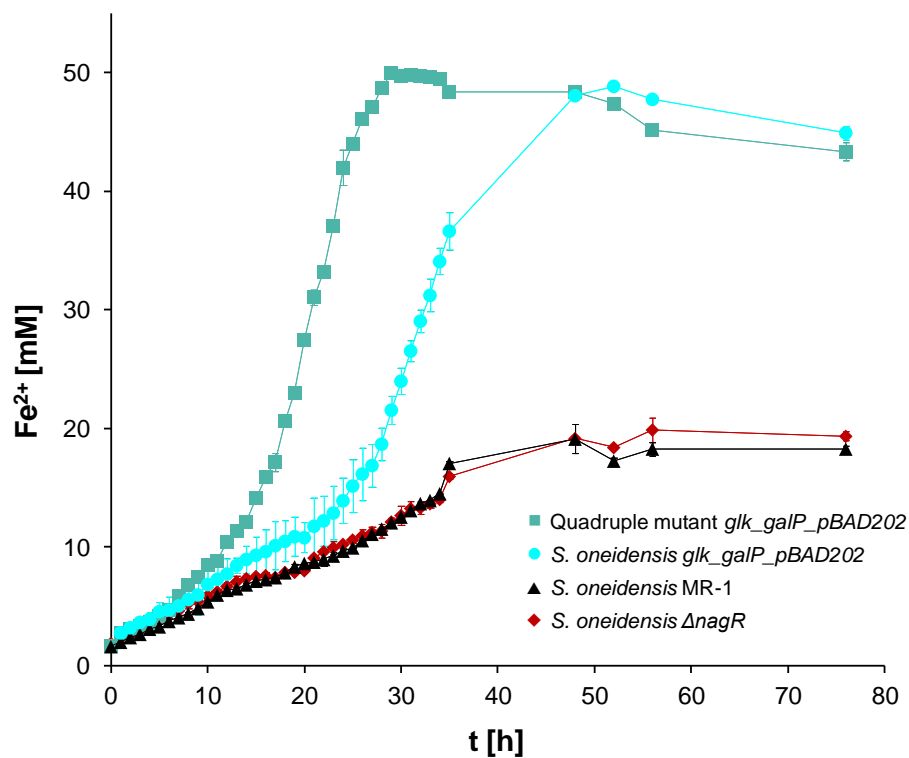
Figure 22: Growth experiments with *S. oneidensis* MR-1, *S. oneidensis ΔnagR* as well as the wild type and quadruple mutant containing the glucose module. All strains were previously adapted to glucose. The experiments were started at an OD of 0.05 using 50 mM glucose as carbon and energy source and 50 mM Fe(III)-citrate as TEA.

In order to quantify the glucose consumption, samples taken at 0, 10, 24 and 48 h were analyzed via HPLC (cf. section 2.9.1). As can be seen in Figure 23, the engineered strains containing the glucose module metabolized glucose more efficiently than the *nagR* phenotype or the naturally adapted wild type. The quadruple mutant containing the glucose module exhibits a 4.4-fold higher glucose consumption in comparison with the wild type after 24 h. Even though the final glucose consumption of both glucose module comprising strains was similar, the modified quadruple mutant demonstrated a faster glucose consumption at the beginning of the experiment, which resulted in a 2.3-fold higher glucose consumption of the quadruple mutant after 24 h. The observed increases in glucose metabolization correlate with the shown increases in the ferric iron reduction rates.
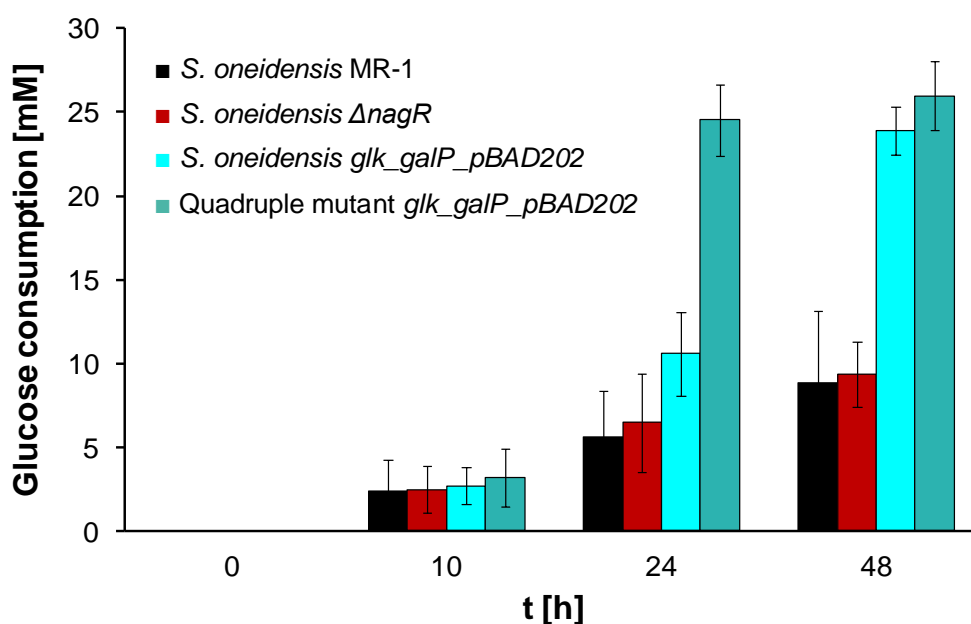
Figure 23: Glucose consumption during the growth experiments with *S. oneidensis* MR-1, *S. oneidensis ΔnagR* as well as the wild type and quadruple mutant containing the glucose module.

3.3 Production of itaconic acid using glucose as substrate

As already described in the introduction, *S. oneidensis* MR-1 is not able to produce itaconic acid naturally. To enable the production of itaconic acid using *S. oneidensis* could open doors for new biotechnological processes. Therefore, in this section, three developed strains for the production of IA based on glucose will be put to the test, combining the findings that *cadA* is pivotal for the production of IA and that a glucose consumption module consisting of *glk* and *galP* has been proven to be effective (section 3.2).

Additionally, the questions arose whether the production of undesired by-products could be suppressed by deleting the responsible genes and whether, thereby, the conversion potential could be shifted towards itaconic acid. This approach originates from *E. coli* studies of Okamoto and Harder (Okamoto et al. 2015; Harder et al. 2016), in which they aimed to facilitate and improve the production of itaconic acid. Therefore, three metabolic pathways were designed and tested:

1. The first strain comprises just the glucose module from *E. coli* and *cadA* from *A. terreus*, which should enable *S. oneidensis* to produce itaconic acid from glucose: *S. oneidensis glk_galP_cadA_pBAD202*. This strain will be called "GlucItac1" in the following.

2. Additionally, in the second strain, the genes *sucCD, aceA* and *pkyA* were deleted to avoid the formation of succinyl-CoA and glyoxylate as well as to disrupt the conversion of PEP to pyruvate:
   S. oneidensis ΔsucCD_ΔpykA_ΔaceA_glk_galP_cadA_pBAD202. In the following, this strain will be called "GlucItac2".

3. In the third strain, the genes *ptA* and *ackA* were also deleted to suppress the production of acetate:
   S. *oneidensis ΔsucCD_ΔpykA_ΔaceA_ΔptA_ΔackA_glk_galP_cadA_ pBAD202*. This strain will be called "GlucItac3" in the following.

Figure 24 depicts the designed metabolic pathway highlighting which genes were inserted and deleted. In order to study whether the designed strains are able to produce itaconic acid and the gene deletions have the intended effect, cell suspension assays were conducted.

Since so far published research on itaconic acid production only reported about successful strategies under oxic conditions (Okabe et al. 2009; van der Straat et al. 2014; Harder et al. 2016), the first series of experiments was also performed under oxic conditions. Subsequently, another series of experiments was performed under anoxic conditions with ferric iron citrate as electron acceptor in order to investigate in a first step if it could be possible to produce itaconic acid with these strains in BESs.

Figure 24: Designed metabolic pathway for the production of itaconic acid. Inserted genes are highlighted in blue and deleted genes are marked with a red cross.

3.3.1 Cell suspension assays under oxic conditions

In preparation for these experiments, the cells were cultivated previously in LB medium with 10 mM glucose and, afterwards, in M4 with 50 mM glucose as electron donor and atmospheric oxygen as electron acceptor. After this adaptation, the experiments were started with 50 mM glucose and atmospheric oxygen at an OD of 10.

The composition of samples taken during the cell suspension assays was analyzed via HPLC in order to determine the glucose consumption and to identify and quantify the chemical compounds produced throughout the experiment. In particular, the concentrations of acetate, citrate, itaconic acid, lactate, pyruvate and succinate were measured.

Figure 25 illustrates the development of the optical cell density of GlucItac1-3 with *S. oneidensis* MR-1 and *S. oneidensis pBAD202* as reference. During the first 5 h of the experiment, the OD of all strains remained more or less on the high initial level. However, after 5 to 7 h all strains showed a strong decrease in OD, whereby GlucItac3 dropped even faster than the reference strains. GlucItac1-3 reached a plateau OD after 20 h, while the OD of the reference strains continued to decrease.
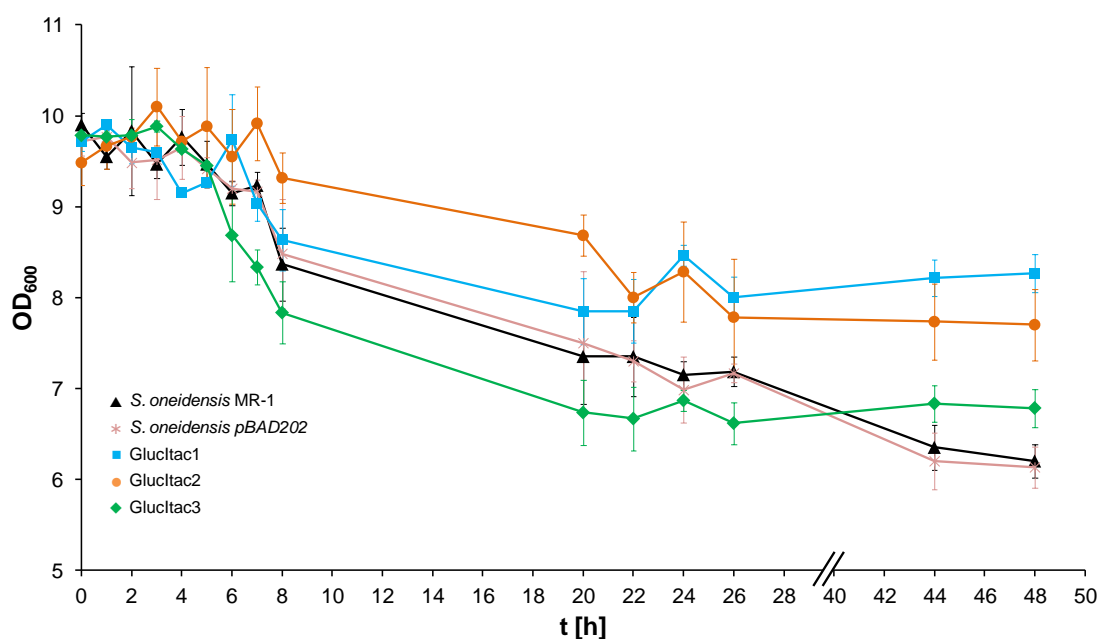
Figure 25: Development of the optical cell density measured during cell suspension assays in M4 with 50 mM glucose as substrate and atmospheric oxygen as electron acceptor started at an OD_{600} of 10. GlucItac1-3 are compared with *S. oneidensis* MR-1 and *S. oneidensis pBAD202*.

When comparing the glucose consumption (depicted in Figure 26) with the measured OD, it can be noted that the major glucose consumption of GlucItac1 (11.38 ± 1.20 mM) and GlucItac2 (12.94 ± 0.57 mM) took place within the first 5 hours of the experiment in which the OD was still on a high level.
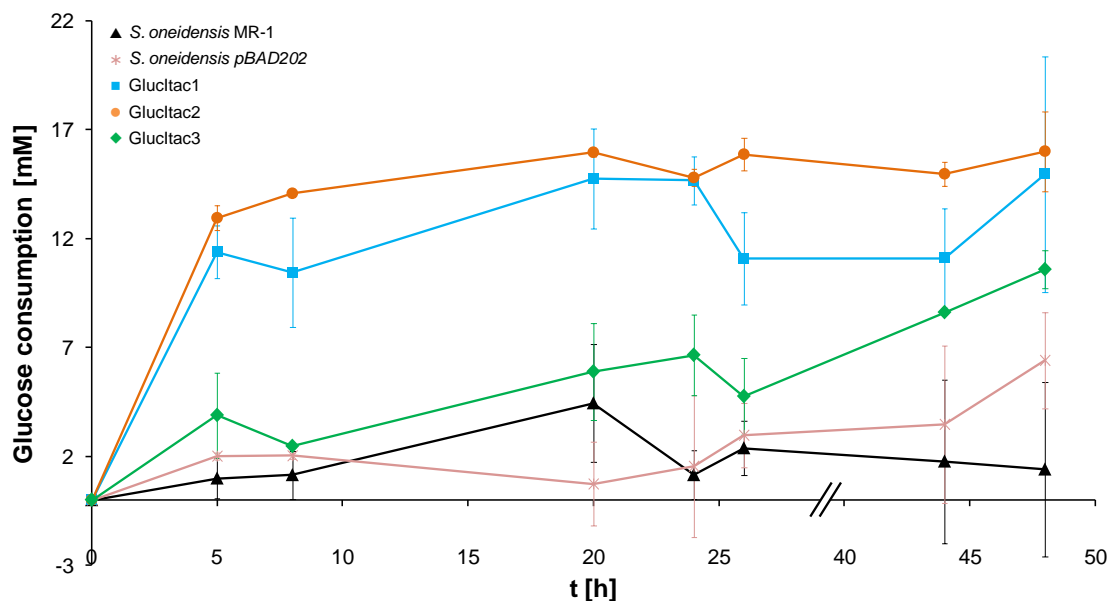
Figure 26: Glucose consumption in cell suspension assays under oxic conditions measured via HPLC. GlucItac1-3 are compared with *S. oneidensis* MR-1 and *S. oneidensis pBAD202*.

The highest acetate concentration was detected in GlucItac2: 4.82 ± 0.10 mM after 5 h and 6.79 ± 0.76 mM after 48 h. GlucItac1 began with only small concentrations and reached its peak concentration of 2.36 ± 0.72 mM after 44 h, while GlucItac3 did not show any noteworthy acetate concentrations. The reference strains, on the other hand, showed an inverse concentration development. Starting with their peak concentration at the 5 h measurement, both strains' acetate concentration diminished in the following. Figure 27 gives a graphical summary of all acetate measurements.
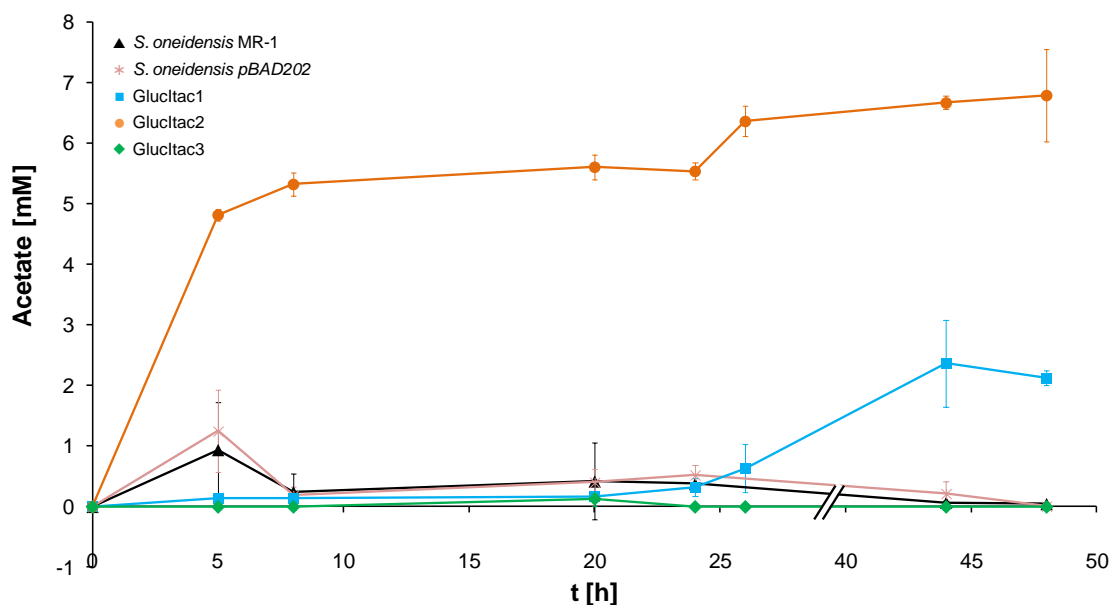
Figure 27: Production of acetate in cell suspension assays under oxic conditions measured via HPLC. GlucItac1-3 are compared with *S. oneidensis* MR-1 and *S. oneidensis pBAD202*.

In the case of citrate (Figure 28), it was only possible to detect small amounts for GlucItac1 throughout the whole experiment and for GlucItac3 at the beginning and at the end of the experiment. For the reference strains, notable quantities of citrate were only detected after 44 h. In GlucItac2 samples, no citrate could be quantified at all.
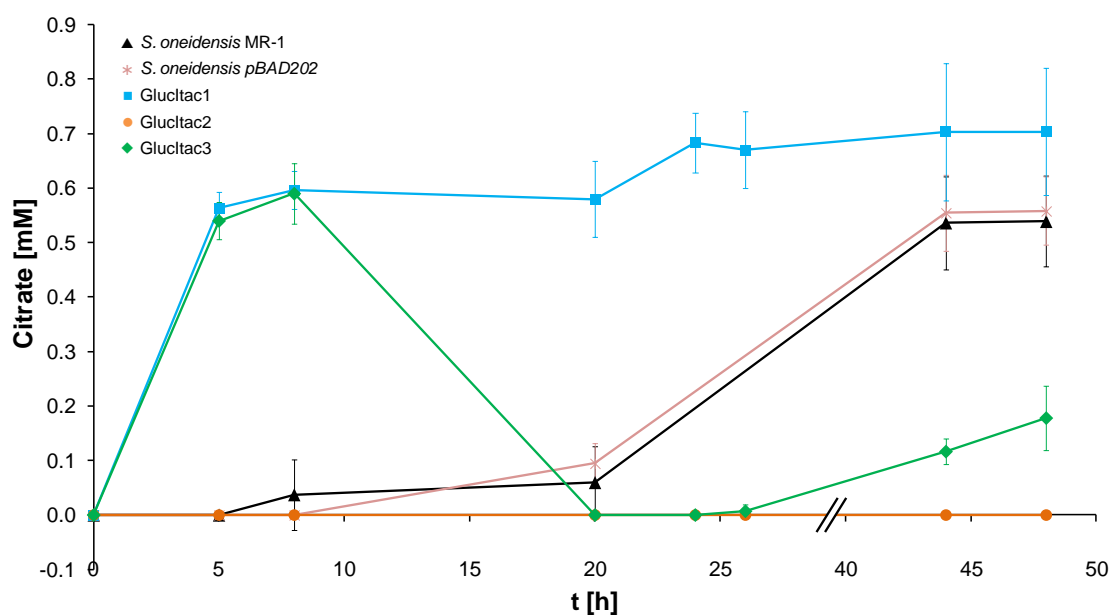
Figure 28: Production of citrate in cell suspension assays under oxic conditions measured via HPLC. GlucItac1-3 are compared with *S. oneidensis* MR-1 and *S. oneidensis pBAD202*.

The analyses of itaconic acid resulted in even lower concentrations than citrate (Figure 29). As anticipated, the reference strains were not able to produce itaconic acid but neither was GlucItac3. However, GlucItac1+2 presented a slight production of itaconic acid with a respective maximum concentration of 0.07 ± 0.06 mM and 0.30 ± 0.02 mM after 44 h. Even though these itaconic acid quantities are not able to compete with established itaconic acid production processes, still, they proof that the insertion of *cadA* enables the production of itaconic acid with *S. oneidensis*.

Apparently, the double-deletion of *ptA* and *ackA* in GlucItac3 led to an inhibition of itaconic acid production. From these results alone, it is not possible to identify unambiguously the reason for this inhibition. Future research might clarify whether the loss of energy or some unexpected interrelations between the deleted genes and *cadA* caused the observed effect. Also, future investigation could focus on integrating further genes that have been identified as key players for a more efficient synthesis of itaconic acid in other microorganisms (Okamoto et al. 2015; Vuoristo et al. 2015a; Tran et al. 2019).
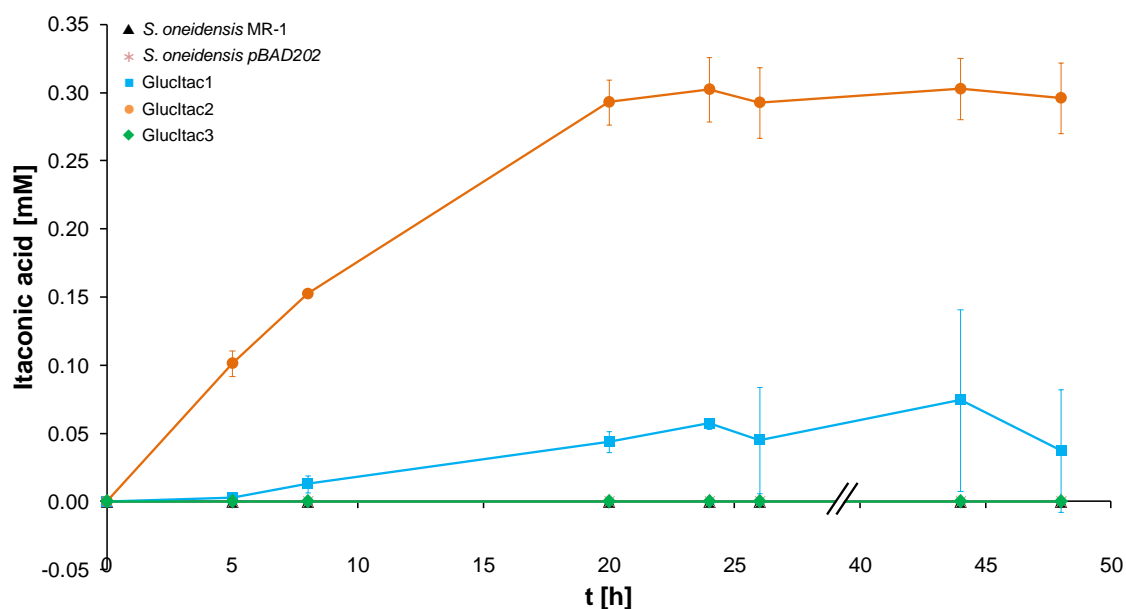
Figure 29: Production of itaconic acid in cell suspension assays under oxic conditions measured via HPLC. GlucItac1-3 are compared with *S. oneidensis* MR-1 and *S. oneidensis* pBAD202.

The identified lactate concentrations of GlucItac1 and GlucItac3 were of similar magnitudes as the citrate concentration and no lactate could be measured in the reference samples. Surprisingly, GlucItac2 began to produce considerable amounts of lactate. Starting with 9.09 ± 0.84 mM after 5 h, the concentration rose up to 23.83 ± 1.23 mM in the 20 h sample at which level the concentration stabilized for the rest of the experiment, as can be observed in Figure 30.

It seems that the combination of the deletions performed in GlucItac2 leads to a significant lactate production based on glucose under oxic conditions. Whether this behavior is only observable with glucose as substrate and whether one specific deletion is the trigger still has to be investigated.
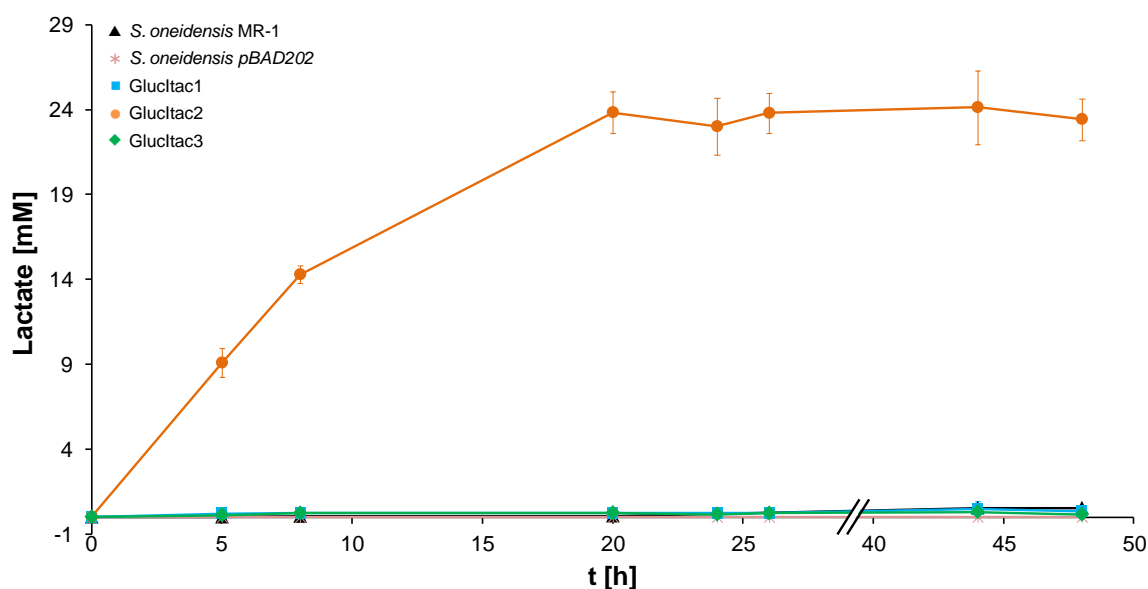
Figure 30: Production of lactate in cell suspension assays under oxic conditions measured via HPLC. GlucItac1-3 are compared with *S. oneidensis* MR-1 and *S. oneidensis pBAD202*.

Succinate was produced in similar quantities as acetate but from other strains (Figure 31). GlucItac2+3 were not able to produce succinate, which could be explained with the deletion of *aceA*. GlucItac1, however, produced a maximum of 9.58 ± 0.36 mM after 20 h, whereupon the concentration sank again. Both reference strains were able to produce small quantities of succinate during the first 24 h, after which a presence of succinate was not detectable anymore.
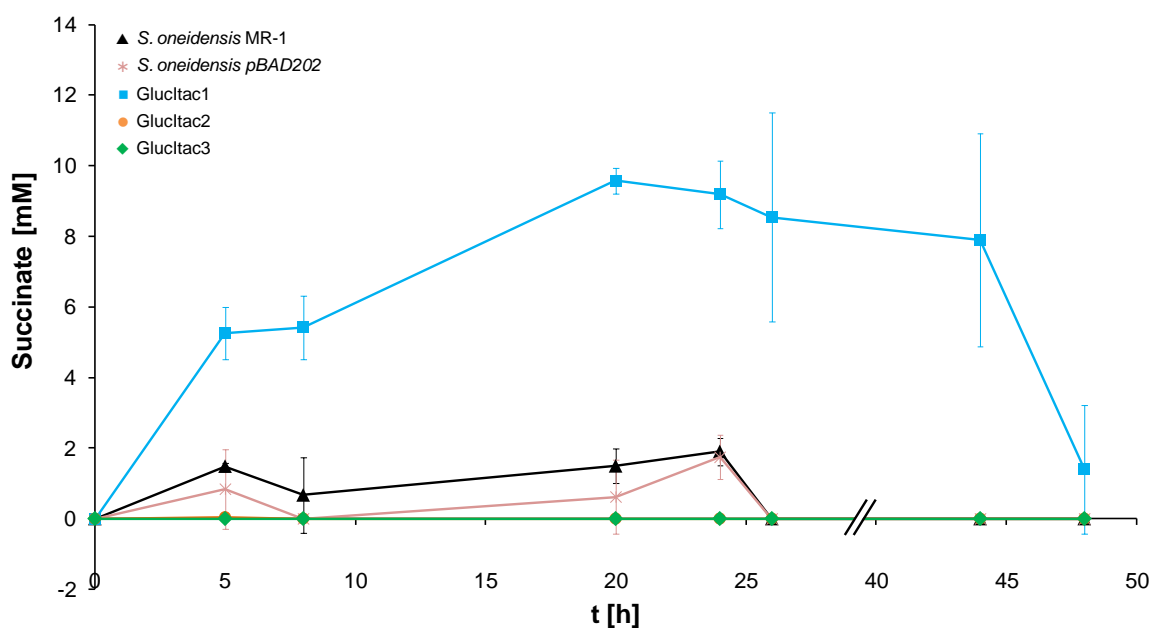
Figure 31: Production of succinate in cell suspension assays under oxic conditions measured via HPLC. GlucItac1-3 are compared with *S. oneidensis* MR-1 and *S. oneidensis pBAD202*.

The HPLC analysis of these experiments did not show any detectable pyruvate concentrations.

After these promising first results, anoxic cell suspension assays were carried out, as a first step towards a potential application in BESs.

3.3.2 Cell suspension assays under anoxic conditions

The cell suspension assays were prepared as already described in section 3.3.1 and started at an OD of 10 under anoxic conditions using 50 mM glucose as electron donor and 50 mM ferric iron citrate as terminal electron acceptor. As can be seen in Figure 32, the strains GlucItac1-3 were able to reduce ferric iron citrate completely, while *S. oneidensis* MR-1 and *S. oneidensis pBAD202* showed only a minimal reduction. Even though GlucItac1-3 were able to reduce ferric iron citrate completely, differences in the electron transfer rates could be observed. GlucItac1 had a higher electron transfer rate (1.07 mM min^{-1}) compared to GlucItac2 (0.40 mM min^{-1}) and GlucItac3 (0.36 mM min^{-1}).
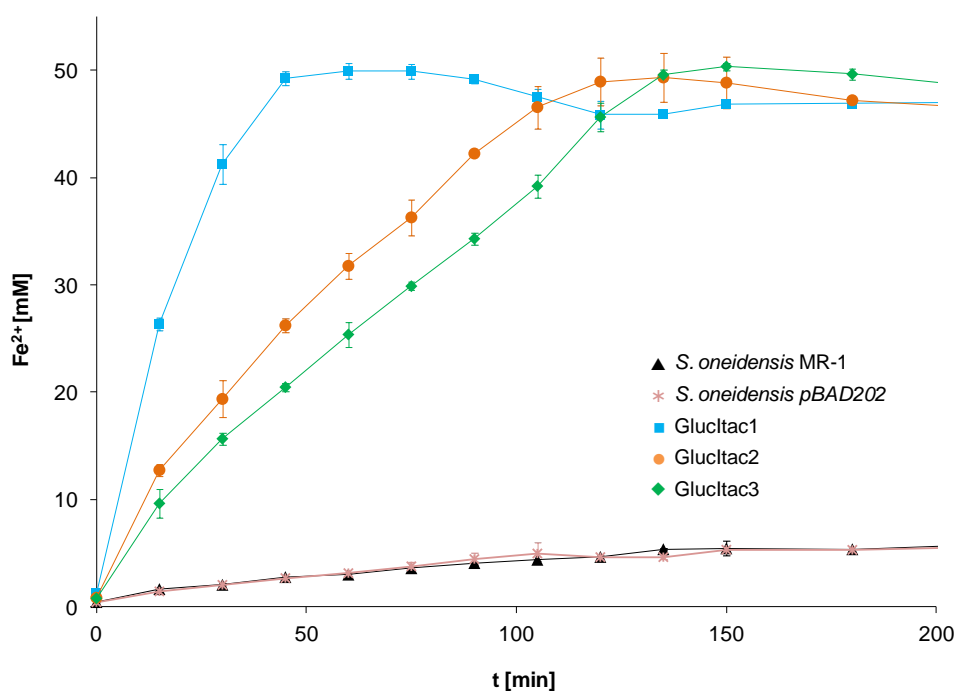
Figure 32: Ferric iron reduction of *S. oneidensis* MR-1, *S. oneidensis pBAD202* and GlucItac1-3. The cell suspension assays were started at an OD of 10 under anoxic conditions with 50 mM ferric iron citrate as TEA and 50 mM glucose as carbon and electron donor.

While the reference strains (*S. oneidensis* MR-1 and *S. oneidensis pBAD202*) were not able to consume a significant amount of glucose within the first 8 hours of the experiment, the strains GlucItac1-3 consumed 35.76 to 43.07 mM

glucose (Figure 33). GlucItac1 and GlucItac2 consumed the glucose in the first hour, whereas GlucItac3 presented a more gradual consumption over the first two hours.

After the first two hours, no noteworthy further glucose consumption took place, which correlates with the measured ferric iron reduction rate that reached its peak after roughly 2 h in case of GlucItac1-3.
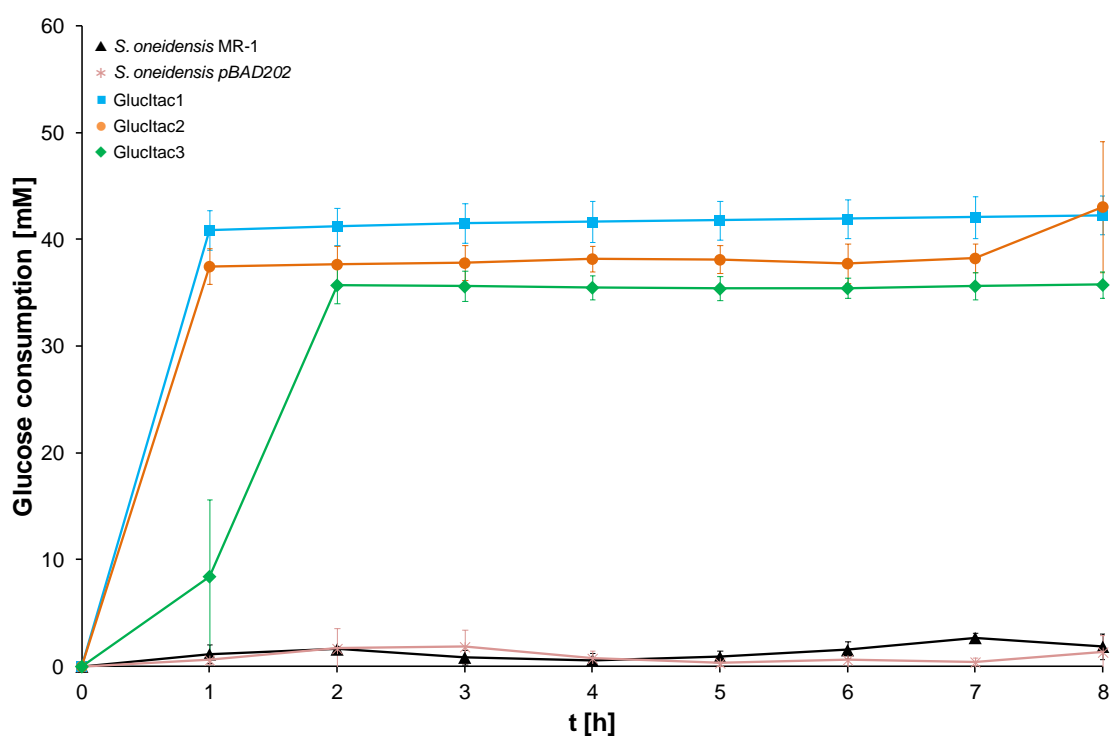
Figure 33: Glucose consumption in cell suspension assays under anoxic conditions measured via HPLC. GlucItac1-3 are compared with *S. oneidensis* MR-1 and *S. oneidensis pBAD202*.

Still, although all developed strains showed considerable ferric citrate consumption, it was not possible to detect any itaconic acid, which might have to do with the downregulation of the citric acid cycle by *S. oneidensis* under anoxic conditions.

4. Discussion

4.1 Improvement of the ET rate in *S. oneidensis* MR-1

The research performed in the course of the first sub-project of this thesis revealed that an overexpression of STC in combination with the reduction of complexity of the periplasmic electron transfer network results in a 1.7-fold increase of the ET rate when using ferric iron citrate or an anode as TEA. Earlier studies showed that an overexpression of the heterotrimeric outer membrane protein complex can lead to an increase of the ET rate, which appears to be a logical consequence since this overexpression causes a higher concentration of the terminal reductase on the cell surface (Golitsch et al. 2013). Still, it remains to be clarified why changes of the redox species configuration in the periplasm increase the ET rate. There are two hypotheses which might elucidate the observed phenomenon of ET acceleration:

In a first scenario, the redox gradient between CymA and the TEA could have been altered by simplifying the periplasmic network of electron transporting proteins and by overexpressing STC, which most likely evolved to bridge the periplasmic gap between CymA and MtrA. Put differently, imagining a simple picture in which the MtrABC complex has periplasmic electrons and ferric iron (or an anode) as substrates, the kinetics of the enzyme complex was increased by augmenting the availability of one of these two substrates. Based on the findings that STC has to change its localization in order to interact with CymA and MtrA and, therefore, a sort of shuttling process has to take place (Alves et al. 2015), one could assume that an increase of STC expression could lead to a higher frequency in which STC interchanges its electrons with MtrA. Figure 34 illustrates this assumed shuttling process. Besides, one could assume that the low molecular weight of STC (12.26 kDa) could allow an easy and, therefore, fast shuttling through the periplasm to transport the electrons from the inner to the outer membrane.
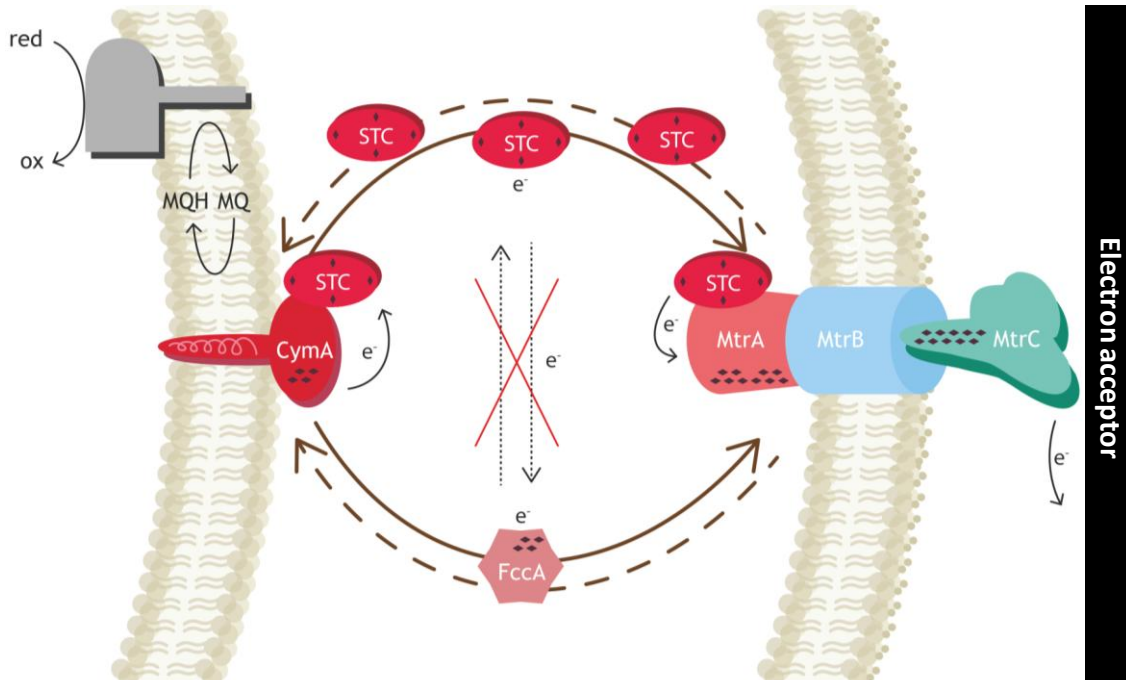
Figure 34: Scheme of electron shuttling between the cytoplasmic membrane cytochrome CymA and the outer membrane protein complex MtrABC via STC and FccA. Brown arrows with continuous lines represent movements with electrons and the arrows with dashed lines represent movements without electrons.

The results of the quintuple mutant experiments would also underpin this hypothesis. As confirmed via transcriptomic analysis, the overexpression of STC could not be further increased by deleting *fccA* and inserting *cctA* in its locus. In fact, the additional deletion of *fccA* led to a reduction of the *cctA* fold-change by 0.21 when comparing the quadruple and the quintuple mutant with the wild type. Furthermore, the deletion of *fccA* led to a decrease of the periplasmic heme and flavin concentration. Based on the measured periplasmic heme concentration, a hypothesis formulated in section 3.1.4 assumed that the substitution of FccA with STC did not lead to the expected increase in STC expression. This assumption is confirmed by the above mentioned finding that the STC expression even decreased in the quintuple mutant compared to the quadruple mutant. Thus, deleting *fccA* resulted in a reduction of periplasmic electrons available for the MtrABC complex. When comparing the periplasmic

heme and overall redox species content of the quintuple mutant and the wild type, only a – if any – slight increase could be observed in the quintuple mutant, which might be the reason for the similar Fe(III)-citrate reduction rates.

The second hypothesis is that the availability of flavins as cofactors for outer membrane cytochromes could have been increased. Still, even though the cells were washed and put into fresh medium before starting the cell suspension assays, these experiments showed higher ferric iron reduction rates. Therefore, it seems doubtful that the flavins could function exclusively as electron shuttles. However, the outer membrane cytochromes could potentially acquire more flavins while migrating through the periplasm due to the high periplasmic flavin concentration, which was detected through cycling voltammetry experiments. The enrichment of the MtrABC complex with periplasmic flavins could lead to the observed enhancement of the ET rates (illustrated schematically in Figure 35).
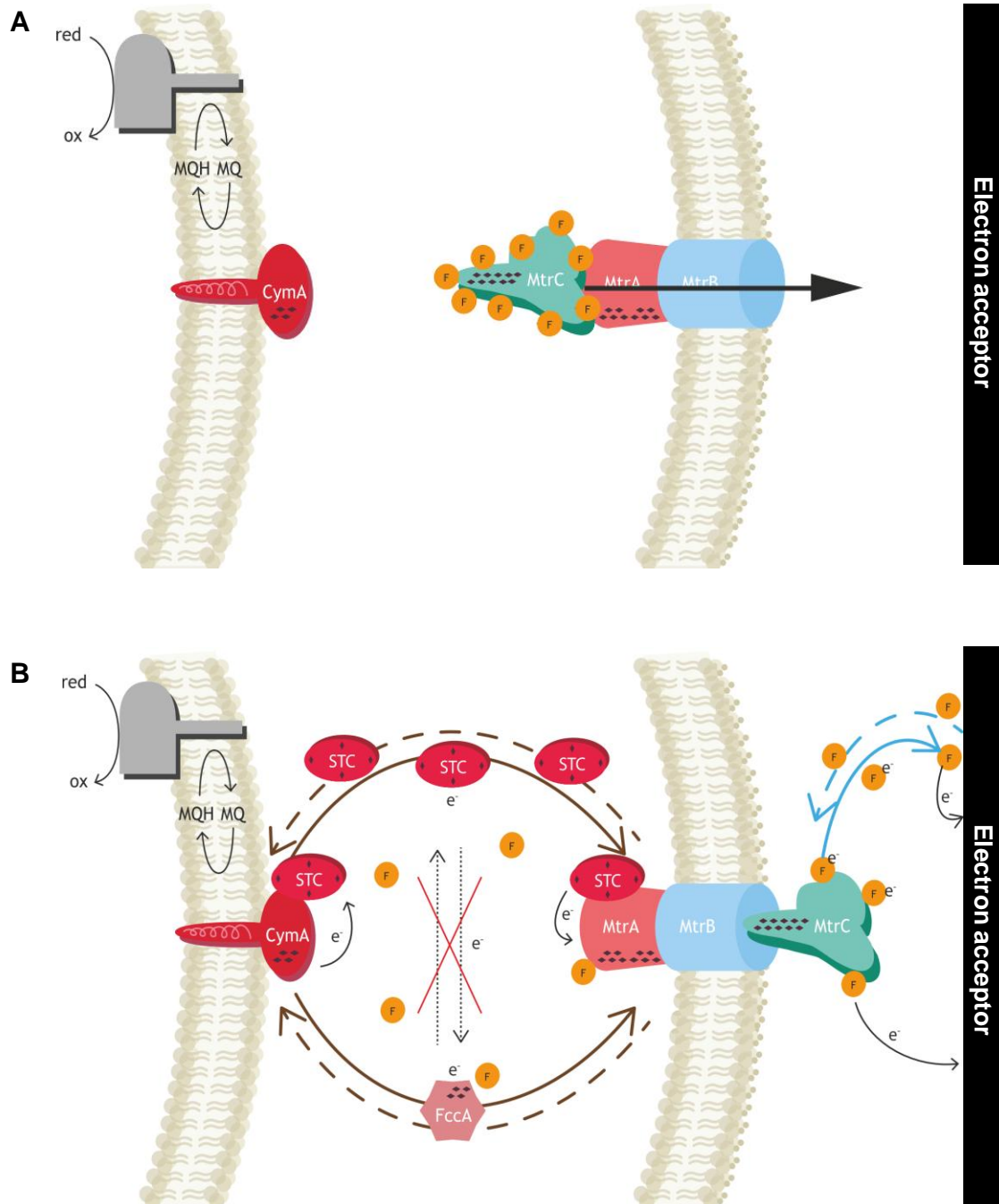
Figure 35: Scheme of electron transfer facilitation via flavins. **A:** MtrC acquires periplasmic flavins as cofactor during its migration towards the outer membrane. **B:** MtrC has reached its final position and flavins act as electron transferring cofactors and as electron shuttles between MtrC and the electron acceptor. Brown arrows with continuous lines represent movements of cytochromes with electrons and the arrows with dashed lines represent movements without electrons. The blue arrow with continuous line represents flavins transporting electrons, while a dashed line indicates a movement without electrons. Black arrows illustrate the transfer of electrons.

Previous studies showed that the most important periplasmic cytochromes regarding ET are STC and FccA and it was suggested that both cytochromes could have redundant or at least similar functions (Fonseca et al. 2013; Sturm et al. 2015). In this thesis, it was possible to proof that both cytochromes do not have completely redundant functions. This was demonstrated by comparing the quintuple mutant, in which FccA had been replaced with STC, with the quadruple mutant and *S. oneidensis* MR-1 in various experiments. In particular, these three strains were tested in anoxic cell suspension assays with ferric iron citrate and fumarate as TEA as well as in anoxic BES experiments with a graphite fleece electrode as anode. In the case of ferric iron citrate and a graphite anode, it was possible to see that the replacement of FccA caused a decrease of the ET rate.

To put it in a nutshell, a chassis strain with high efficiency regarding ET has been created. Recent, still ongoing research of AG Gescher revealed that it is possible to improve the ET rate further by combining the created chassis strain with an overexpression of the outer membrane complex MtrABC.

4.2   Facilitation of a new carbon and electron source: Glucose

The work on the second sub-project confirmed that the insertion of a glucose consumption module consisting of the transporter GalP and the kinase Glk from *E. coli* enables *S. oneidensis* to use glucose as a substrate as was already shown by Nakawaga and colleagues (Nakagawa et al. 2015). Integrating this glucose module into the quadruple mutant developed in the first sub-project led to an increased glucose consumption and ET rate in comparison to the naturally adapted wild type and the wild type comprising the glucose module.

At the beginning of the research on this sub-project, three approaches to facilitate glucose consumption were chosen for testing: First, the natural adaptation (Biffinger et al. 2008; Biffinger et al. 2009; Howard et al. 2012) of the wild type, second, the deletion of the transcriptional repressor NagR (Chubiz and Marx 2017) and, third, the insertion of the transporter GalP and the kinase GlK from *E. coli* (Nakagawa et al. 2015). Besides *E. coli* there are also other microorganisms such as *Zymomonas mobilis* (Choi et al. 2014a) possessing a similar glucose transporter and kinase. For the present study, the enzymes from *E. coli* were chosen because of the organism's phylogenetic relatedness to *Shewanella*.

The naturally adapted wild type strain showed only a low glucose consumption of 8.84 ± 4.31 mM within 48 h and, thus, had the lowest glucose consumption of all tested strains. Deleting *nagR* led to a strain with very low glucose consumption and ferric iron reduction rates under anoxic conditions similar to the adapted wild type. Hence, the positive effect of deleting *nagR* reported by Chubiz and Marx (Chubiz and Marx 2017) most likely only occurs under oxic conditions.

Both mutants containing the glucose module showed far better ferric iron reduction and glucose consumption behaviors. *S. oneidensis glk_galP_pBAD202* was able to reduce ferric iron citrate completely after 48 h and the quadruple mutant *glk_galP_pBAD202* even after 29 h, which implies a 1.7-fold improvement of the ET rate when comparing these two strains. This improvement of the ET rate coincides with the observed ET rate improvement when using lactate as carbon and electron source.

These promising results could be key for the use of complex molecules from sustainable and environmentally friendly sources. In the last years, environmental protection has become the focus of attention for many research projects due to the escalating climate crisis and a raising global awareness of the finite nature of the resources our current industry is built on. One of the most abundant organic compounds on Earth is cellulose, which is primarily originating from plants and is readily available in great quantities in form of agricultural wastes.

Cellulose is composed of linear chains of roughly 8,000 to 12,000 residues of D-glucose bound by β-1,4 bonds (Timell 1967; Aro et al. 2005). The monomeric unit of cellulose is glucose and the repetitive structural unit of the chain is the dimer cellobiose (Brown et al. 1996). Internal hydrogen bonds stabilize the flat structure of cellulose chains and the synergy of hydrogen bonds and van der Waals forces allow parallel cellulose chains to interact, resulting in very extensive and crystalline aggregates called microfibriles (Somerville et al. 2004; Glazer and Nikaido 2008). In one cellulose chain, all alternate glucose residues are rotated 180°.

In order to pave the way for the use of cellulose as a substrate for the production of platform chemicals with *Shewanella*, a multi-step strategy seems to be suitable (illustrated in Figure 36): First of all, the cellulose has to be transported into the cell. Afterwards, it has to be broken down into cellobiose, whereupon the cellobiose has to be broken down into glucose which, then, can be metabolized by *Shewanella* as shown in this thesis. Due to the high complexity of this strategy, a reverse approach is advisable. The consumption of glucose has already been facilitated. Hence, the next step would be to enable *Shewanella* to transport cellobiose into the cell and break it down.

It has been shown that β-glucosidases are necessary for the hydrolyzation of cellobiose into glucose, once the cellobiose has entered the cell. Therefore, different transporters and β-glucosidases would have to be tested in *S. oneidensis* to identify the most suiting and efficient enzymes. Some examples for microorganisms capable of metabolizing cellobiose are *Clostridium cellolyticum* (Fierobe et al. 1991) and *Lactococcus lactis*

(Rosenbaum et al. 2011). Searching for the best suited enzymes, one must have in mind that *Shewanella* operates at temperatures around 30⁰C, hence, the chosen enzymes would have to be active at this temperature as well.

After achieving this milestone, the next challenge would be to find an efficient and fast way to import cellulose and to hydrolyze the β-1,4-linkages of the cellulose structure in order to obtain cellobiose.
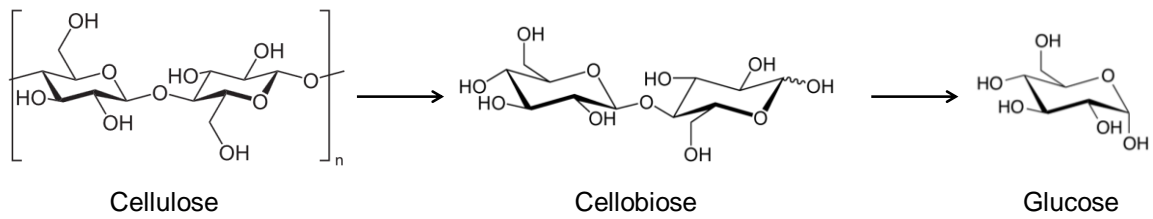
Figure 36: Schematic of break down steps of cellulose to glucose.

4.3   Production of itaconic acid using glucose as substrate

For the experiments of the third sub-project, the basic idea was to insert the *cadA* gene from *A. terreus* for itaconic acid production as well as the transporter GalP and the kinase Glk from *E. coli* for glucose utilization into the plasmid *pBAD202*. CadA is a *cis*-aconitate decarboxylase which has been demonstrated to enable the production of itaconic acid in *A. terreus* (Bentley and Thiessen 1957a, 1957b, 1957c; Bonnarme et al. 1995; Dwiarti et al. 2002) and in other microorganisms after its insertion (van der Straat et al. 2014; Vuoristo et al. 2015a; Otten et al. 2015; Okamoto et al. 2015; Geiser et al. 2016). Furthermore, various gene deletions were performed with the goal of increasing the production of IA through minimization of the production of by-products. The created mutant strains GlucItac1-3 were tested under oxic and anoxic conditions together with the wild type and *S. oneidensis pBAD202* for reference.

The oxic cell suspension assays were performed at an initial OD of 10 with glucose as carbon and electron source and atmospheric oxygen as electron acceptor.

For anoxic experiments with ferric iron citrate as TEA, it was easy to determine the period of time that is needed for the main reaction to take place because at some point of time all of the electron acceptor is reduced. However, this is not the case for the conducted oxic experiments with atmospheric oxygen, which is why an experiment duration of 48 h was chosen.

The total glucose consumption measured throughout the experiment amounted to only 10.58 to 16.00 mM in case of the GlucItac mutants and 1.41 to 6.41 mM in case of the reference strains. The major glucose consumption of GlucItac1+2 took place within the first 5 h of the experiment, which correlates with a more or less constant OD in this period of time. Afterwards, the OD of all tested strains began to decrease and only slight glucose consumptions could be detected.

Most likely, the reason for this less efficient glucose consumption is the decreasing pH value. *Shewanella oneidensis* works optimally at a pH between 7.0 and 7.5. However, the pH sank to values around 6.7 during these experiments, which causes hampered conversion rates. New media could be

put to the test in order to avoid this decrease of pH via applying high buffering. Another possible explanation could be that the atmospheric oxygen was only in contact with the surface of the medium and, therefore, fewer cells could be in contact at the same time. Experiments with a longer duration, larger medium surface or aeration could validate this hypothesis but could not be performed within the scope of this thesis.

The – in comparison with the other tested strains – relatively high acetate concentration of 6.79 ± 0.76 mM after 48 h could be seen as an indicator for the disruption of the TCA cycle in GlucItac2 under oxic conditions. It could be that the conversion of acetyl-CoA to acetate is favored over the conversion to citrate because the cell gains energy in form of 1 ATP. This assumption seems to be underpinned by the results of the measurements of the other chemical compounds.

In contrast to all other strains, it was not possible to detect citrate in GlucItac2 samples, which could either be a sign that all produced citrate was converted into other compounds (e.g. itaconic acid) or that there was no citrate production at all. The other strains showed only small citrate concentrations below 1 mM.

Unfortunately, it was not possible to produce larger quantities of itaconic acid, but the small concentrations in GlucItac1+2 can be considered as proof of concept that the introduction of *cadA* into *Shewanella* can facilitate itaconic acid production. Besides, the presence of itaconic acid in GlucItac2 samples indicates that the TCA cycle has not been completely inhibited as hypothesized above. Independently of the mutant strain, an optimization of the *cadA* codon could probably enhance the synthesis of itaconic acid.

Apparently, the double-deletion of *ptA* and *ackA* in GlucItac3 led to an inhibition of itaconic acid production, but from these results alone, it is not possible to identify unambiguously the reason for this inhibition. Future research might clarify whether the loss of energy or some unexpected interrelations between the deleted genes and *cadA* caused the observed effect.

The unexpectedly high production of lactate with GlucItac2 could be a further indication that deletions of *sucCD*, *pykA* and *aceA* led to a disruption of the TCA

cycle and, thus to a shift of the conversion potential in this mutant strain. Either way, the small lactate concentration measured in GlucItac1 samples indicates that even without the deletions performed in GlucItac2 an, at least, low lactate production is possible. Looking at GlucItac3, the question arises why this strain could not produce lactate similarly to GlucItac2. As described earlier, the two additional deletions of *ptA* and *ackA* most probably result in a loss of cell energy which, in turn, might block the production of chemical compounds because the cell needs the remaining energy for survival.

The primary strategy for further work with GlucItac2 would be to avoid the formation of lactate by deleting the putative fermentative NADH-dependent D-lactate dehydrogenase ldhA, which has been proven to be a crucial enzyme for the conversion of pyruvate to lactate (Pinchuk et al. 2008). Another strategy could be to enhance the already high lactate production by deleting *nagR*. This deletion could be beneficial because it can be assumed that some of the produced lactate is metabolized since lactate is one of the preferred substrates of *Shewanella*. A deletion of *nagR* should avoid this metabolization or at least slow it down. Nevertheless, there are already highly efficient processes for lactate production in place and a further pursue of this approach seems not recommendable (Bai et al. 2003).

GlucItac1 was the only tested strain that was able to produce notable amounts of succinate with a maximum concentration of 9.58 ± 0.30 mM. It is not surprising that GlucItac2+3 did not produce any succinate because the deletion of *aceA* prohibited the conversion of isocitrate to succinate. The presence of succinate in the GlucItac1 samples point towards a functioning TCA cycle in this strain, which also allows for the production of small amounts of itaconic acid.

To summarize the findings of the oxic cell suspension assays, it can be stated that the general concept of introducing *cadA* from *A. terreus* into *S. oneidensis* in order to produce itaconic acid has been proven, even though the produced quantities cannot compete with other microorganisms, yet. GlucItac2 can be considered the most promising strain for successive research.

Like the oxic cell suspensions assays, the anoxic experiments were started at OD 10 with glucose as carbon and electron source but ferric iron citrate was used as electron acceptor instead of atmospheric oxygen.

While the reference strains only reduced small amounts of the electron acceptor (approximately 5 mM), all GlucItac mutants were able to reduce the ferric iron citrate completely within the first 2.5 h. Nevertheless, significant differences between the individual mutants could be observed: GlucItac2+3 developed similarly, reaching maximum ferric iron reduction after 135 min and 150 min, respectively. In contrast, GlucItac1 reached the peak reduction after only 45 min and, thereby, presented a 2.66-fold increased ferric iron reduction rate compared to GlucItac2 and 2.95-fold compared to GlucItac3. Hence, the deletion of the genes *sucCD*, *pykA, aceA, ptA* and *ackA*, which was intended to minimize by-product formation, seems to have the side effect of slowing down the ferric iron reduction. A possible explanation for this effect might be that by deleting these genes, the cells lost to some extent their capability of forming ATP and NADH, which could have led to a loss of cell energy.

Since glucose was the sole carbon and electron donor, the analysis of the ferric iron reduction led to the assumptions that the reference strains would not consume significant amounts of glucose, that GlucItac1 would show the main glucose consumption within the first hour and that GlucItac2+3 would take roughly 2 h for their major glucose consumption. This hypothesis was verified via HPLC analysis, which confirmed in general the expected development of glucose concentrations in the samples but, in case of GlucItac2, also entailed a surprise. Instead of taking 2 h for the major glucose consumption, the glucose consumption velocity of GlucItac2 was equally fast as GlucItac1's. The experiments conducted throughout this study could not explain the fast glucose consumption of GlucItac2 sufficiently, wherefore further investigation would be needed for clarification.

Unfortunately, it was not possible to produce detectable amounts of itaconic acid under anoxic conditions. This concurs with the fact that – to the author's best knowledge – no anoxic production of itaconic acid has been reported in the

literature so far. This hypothesis gains plausibility considering reports about the citric acid cycle being partly inactive under anoxic conditions (Tang et al. 2007).

All in all, the anoxic cell suspension assays did not lead to the expected results. Probably, the carbon and energy obtained from glucose were mainly used for biomass formation instead of chemical production or the cells were not able to transport products out of the cell. Based on the findings presented in this thesis and the so far reported attempts to produce itaconic acid, it can be concluded that further attempts to produce itaconic acid with *S. oneidensis* should focus on oxic processes.

Future investigation could focus on integrating further genes in *Shewanella* that have been identified as key players for a more efficient synthesis of itaconic acid in other microorganisms (Okamoto et al. 2015; Vuoristo et al. 2015a; Tran et al. 2019). More specifically, the citrate synthase GltA from *Corynebacterium glutamicum* and the aconitase synthase AcnA from *E. coli* could improve the currently very low production of itaconic acid. GltA has been shown to catalyze the reaction from oxaloacetate to citrate in the TCA cycle. AcnA has been reported to catalyze the reversible isomerization of citrate to isocitrate via *cis*-aconitate in *E. coli* and, therefore, might be beneficial for an increased formation of aconitate, which then could be converted to itaconic acid. *Shewanella* already comprises similar enzymes but it could be possible that these *Shewanella* inherent enzymes are not as active for the synthesis of IA as the mentioned exogenous enzymes. Thus, the insertion of *gltA* and *acnA* has the potential of strengthening the TCA cycle and, thereby, building a solid pathway for the production of itaconic acid.

A plasmid containing *glk*, *galP*, *cadA* and *gltA* has already been prepared in the course of this thesis but could not be tested yet. The gene *acnA* has been amplified but not yet introduced into the plasmid.

5. Outlook

Future research endeavors with a main focus on ET rate improvement could combine the developed quadruple mutant with the overexpression of the OMC complex MtrABC, the recent discovery that current densities can also be enhanced by deletion of the λ-phage gene cluster from the *S. oneidensis* chromosome (Bursac et al. 2017) or both. Furthermore, investigation could be directed towards improving the biofilm adhesion to the anode in BESs in order to achieve higher current densities, which might also be key for efficient electrode-assisted fermentations. First research projects working with hydrogels have already been started in AG Gescher.

With regard to the utilization of new, sustainable substrates, cellulose and cellobiose seem to be promising compounds due to their availability in large amounts in form of agricultural waste. These eco-friendly and cheap substances bare a great potential for the production of platform chemicals. After establishing glucose as a substrate, the next steps towards the use of cellulose could be the use of cellobiose, which might be achieved by integrating cellobiose transporters and β-glucosidases from other microorganisms such as *Clostridium cellolyticum* (Fierobe et al. 1991) or *Lactococcus lactis* (Rosenbaum et al. 2011) into *Shewanella* for breaking down cellobiose into glucose inside the cell.

Relating to the production of itaconic acid, the most promising tested strain was GlucItac2, which might be enabled to produce larger quantities of itaconic acid by either inserting the plasmid *glk_galP_cadA_gltA_pBAD202* or the plasmid *glk_galP_cadA_gltA_acnA_pBAD202.* GltA and AcnA were shown to be actively involved in the TCA cycle of other microorganisms (Vuoristo et al. 2015a, 2015b) and, thus, could also improve the synthesis of itaconic acid in *S. oneidensis* by activating the TCA cycle. The first plasmid has already been prepared in the course of this thesis and the gene encoding AcnA has already been amplified for the subsequent insertion into the plasmid.

6. References

Aelterman, P.; Freguia, S.; Keller, J.; Verstraete, W.; Rabaey, K. (2008): The anode potential regulates bacterial activity in microbial fuel cells. In *Applied microbiology and biotechnology* 78 (3), pp. 409–418. DOI: 10.1007/s00253-007-1327-8.

Alves, M. N.; Neto, S. E.; Alves, A. S.; Fonseca, B. M.; Carrêlo, A.; Pacheco, I. et al. (2015): Characterization of the periplasmic redox network that sustains the versatile anaerobic metabolism of *Shewanella oneidensis* MR-1. In *Frontiers in microbiology* 6 (665), 1-10. DOI: 10.3389/fmicb.2015.00665.

Aro, N.; Pakula, T.; Penttilä, M. (2005): Transcriptional regulation of plant cell wall degradation by filamentous fungi. In *FEMS Microbiology Reviews* 29 (4), pp. 719–739. DOI: 10.1016/j.femsre.2004.11.006.

Bai, D.-M.; Wei, Q.; Yan, Z.-H.; Zhao, X.-M.; Li, X.-G.; Xu, S.-M. (2003): Fed-batch fermentation of *Lactobacillus lactis* for hyper-production of L-lactic acid. In *Biotechnology Letters* 25 (21), pp. 1833–1835.

Bard, A. J.; Faulkner, L. R. (2002): Electrochemical methods: fundamentals and applications, New York: Wiley, 2001, 2nd ed. In *Russian Journal of Electrochemistry* 38 (12), pp. 1364–1365. DOI: 10.1046/j.1464-410x.2001.02215.x.

Batti, M.; Schweiger, L. B. (1963): Process for the production of itaconic acid. App. no. 40182.

Bauer, W., Jr. (2000): Methacrylic Acid and Derivatives. In J. E. Bailey, M. Bohnet, C. J. Brinker (Eds.): Ullmann's Encyclopedia of Industrial Chemistry. 6th ed. Weinheim, Germany: Wiley-VCH Verlag GmbH & Co. KGaA.

Beliaev, A. S.; Saffarini, D. A. (1998): *Shewanella putrefaciens mtrB* encodes an outer membrane protein required for Fe(III) and Mn(IV) reduction. In *Journal of Bacteriology* 180 (23).

Beliaev, A. S.; Saffarini, D. A.; McLaughlin, J. L.; Hunnicutt, D. (2001): MtrC, an outer membrane decahaem c cytochrome required for metal reduction in *Shewanella putrefaciens* MR-1. In *Molecular microbiology* 39 (3), pp. 722–730.

Beliaev, A. S.; Thompson, D. K.; Fields, M. W.; Wu, L.; Lies, D. P.; Nealson, K. H.; Zhou, J. (2002): Microarray transcription profiling of a *Shewanella oneidensis* etrA mutant. In *Journal of Bacteriology* 184 (16), pp. 4612–4616. DOI: 10.1128/jb.184.16.4612-4616.2002.

Bentley, R.; Thiessen, C. P. (1955): *Cis*-aconitic decarboxylase. In *Science (New York, N.Y.)* 122 (3164), p. 330. DOI: 10.1126/science.122.3164.330.

Bentley, R.; Thiessen, C. P. (1957a): Biosynthesis of itaconic acid in *Aspergillus terreus*. I. Tracer studies with ^{14}C-labeled substrates. In *Journal of biological chemistry* 226 (2), pp. 673–687.

Bentley, R.; Thiessen, C. P. (1957b): Biosynthesis of itaconic acid in *Aspergillus terreus*. II. Early stages in glucose dissimilation and the role of citrate. In *Journal of biological chemistry* 226 (2), pp. 689–701.

Bentley, R.; Thiessen, C. P. (1957c): Biosynthesis of itaconic acid in *Aspergillus terreus*. III. The properties and reaction mechanism of *cis*-aconitic acid decarboxylase. In *Journal of biological chemistry* 226 (2), pp. 703–720.

Berry, E. A.; Trumpower, B. L. (1987): Simultaneous determination of hemes *a*, *b* and *c* from pyridine hemochrome[1] spectra. In *Analytical Biochemistry* 161 (1).

Biffinger, J. C.; Byrd, J. N.; Dudley, B. L.; Ringeisen, B. R. (2008): Oxygen exposure promotes fuel diversity for *Shewanella oneidensis* microbial fuel cells. In *Biosensors & bioelectronics* 23 (6), pp. 820–826. DOI: 10.1016/j.bios.2007.08.021.

Biffinger, J. C.; Ray, R.; Little, B. J.; Fitzgerald, L. A.; Ribbens, M.; Finkel, S. E.; Ringeisen, B. R. (2009): Simultaneous analysis of physiological and electrical output changes in an operating microbial fuel cell with *Shewanella oneidensis*. In *Biotechnology and bioengineering* 103 (3), pp. 524–531. DOI: 10.1002/bit.22266.

Bonnarme, P.; Gillet, B.; Sepulchre, A. M.; Role, C.; Beloeil, J. C.; Ducrocq, C. (1995): Itaconate biosynthesis in *Aspergillus terreus*. In *Journal of Bacteriology* 177 (12), pp. 3573–3578.

Bouhenni, R. A.; Vora, G. J.; Biffinger, J. C.; Shirodkar, S.; Brockman, K.; Ray, R. et al. (2010): The Role of *Shewanella oneidensis* MR-1 Outer Surface Structures in Extracellular Electron Transfer. In *Electroanalysis* 22 (7-8), pp. 856–864. DOI: 10.1002/elan.200880006.

Bradford, M. M. (1976): A rapid and sensitive method for the quantitation of microgram quantities of protein utilizing the principle of protein-dye binding. In *Analytical Biochemistry* 72, pp. 248–254.

Bretschger, O.; Obraztsova, A.; Sturm, C. A.; Chang, I. S.; Gorby, Y. A.; Reed, S. B. et al. (2007): Current production and metal oxide reduction by *Shewanella oneidensis* MR-1 wild type and mutants. In *Applied and environmental microbiology* 73 (21), pp. 7003–7012. DOI: 10.1128/AEM.01087-07.

Brown, R. M. [J.]; Saxena, I. M.; Kudlicka, K. (1996): Cellulose biosynthesis in higher plants. In *Trends in Plant Science* 1 (5), pp. 149–156. DOI: 10.1016/S1360-1385(96)80050-1.

Brutinel, E. D.; Gralnick, J. A. (2012a): Preferential utilization of D-lactate by *Shewanella oneidensis*. In *Applied and environmental microbiology* 78 (23), pp. 8474–8476. DOI: 10.1128/AEM.02183-12.

Brutinel, E. D.; Gralnick, J. A. (2012b): Shuttling happens: soluble flavin mediators of extracellular electron transfer in *Shewanella*. In *Applied microbiology and biotechnology* 93 (1), pp. 41–48. DOI: 10.1007/s00253-011-3653-0.

Bursac, T.; Gralnick, J. A.; Gescher, J. (2017): Acetoin production via unbalanced fermentation in *Shewanella oneidensis*. In *Biotechnology and bioengineering* 114 (6), pp. 1283–1289. DOI: 10.1002/bit.26243.

Calam, C. T.; Oxford, A. E.; Raistrick, H. (1939): Studies in the biochemistry of micro-organisms. LXIII. Itaconic acid, a metabolic product of a strain of *Aspergillus terreus* Thom. In *The Biochemical journal* 33 (9), pp. 1488–1495.

Carlsson, M.; Habenicht, C.; Kam, L. C.; Antal, M. J., Jr. (1994): Study of the sequential conversion of citric to itaconic to methacrylic acid in near-critical and supercritical water. In *Industrial and engineering chemistry research* 33 (8), pp. 1989–1996.

Carvalho, J. C.; Magalhães, A. I., Jr.; Soccol, C. R. (2018): Biobased itaconic acid market and research trends - is it really a promising chemical? In *Chimica oggi-chemistry today* 36 (4), pp. 56–58.

Cerny, G.; Teuber, M. (1971): Differential release of periplasmic *versus* cytoplasmic enzymes from *Escherichia coli B* by polymyxin B. In *Archiv. Mikrobiol.* 78 (2), pp. 166–179. DOI: 10.1007/BF00424873.

Choi, D.; Lee, S. B.; Kim, S.; Min, B.; Choi, I.-G.; Chang, I. S. (2014a): Metabolically engineered glucose-utilizing *Shewanella* strains under anaerobic conditions. In *Bioresource technology* 154, pp. 59–66. DOI: 10.1016/j.biortech.2013.12.025.

Choi, O.; Kim, T.; Woo, H. M.; Um, Y. (2014b): Electricity-driven metabolic shift through direct electron uptake by electroactive heterotroph *Clostridium pasteurianum*. In *Scientific reports* 4, p. 6961. DOI: 10.1038/srep06961.

Chubiz, L. M.; Marx, C. J. (2017): Growth Trade-Offs Accompany the Emergence of Glycolytic Metabolism in *Shewanella oneidensis* MR-1. In *Journal of Bacteriology* 199 (11), pp. 1–15. DOI: 10.1128/JB.00827-16.

Climent, M. J.; Corma, A.; Iborra, S. (2011): Converting carbohydrates to bulk chemicals and fine chemicals over heterogeneous catalysts. In *Green Chem.* 13 (3), pp. 520–540. DOI: 10.1039/c0gc00639d.

Coursolle, D.; Gralnick, J. A. (2010): Modularity of the Mtr respiratory pathway of *Shewanella oneidensis* strain MR-1. In *Molecular microbiology* 77 (4), pp. 995–1008. DOI: 10.1111/j.1365-2958.2010.07266.x.

Covington, E. D.; Gelbmann, C. B.; Kotloski, N. J.; Gralnick, J. A. (2010): An essential role for UshA in processing of extracellular flavin electron shuttles by *Shewanella oneidensis*. In *Molecular microbiology* 78 (2), pp. 519–532. DOI: 10.1111/j.1365-2958.2010.07353.x.

da Cruz, J. C.; Camporese Sérvulo, E. F.; de Castro, A. M. (2017): Microbial Production of Itaconic Acid. In : Microbial Production of Food Ingredients and Additives: Elsevier, pp. 291–315.

da Cruz, J. C.; de Castro, A. M.; Camporese Sérvulo, E. F. (2018): World market and biotechnological production of itaconic acid. In *Biotech* 8 (3), pp. 1–15. DOI: 10.1007/s13205-018-1151-0.

Delgado, V. P.; Paquete, C. M.; Sturm, G.; Gescher, J. (2019): Improvement of the electron transfer rate in *Shewanella oneidensis* MR-1 using a tailored periplasmic protein composition. In *Bioelectrochemistry* 129, pp. 18–25. DOI: 10.1016/j.bioelechem.2019.04.022.

Dobbin, P. S.; Butt, J. N.; Powell, A. K.; Reid, G. A.; Richardson, D. J. (1999): Characterization of a flavocytochrome that is induced during the anaerobic respiration of Fe^{3+} by *Shewanella frigidimarina* NCIMB400. In *Biochemical Journal* 342 (Pt 2), pp. 439–448.

Dwiarti, L.; Yamane, K.; Yamatani, H.; Kahar, P.; Okabe, M. (2002): Purification and characterization of *cis*-aconitic acid decarboxylase from *Aspergillus terreus* TN484-M1. In *Bioscience and bioengineering* 94 (1), pp. 29–33.

El-Halah, A.; Machado, D.; González, N.; Contreras, J.; López-Carrasquero, F. (2019): Use of super absorbent hydrogels derivative from acrylamide with itaconic acid and itaconates to remove metal ions from aqueous solutions. In *J Appl Polym Sci* 136 (4). DOI: 10.1002/app.46999.

El-Naggar, M. Y.; Wanger, G.; Leung, K. M.; Yuzvinsky, T. D.; Southam, G.; Yang, J. et al. (2010): Electrical transport along bacterial nanowires from *Shewanella oneidensis* MR-1. In *Proceedings of the National Academy of Sciences of the United States of America* 107 (42), pp. 18127–18131. DOI: 10.1073/pnas.1004880107.

Fierobe, H.-P.; Gaudin, C.; Belaich, A.; Loutfi, M.; Faure E.; Bagnara, C. et al. (1991): Characterization of Endoglucanase A from *Clostridium cellulolyticum*. In *Journal of Bacteriology* 173 (24), pp. 7956–7962.

Firer-Sherwood, M.; Pulcu, G. S.; Elliott, S. J. (2008): Electrochemical interrogations of the Mtr cytochromes from *Shewanella*: opening a potential window. In *Journal of biological inorganic chemistry : JBIC : a publication of the Society of Biological Inorganic Chemistry* 13 (6), pp. 849–854. DOI: 10.1007/s00775-008-0398-z.

Flores, N.; Xiao, J.; Berry, A.; Bolivar, F.; Valle, F. (1996): Pathway engineering for the production of aromatic compounds in *Escherichia coli*. In *Nature biotechnology* 14 (5), pp. 620–623.

Flores, S.; Gosset, G.; Flores, N.; Graaf, A. A. de; Bolívar, F. (2002): Analysis of carbon metabolism in *Escherichia coli* strains with an inactive

phosphotransferase system by (13)C labeling and NMR spectroscopy. In *Metabolic engineering* 4 (2), pp. 124–137. DOI: 10.1006/mben.2001.0209.

Flynn, J. M.; Ross, D. E.; Hunt, K. A.; Bond, D. R.; Gralnick, J. A. (2010): Enabling unbalanced fermentations by using engineered electrode-interfaced bacteria. In *mBio* 1 (5), pp. 1–8. DOI: 10.1128/mBio.00190-10.

Fonseca, B. M.; Paquete, C. M.; Neto, S. E.; Pacheco, I.; Soares, C. M.; Louro, R. O. (2013): Mind the gap: cytochrome interactions reveal electron pathways across the periplasm of *Shewanella oneidensis* MR-1. In *The Biochemical journal* 449 (1), pp. 101–108. DOI: 10.1042/BJ20121467.

Förster, A. H.; Beblawy, S.; Golitsch, F.; Gescher, J. (2017): Electrode-assisted acetoin production in a metabolically engineered *Escherichia coli* strain. In *Biotechnology for biofuels* 10 (65), pp. 1–11. DOI: 10.1186/s13068-017-0745-9.

Fourmond, V. (2016): QSoas: A versatile software for data analysis. In *Analytical chemistry* 88 (10), pp. 5050–5052. DOI: 10.1021/acs.analchem.6b00224.

Fredrickson, J. K.; Romine, M. F.; Beliaev, A. S.; Auchtung, J. M.; Driscoll, M. E.; Gardner, T. S. et al. (2008): Towards environmental systems biology of *Shewanella*. In *Nature reviews. Microbiology* 6 (8), pp. 592–603. DOI: 10.1038/nrmicro1947.

Gao, H.; Barua, S.; Liang, Y.; Wu, L.; Dong, Y.; Reed, S. et al. (2010): Impacts of *Shewanella oneidensis c*-type cytochromes on aerobic and anaerobic respiration. In *Microbial biotechnology* 3 (4), pp. 455–466. DOI: 10.1111/j.1751-7915.2010.00181.x.

Geiser, E.; Przybilla, S. K.; Friedrich, A.; Buckel, W.; Wierckx, N.; Blank, L. M.; Bölker, M. (2016): *Ustilago maydis* produces itaconic acid via the unusual intermediate trans-aconitate. In *Microbial biotechnology* 9 (1), pp. 116–126. DOI: 10.1111/1751-7915.12329.

Gibson, D. G.; Young, L.; Chuang, R.-Y.; Venter, J. C.; Hutchison, C. A.; Smith, H. O. (2009): Enzymatic assembly of DNA molecules up to several hundred kilobases. In *Nature methods* 6 (5), pp. 343–345. DOI: 10.1038/nmeth.1318.

Glazer, A. N.; Nikaido, H. (2008): Microbial biotechnology. Fundamentals of applied microbiology. 2nd ed., [international student ed.]. Singapore: Cambridge University Press.

Golitsch, F.; Bücking, C.; Gescher, J. (2013): Proof of principle for an engineered microbial biosensor based on *Shewanella oneidensis* outer membrane protein complexes. In *Biosensors & bioelectronics* 47, pp. 285–291. DOI: 10.1016/j.bios.2013.03.010.

Gorby, Y. A.; Yanina, S.; McLean, J. S.; Rosso, K. M.; Moyles, D.; Dohnalkova, A. et al. (2006): Electrically conductive bacterial nanowires produced by *Shewanella oneidensis* strain MR-1 and other microorganisms. In *Proceedings*

of the National Academy of Sciences of the United States of America 103 (30), pp. 11358–11363. DOI: 10.1073/pnas.0604517103.

Gralnick, J. A.; Newman, D. K. (2007): Extracellular respiration. In *Molecular microbiology* 65 (1), pp. 1–11. DOI: 10.1111/j.1365-2958.2007.05778.x.

Harder, B.-J.; Bettenbrock, K.; Klamt, S. (2016): Model-based metabolic engineering enables high yield itaconic acid production by *Escherichia coli*. In *Metabolic engineering* 38, pp. 29–37. DOI: 10.1016/j.ymben.2016.05.008.

Hartshorne, R. S.; Jepson, B. N.; Clarke, T. A.; Field, S. J.; Fredrickson, J.; Zachara, J. et al. (2007): Characterization of *Shewanella oneidensis* MtrC: a cell-surface decaheme cytochrome involved in respiratory electron transport to extracellular electron acceptors. In *Journal of biological inorganic chemistry : JBIC : a publication of the Society of Biological Inorganic Chemistry* 12 (7), pp. 1083–1094. DOI: 10.1007/s00775-007-0278-y.

Hau, H. H.; Gralnick, J. A. (2007): Ecology and biotechnology of the genus *Shewanella*. In *Annual review of microbiology* 61, pp. 237–258. DOI: 10.1146/annurev.micro.61.080706.093257.

Heidelberg, J. F.; Paulsen, I. T.; Nelson, K. E.; Gaidos, E. J.; Nelson, W. C.; Read, T. D. et al. (2002): Genome sequence of the dissimilatory metal ion-reducing bacterium *Shewanella oneidensis*. In *Nature biotechnology* 20 (11), pp. 1118–1123. DOI: 10.1038/nbt749.

Hernández-Montalvo, V.; Martínez, A.; Hernández-Chavez, G.; Bolivar, F.; Valle, F.; Gosset, G. (2003): Expression of *galP* and *glk* in a *Escherichia coli* PTS mutant restores glucose transport and increases glycolytic flux to fermentation products. In *Biotechnology and bioengineering* 83 (6), pp. 687–694. DOI: 10.1002/bit.10702.

Hirsch, R. L.; Bezdek, R.; Wendling, R. (2006): Peaking of World Oil Production and Its Mitigation. In *AIChE J.* 52 (1), pp. 2–8. DOI: 10.1002/aic.10747.

Howard, E. C.; Hamdan, L. J.; Lizewski, S. E.; Ringeisen, B. R. (2012): High frequency of glucose-utilizing mutants in *Shewanella oneidensis* MR-1. In *FEMS microbiology letters* 327 (1), pp. 9–14. DOI: 10.1111/j.1574-6968.2011.02450.x.

Hunt, K. A.; Flynn, J. M.; Naranjo, B.; Shikhare, I. D.; Gralnick, J. A. (2010): Substrate-level phosphorylation is the primary source of energy conservation during anaerobic respiration of *Shewanella oneidensis* strain MR-1. In *Journal of Bacteriology* 192 (13), pp. 3345–3351. DOI: 10.1128/JB.00090-10.

Jaklitsch, W. M.; Kubicek, C. P.; Scrutton, M. C. (1991): The subcellular organization of itaconate biosynthesis in *Aspergillus terreus*. In *Journal of General Microbiology* 137 (3), pp. 533–539. DOI: 10.1099/00221287-137-3-533.

Kanamasa, S.; Dwiarti, L.; Okabe, M.; Park, E. Y. (2008): Cloning and functional characterization of the *cis*-aconitic acid decarboxylase (CAD) gene from

Aspergillus terreus. In *Applied microbiology and biotechnology* 80 (2), pp. 223–229. DOI: 10.1007/s00253-008-1523-1.

Kim, B. H.; Chang, I. S.; Gil, G. C.; Park, H. S.; Kim, H. J. (2003): Novel BOD (biological oxygen demand) sensor using mediator-less microbial fuel cell. In *Biotechnology Letters* 25 (7), pp. 541–545.

Kim, H. J.; Park, H. S.; Hyun, M. S.; Chang, I. S.; Kim, M.; Kim, B. H. (2002): A mediator-less microbial fuel cell using a metal reducing bacterium, *Shewanella putrefaciens* 30 (2), pp. 145–152.

Kotloski, N. J.; Gralnick, J. A. (2013): Flavin electron shuttles dominate extracellular electron transfer by *Shewanella oneidensis*. In *mBio* 4 (1), pp. 1–4. DOI: 10.1128/mBio.00553-12.

Kracke, F.; Krömer, J. O. (2014): Identifying target processes for microbial electrosynthesis by elementary mode analysis. In *BMC bioinformatics* 15. DOI: 10.1186/s12859-014-0410-2.

Kuenz, A.; Krull, S. (2018): Biotechnological production of itaconic acid—things you have to know. In *Applied microbiology and biotechnology* 102 (9), pp. 3901–3914. DOI: 10.1007/s00253-018-8895-7.

Laemmli, U. K. (1970): Cleavage of structural proteins during the assembly of the head of bacteriophage T4. In *Nature* 227 (5259), 680-685.

Lies, D. P.; Hernandez, M. E.; Kappler, A.; Mielke, R. E.; Gralnick, J. A.; Newman, D. K. (2005): *Shewanella oneidensis* MR-1 uses overlapping pathways for iron reduction at a distance and by direct contact under conditions relevant for biofilms. In *Applied and environmental microbiology* 71 (8), pp. 4414–4426. DOI: 10.1128/AEM.71.8.4414-4426.2005.

Logan, B. E.; Murano, C.; Scott, K.; Gray, N. D.; Head, I. M. (2005): Electricity generation from cysteine in a microbial fuel cell. In *Water research* 39 (5), pp. 942–952. DOI: 10.1016/j.watres.2004.11.019.

Lovley, D. R. (2006): Bug juice. Harvesting electricity with microorganisms. In *Nature reviews. Microbiology* 4 (7), pp. 497–508. DOI: 10.1038/nrmicro1442.

Lovley, D. R.; Phillips, E. J. P.; Lonergan, D. J. (1989): Hydrogen and Formate Oxidation Coupled to Dissimilatory Reduction of Iron or Manganese by *Alteromonas putrefaciens*. In *Applied and environmental microbiology* 55 (3), pp. 700–706.

Maier, T. M.; Myers, C. R. (2001): Isolation and characterization of a *Shewanella putrefaciens* MR-1 electron transport regulator *etrA* mutant: reassessment of the role of EtrA. In *Journal of Bacteriology* 183 (16), pp. 4918–4926. DOI: 10.1128/JB.183.16.4918-4926.2001.

Marmur, J. (1961): A procedure for the isolation of deoxyribonucleic acid for micro-organisms. J. Mol. Biol. 3:208-18. In *J. Mol. Biol.* 3, pp. 208–218.

Marsili, E.; Baron, D. B.; Shikhare, I. D.; Coursolle, D.; Gralnick, J. A.; Bond, D. R. (2008): *Shewanella* secretes flavins that mediate extracellular electron transfer. In *PNAS* 105 (10), pp. 3968–3973.

Max, B.; Salgado, J. M.; Rodríguez, N.; Cortés, S.; Converti, A.; Domínguez, J. M. (2010): Biotechnological production of citric acid. In *Brazilian journal of microbiology : [publication of the Brazilian Society for Microbiology]* 41 (4), pp. 862–875. DOI: 10.1590/S1517-83822010000400005.

Meshulam-Simon, G.; Behrens, S.; Choo, A. D.; Spormann, A. M. (2007): Hydrogen metabolism in *Shewanella oneidensis* MR-1. In *Applied and environmental microbiology* 73 (4), pp. 1153–1165. DOI: 10.1128/AEM.01588-06.

Middleton, S. S.; Latmani, R. B.; Mackey, M. R.; Ellisman, M. H.; Tebo, B. M.; Criddle, C. S. (2003): Cometabolism of Cr(VI) by *Shewanella oneidensis* MR-1 produces cell-associated reduced chromium and inhibits growth. In *Biotechnology and bioengineering* 83 (6), pp. 627–637. DOI: 10.1002/bit.10725.

Moat, A. G.; Foster, J. W.; Spector, M. P. (2002): Fermentation pathways. 4th ed. New York: Wiley-Liss.

Mortazavi, A.; Williams, B. A.; McCue, K.; Schaeffer, L.; Wold, B. (2008): Mapping and quantifying mammalian transcriptomes by RNA-Seq. In *Nature methods* 5 (7), pp. 621–628. DOI: 10.1038/nmeth.1226.

Myers, C. R.; Carstens, B. P.; Antholine, W. E.; Myers, J. M. (2000): Chromium(VI) reductase activity is associated with the cytoplasmic membrane of anaerobically grown *Shewanella putrefaciens* MR1. In *Applied Microbiology* 88 (1), pp. 98–106.

Myers, C. R.; Myers, J. M. (1997): Cloning and sequence of *cymA*, a gene encoding a tetraheme cytochrome *c* required for reduction of iron(III), fumarate, and nitrate by *Shewanella putrefaciens* MR-1. In *Journal of Bacteriology* 179 (4), pp. 1143–1152.

Myers, C. R.; Nealson, K. H. (1988): Bacterial manganese reduction and growth with manganese oxide as the sole electron acceptor. In *Science* 240 (4857), pp. 1319-1321.

Nakagawa, G.; Kouzuma, A.; Hirose, A.; Kasai, T.; Yoshida, G.; Watanabe, K. (2015): Metabolic characteristics of a glucose-utilizing *Shewanella oneidensis* strain grown under electrode-respiring conditions. In *PloS one* 10 (9). DOI: 10.1371/journal.pone.0138813.

Okabe, M.; Lies, D.; Kanamasa, S.; Park, E. Y. (2009): Biotechnological production of itaconic acid and its biosynthesis in *Aspergillus terreus*. In *Applied microbiology and biotechnology* 84 (4), pp. 597–606. DOI: 10.1007/s00253-009-2132-3.

Okamoto, A.; Hashimoto, K.; Nealson, K. H. (2014a): Flavin redox bifurcation as a mechanism for controlling the direction of electron flow during extracellular electron transfer. In *Angewandte Chemie (International ed. in English)* 53 (41), pp. 10988–10991. DOI: 10.1002/anie.201407004.

Okamoto, A.; Hashimoto, K.; Nealson, K. H.; Nakamura, R. (2013): Rate enhancement of bacterial extracellular electron transport involves bound flavin semiquinones. In *PNAS* 110 (19), pp. 7856–7861. DOI: 10.1073/pnas.1220823110.

Okamoto, A.; Kalathil, S.; Deng, X.; Hashimoto, K.; Nakamura, R.; Nealson, K. H. (2014b): Cell-secreted flavins bound to membrane cytochromes dictate electron transfer reactions to surfaces with diverse charge and pH. In *Scientific reports* 4, p. 5628. DOI: 10.1038/srep05628.

Okamoto, S.; Chin, T.; Nagata, K.; Takahashi, T.; Ohara, H.; Aso, Y. (2015): Production of itaconic acid in *Escherichia coli* expressing recombinant α-amylase using starch as substrate. In *Journal of bioscience and bioengineering* 119 (5), pp. 548–553. DOI: 10.1016/j.jbiosc.2014.10.021.

Otten, A.; Brocker, M.; Bott, M. (2015): Metabolic engineering of *Corynebacterium glutamicum* for the production of itaconate. In *Metabolic engineering* 30, pp. 156–165. DOI: 10.1016/j.ymben.2015.06.003.

Park, D. H.; Zeikus, J. G. (2002): Impact of electrode composition on electricity generation in a single-compartment fuel cell using *Shewanella putrefaciens*. In *Applied microbiology and biotechnology* 59 (1), pp. 58–61. DOI: 10.1007/s00253-002-0972-1.

Pinchuk, G. E.; Rodionov, D. A.; Yang, C.; Li, X.; Osterman, A. L.; Dervyn, E. et al. (2008): Genomic reconstruction of *Shewanella oneidensis* MR-1 metabolism reveals a previously uncharacterized machinery for lactate utilization. In *PNAS* 106 (8), pp. 2874–2879.

Pirbadian, S.; Barchinger, S. E.; Leung, K. M.; Byun, H. S.; Jangir, Y.; Bouhenni, R. A. et al. (2014): *Shewanella oneidensis* MR-1 nanowires are outer membrane and periplasmic extensions of the extracellular electron transport components. In *Proceedings of the National Academy of Sciences of the United States of America* 111 (35), pp. 12883–12888. DOI: 10.1073/pnas.1410551111.

Pitts, K. E.; Dobbin, P. S.; Reyes-Ramirez, F.; Thomson, A. J.; Richardson, D. J.; Seward, H. E. (2003): Characterization of the *Shewanella oneidensis* MR-1 decaheme cytochrome MtrA. Expression in *Escherichia coli* confers the ability to reduce soluble Fe(III) chelates. In *J. Biol. Chem* 278 (30), pp. 27758–27765. DOI: 10.1074/jbc.M302582200.

Ramesh, K.; Vikramachakravarthi, D.; Pal, P. (2014): Production and purification of glutamic acid: A critical review towards process intensification. In

chemical engineering and processing 81, pp. 59–71. DOI: 10.1016/j.cep.2014.04.012.

Robert, T.; Friebel, S. (2016): Itaconic acid – a versatile building block for renewable polyesters with enhanced functionality. In *Green Chem.* 18 (10), pp. 2922–2934. DOI: 10.1039/C6GC00605A.

Romine, M. F.; Carlson, T. S.; Norbeck, A. D.; McCue, L. A.; Lipton, M. S. (2008): Identification of mobile elements and pseudogenes in the *Shewanella oneidensis* MR-1 genome. In *Applied and environmental microbiology* 74 (10), pp. 3257–3265. DOI: 10.1128/AEM.02720-07.

Rosenbaum, M. A.; Bar, H. Y.; Beg, Q. K.; Segrè, D.; Booth, J.; Cotta, M. A.; Angenent, L. T. (2011): *Shewanella oneidensis* in a lactate-fed pure-culture and a glucose-fed co-culture with *Lactococcus lactis* with an electrode as electron acceptor. In *Bioresource technology* 102 (3), pp. 2623–2628. DOI: 10.1016/j.biortech.2010.10.033.

Ross, D. E.; Flynn, J. M.; Baron, D. B.; Gralnick, J. A.; Bond, D. R. (2011): Towards electrosynthesis in *Shewanella*: energetics of reversing the mtr pathway for reductive metabolism. In *PloS one* 6 (2), e16649. DOI: 10.1371/journal.pone.0016649.

Ruebush, S. S.; Brantley, S. L.; Tien, M. (2006): Reduction of soluble and insoluble iron forms by membrane fractions of *Shewanella oneidensis* grown under aerobic and anaerobic conditions. In *Applied and environmental microbiology* 72 (4), pp. 2925–2935. DOI: 10.1128/AEM.72.4.2925-2935.2006.

Saltikov, C. W.; Newman, D. K. (2003): Genetic identification of a respiratory arsenate reductase. In *PNAS* 100 (19), pp. 10983–10988. DOI: 10.1073/pnas.1834303100.

Schicklberger, M.; Bücking, C.; Schuetz, B.; Heide, H.; Gescher, J. (2011): Involvement of the *Shewanella oneidensis* decaheme cytochrome MtrA in the periplasmic stability of the beta-barrel protein MtrB. In *Applied and environmental microbiology* 77 (4), pp. 1520–1523. DOI: 10.1128/AEM.01201-10.

Schuetz, B.; Schicklberger, M.; Kuermann, J.; Spormann, A. M.; Gescher, J. (2009): Periplasmic electron transfer via the *c*-type cytochromes MtrA and FccA of *Shewanella oneidensis* MR-1. In *Applied and environmental microbiology* 75 (24), pp. 7789–7796. DOI: 10.1128/AEM.01834-09.

Schwalb, C.; Chapman, S. K.; Reid, G. A. (2003): The tetraheme cytochrome CymA is required for anaerobic respiration with dimethyl sulfoxide and nitrite in *Shewanella oneidensis*. In *Biochemistry* 42 (31), pp. 9491–9497. DOI: 10.1021/bi034456f.

Serres, M. H.; Riley, M. (2006): Genomic analysis of carbon source metabolism of *Shewanella oneidensis* MR-1. Predictions versus experiments. In *Journal of Bacteriology* 188 (13), pp. 4601–4609. DOI: 10.1128/JB.01787-05.

Shanks, R. M. Q.; Caiazza, N. C.; Hinsa, S. M.; Toutain, C. M.; O'Toole, G. A. (2006): *Saccharomyces cerevisiae*-based molecular tool kit for manipulation of genes from Gram-negative bacteria. In *Applied and environmental microbiology* 72 (7), pp. 5027–5036. DOI: 10.1128/AEM.00682-06.

Shi, L.; Rosso, K. M.; Clarke, T. A.; Richardson, D. J.; Zachara, J. M.; Fredrickson, J. K. (2012): Molecular Underpinnings of Fe(III) Oxide Reduction by *Shewanella Oneidensis* MR-1. In *Frontiers in microbiology* 3, p. 50. DOI: 10.3389/fmicb.2012.00050.

Somerville, C.; Bauer, S.; Brininstool, G.; Facette, M.; Hamann, T.; Milne, J. et al. (2004): Toward a systems approach to understanding plant cell walls. In *Science (New York, N.Y.)* 306 (5705), pp. 2206–2211. DOI: 10.1126/science.1102765.

Song, H.; Lee, S. Y. (2006): Production of succinic acid by bacterial fermentation. In *Enzyme and Microbial Technology* 39 (3), pp. 352–361. DOI: 10.1016/j.enzmictec.2005.11.043.

Steiger, M. G.; Blumhoff, M. L.; Mattanovich, D.; Sauer, M. (2013): Biochemistry of microbial itaconic acid production. In *Frontiers in microbiology* 4 (1), pp. 1–5. DOI: 10.3389/fmicb.2013.00023.

Stookey, L. L. (1970): Ferrozine-A new spectrophotometric reagent for iron. In *Analytical chemistry* 42 (7), pp. 779–781. DOI: 10.1021/ac60289a016.

Sturm, G.; Richter, K.; Doetsch, A.; Heide, H.; Louro, R. O.; Gescher, J. (2015): A dynamic periplasmic electron transfer network enables respiratory flexibility beyond a thermodynamic regulatory regime. In *The ISME journal* 9 (8), pp. 1802–1811. DOI: 10.1038/ismej.2014.264.

Subramanian, P.; Pirbadian, S.; El-Naggar, M. Y.; Jensen, G. J. (2018): Ultrastructure of *Shewanella oneidensis* MR-1 nanowires revealed by electron cryotomography. In *Proceedings of the National Academy of Sciences of the United States of America* 115 (14), E3246-E3255. DOI: 10.1073/pnas.1718810115.

Survase, S.; Bajaj, I. B.; Singhal, R. S. (2006): Biotechnological Production of Vitamins. In *Food technol. biotechnol.* 44 (3), pp. 381–396.

Tang, Y. J.; Laidlaw, D.; Gani, K.; Keasling, J. D. (2006): Evaluation of the effects of various culture conditions on Cr(VI) reduction by *Shewanella oneidensis* MR-1 in a novel high-throughput mini-bioreactor. In *Biotechnology and bioengineering* 95 (1), pp. 176–184. DOI: 10.1002/bit.21002.

Tang, Y. J.; Meadows, A. L.; Kirby, J.; Keasling, J. D. (2007): Anaerobic central metabolic pathways in *Shewanella oneidensis* MR-1 reinterpreted in the light of

isotopic metabolite labeling. In *Journal of Bacteriology* 189 (3), pp. 894–901. DOI: 10.1128/JB.00926-06.

Thomas, P. E.; Ryan, D.; Levin, W. (1976): An improved staining procedure for the detection of the peroxidase activity of cytochrome *P*-450 on sodium dodecyl sulfate polyacrylamide gels. In *Analytical Biochemistry* 75 (1), pp. 168-176.

Tiedje, J. M. (2002): *Shewanella*-the environmentally versatile genome. In *Nature biotechnology* 20, pp. 1093–1094.

Timell, T. E. (1967): Recent progress in the chemistry of wood hemicelluloses. In *Wood Sci.Technol.* 1 (1), pp. 45–70. DOI: 10.1007/BF00592255.

Tomić, S. L.; Mićić, M. M.; Dobić, S. N.; Filipović, J. M.; Suljovrujić, E. H. (2010): Smart poly(2-hydroxyethyl methacrylate/itaconic acid) hydrogels for biomedical application. In *Radiation Physics and Chemistry* 79 (5), pp. 643–649. DOI: 10.1016/j.radphyschem.2009.11.015.

Torres, C. I.; Krajmalnik-Brown, R.; Parameswaran, P.; Marcus, A. K.; Wanger, G.; Gorby, Y. A.; Rittmann, B. E. (2009): Selecting anode-respiring bacteria based on anode potential: phylogenetic, electrochemical, and microscopic characterization. In *Environmental science & technology* 43 (24), pp. 9519–9524. DOI: 10.1021/es902165y.

Tran, K.-N. T.; Somasundaram, S.; Eom, G. T.; Hong, S. H. (2019): Efficient Itaconic acid production via protein-protein scaffold introduction between GltA, AcnA, and CadA in recombinant *Escherichia coli*. In *Biotechnology progress* 35 (3), e2799. DOI: 10.1002/btpr.2799.

van der Straat, L.; Vernooij, M.; Lammers, M.; van den Berg, W.; Schonewille, T.; Cordewener, J. et al. (2014): Expression of the *Aspergillus terreus* itaconic acid biosynthesis cluster in *Aspergillus niger*. In *Microbial cell factories* 13, p. 11. DOI: 10.1186/1475-2859-13-11.

Velasquez-Orta, S. B.; Head, I. M.; Curtis, T. P.; Scott, K.; Lloyd, J. R.; von Canstein, H. (2010): The effect of flavin electron shuttles in microbial fuel cells current production. In *Applied microbiology and biotechnology* 85 (5), pp. 1373–1381. DOI: 10.1007/s00253-009-2172-8.

Venkateswaran, K.; Moser, D. P.; Dollhopf, M. E.; Lies, D. P.; Saffarini, D. A.; MacGregor, B. J. et al. (1999): Polyphasic taxonomy of the genus *Shewanella* and description of *Shewanella oneidensis* sp. nov. In *International Journal of Systematic Bacteriology* 49 (2), pp. 705–724.

Viamajala, S.; Peyton, B. M.; Apel, W. A.; Petersen, J. N. (2002): Chromate/nitrite interactions in *Shewanella oneidensis* MR-1: evidence for multiple hexavalent chromium Cr(VI) reduction mechanisms dependent on physiological growth conditions. In *Biotechnology and bioengineering* 78 (7), pp. 770–778. DOI: 10.1002/bit.10261.

von Canstein, H.; Ogawa, J.; Shimizu, S.; Lloyd, J. R. (2008): Secretion of flavins by *Shewanella* species and their role in extracellular electron transfer. In *Applied and environmental microbiology* 74 (3), pp. 615–623.

Vuoristo, K. S.; Mars, A. E.; Sangra, J. V.; Springer, J.; Eggink, G.; Sanders, J. P. M.; Weusthuis, R. A. (2015a): Metabolic engineering of itaconate production in *Escherichia coli*. In *Applied microbiology and biotechnology* 99 (1), pp. 221–228. DOI: 10.1007/s00253-014-6092-x.

Vuoristo, K. S.; Mars, A. E.; Sangra, J. V.; Springer, J.; Eggink, G.; Sanders, J. P. M.; Weusthuis, R. A. (2015b): Metabolic engineering of the mixed-acid fermentation pathway of *Escherichia coli* for anaerobic production of glutamate and itaconate. In *AMB Express* 5 (1), p. 61. DOI: 10.1186/s13568-015-0147-y.

Walcarius, A.; Minteer, S. D.; Wang, J.; Lin, Y.; Merkoçi, A. (2013): Nanomaterials for bio-functionalized electrodes: recent trends. In *J. Mater. Chem. B* 1 (38), p. 4878. DOI: 10.1039/c3tb20881h.

Weastra s.r.o. (2012): Determination of market potential for selected platform chemicals. Weastra s.r.o. Available online at https://www.cbp.fraunhofer.de/content/dam/cbp/en/documents/project-reports/BioConSepT_Market-potential-for-selected-platform-chemicals_report1.pdf, checked on 7/14/2019.

Wee, Y.-J.; Kim, J.-N.; Ryu, H.-W. (2006): Biotechnological production of lactic acid and its recent applications. In *Food technol. biotechnol.* 44 (2), pp. 163–172.

Werpy, T.; Petersen, G.; Aden, A.; Bozell, J.; Holladay, J.; White, J. et al. (2004): Top Value Added Chemicals from Biomass. Volume I: Results of Screening for Potential Candidates from Sugars and Synthesis Gas.

Willke, T.; Vorlop, K.-D. (2001): Biotechnological production of itaconic acid. In *Applied microbiology and biotechnology* 56 (3-4), pp. 289–295. DOI: 10.1007/s002530100685.

Xu, S.; Jangir, Y.; El-Naggar, M. Y. (2016): Disentangling the roles of free and cytochrome-bound flavins in extracellular electron transport from *Shewanella oneidensis* MR-1. In *Electrochimica Acta* 198, pp. 49–55. DOI: 10.1016/j.electacta.2016.03.074.

Yahiro, K.; Takahama, T.; Park, Y. S.; Okabe, M. (1995): Breeding of *Aspergillus terreus* mutant TN-484 for itaconic acid production with high yield. In *Journal of fermentation and bioengineering* 79 (5), pp. 506-508.

Zhai, D.-D.; Li, B.; Sun, J.-Z.; Sun, D.-Z.; Si, R.-W.; Yong, Y.-C. (2016): Enhanced power production from microbial fuel cells with high cell density culture. In *Water science and technology : a journal of the International Association on Water Pollution Research* 73 (9), pp. 2176–2181. DOI: 10.2166/wst.2016.059.

Zhou, M.; Chen, J.; Freguia, S.; Rabaey, K.; Keller, J. (2013): Carbon and electron fluxes during the electricity driven 1,3-propanediol biosynthesis from glycerol. In *Environmental science & technology* 47 (19), pp. 11199–11205. DOI: 10.1021/es402132r.